

Analysis of Purkinje Cell Responses in the Oculomotor Vermis during the Execution of
Smooth Pursuit Eye Movements

by

Ramanujan T. Raghavan

Department of Neurobiology
Duke University

Date: _____

Approved:

Stephen G. Lisberger, Co-Supervisor

Marc A. Sommer, Co-Supervisor

Lindsey Glickfeld

Court Hull, Chair

Dissertation submitted in partial fulfillment of
the requirements for the degree of Doctor of Philosophy in the Department of
Neurobiology in the Graduate School
of Duke University

2016

ABSTRACT

Analysis of Purkinje Cell Responses in the Oculomotor Vermis during the Execution of
Smooth Pursuit Eye Movements

by

Ramanujan T. Raghavan

Department of Neurobiology
Duke University

Date: _____

Approved:

Stephen G. Lisberger, Co-Supervisor

Marc A. Sommer, Co-Supervisor

Lindsey Glickfeld

Court Hull, Chair

An abstract of a dissertation submitted in partial
fulfillment of the requirements for the degree
of Doctor of Philosophy in the Department of
Neurobiology in the Graduate School of
Duke University

2016

Copyright by
Ramanujan T. Raghavan
2016

Abstract

Smooth pursuit eye movements are movements of the eyes that are used to foveate moving objects. Their precision and adaptation is believed to depend on a constellation of sites across the cerebellum, but only one region's contribution is well characterized, the floccular complex. Here, I characterize the response properties of neurons in the oculomotor vermis, another major division of the oculomotor cerebellum whose role in pursuit remains unknown. I recorded Purkinje cells, the output neurons of this region, in two monkeys as they executed pursuit eye movements in response to step ramp target motion. The responses of these Purkinje cells in the oculomotor vermis were very different from responses that have been documented in the floccular complex. The simple spikes of these cells encoded movement direction in retinal, as opposed to muscle coordinates. They were less related to movement kinematics, and had smaller values of trial-by-trial correlations with pursuit speed, latency, and direction than their floccular complex counterparts. Unlike Purkinje cells in the floccular complex, simple spike firing rates in the oculomotor vermis remained unchanged over the course of pursuit adaptation, likely excluding the oculomotor vermis as a site of directional plasticity. Complex spikes of these Purkinje cells were only partially responsive to target motion, and did not fall into any clear opponent directional organization with simple spikes, as has been found in the floccular complex. In general, Purkinje cells in the

oculomotor vermis were responsive to both pursuit and to saccadic eye movements, but maintained tuning for the direction of these movements along separate directions at a population level. Predictions of caudal fastigial nucleus activity, generated on the basis of our population of oculomotor vermal Purkinje cells, faithfully tracked moment-by-movement changes in pursuit kinematics. By contrast, these responses did not faithfully track moment-by-moments changes in saccade kinematics. These results suggest that the oculomotor vermis is likely to play a smaller role in influencing pursuit eye movements by comparison to the floccular complex.

Dedication

Dedicated to the memory of my dearest uncle, Dr. C.S. Rangarathnam. In life and in science, I hope to approach a fraction of his kindness and brilliance.

Contents

Abstract	iv
List of Tables.....	xi
List of Figures	xii
Acknowledgements.....	xvii
1. Introduction: Why study eye movements?.....	1
1.1 Behavioral characteristics of voluntary eye movements.....	7
1.1.1 Behavioral characteristics of smooth pursuit eye movements	7
1.1.2 Behavioral characteristics of saccadic eye movements.....	10
1.2 Anatomical substrates underlying voluntary eye movement control.....	11
1.2.1 Functional anatomy of the smooth pursuit eye movement system	11
1.2.2 Functional anatomy of the saccadic eye movement system	13
1.3 The contribution of the cerebellum to voluntary eye movement control.....	14
1.3.1 Functional anatomy and physiology of the floccular complex	15
1.3.2 Functional anatomy and physiology of the oculomotor vermis	17
1.3.3 Major anatomical differences between the floccular complex and oculomotor vermis	20
1.4 Outline of the chapters presented henceforth.....	21
2.The directional organization of pursuit eye movement signals in the oculomotor vermis and their consequences for motor learning	22
2.1 Introduction	22
2.2 Methods	26

2.2.1 Subjects	26
2.2.2 Visual stimuli and Experimental Design	27
2.2.3 Neural Recording	28
2.2.4 Data Analysis	30
2.3 Results	32
2.3.1 Psychophysics of Pursuit	32
2.3.2 Example response	34
2.3.3 Summary of population simple spiking directional selectivity	38
2.3.4 Directional tuning of Purkinje cell complex spikes during pursuit in eight directions	43
2.3.5 Summary of findings on tuning properties	47
2.3.6 Methods for studying directional adaptation	48
2.3.7 Structure of our learning population, experimental setup	50
2.3.8 Simple spike changes over the course of learning	53
2.3.9 Complex spiking changes over the course of learning	55
2.4 Discussion	60
3. A quantitative comparison of the encoding of smooth pursuit eye movements by the oculomotor vermis and floccular complex	62
3.1 Introduction	62
3.2 Methods	65
3.2.1 Visual stimuli and Experimental Design	66
3.2.2 Data Analysis	67
3.3 Results	69

3.3.1 Pursuit Kinematics	69
3.3.2 Properties of Purkinje cell responses in the oculomotor vermis and floccular complex during fixation	70
3.3.3 Kinematic sensitivity of pursuit responses as compared between the Oculomotor Vermis and Floccular Complex	73
3.3.4 Neuron-Behavior correlations during fixation and the open loop of pursuit: comparing the Oculomotor Vermis and Floccular Complex	77
3.3.5 Discussion	84
4. A quantitative comparison of the encoding of smooth pursuit eye movements and saccadic eye movements by Purkinje cells in the oculomotor vermis	88
4.1 Introduction	88
4.2 Methods	92
4.2.1 Visual stimuli and Experimental Design	92
4.2.2 Data Analysis	93
4.3 Results	96
4.3.1 Task Differences	96
4.3.2 Directional Selectivity of Individual Purkinje Cells During Pursuit and Saccades	97
4.3.3 Directional selectivity at a population level during pursuit and saccade trials	102
4.3.4 Kinematic sensitivity of Individual Purkinje Cells during Pursuit and Saccade Trials	106
4.3.5 Kinematic sensitivity at a population level during pursuit and saccade Trials	109
4.3.6 Discussion	114

5. Discussion	115
5.1 Core Findings.....	115
5.2 Conclusions and future lines of research.....	119
References	125
Biography.....	136

List of Tables

Table 1: Summary of statistical tests on firing rates across three intervals	38
Table 2: Classification of Neurons on the basis of their firing rate during movement windows.....	43

List of Figures

Figure 1: A, Eye position trace for rightward pursuit (smooth line) against target position (dashed line). B, Eye velocity trace for rightward pursuit (smooth line) against target velocity (dashed line). C, Eye acceleration trace for rightward pursuit with three relevant intervals highlighted. FW = fixation window (grey), AW = acceleration window (green), SW = sustained window (red).	34
Figure 2: Firing rate of an example Purkinje cell for pursuit in eight directions. This example neuron preferred down-left pursuit reaching peak firing rate during the acceleration interval, before settling at a constant rate of firing rate during the sustained window.	35
Figure 3: A, Average firing rates in the acceleration window of an example Purkinje cell as a function of pursuit direction. Smooth lines denote von mises tuning curve fits, dashed lines denote the average fixation interval firing rate. B, A second example of tuning, generated from a second Purkinje cell's simple spike response during the acceleration interval.	36
Figure 4: A,C The distribution of simple spike preferred directions as determined during the acceleration and sustained windows respectively, calibration bar indicates number of cells with tuning in a given direction. B and D, Directional sector widths for these same windows of time.	40
Figure 5: A, Preferred direction for all neurons, calculated in the acceleration window, relative to the preferred direction calculated from the firing rates in the sustained window. B, Difference in directional sector widths between the sustained and acceleration windows.....	41
Figure 6: Complex spike tuning of Purkinje cell from Figure 1. Neuron responded with the highest spiking probability towards movements down and to the left.	44
Figure 7: A, Distribution for preferred directions for Purkinje cell complex spikes assessed during the open loop interval of pursuit. B, Distribution of directional sector widths of Purkinje cell complex spikes.	46
Figure 8: A, Preferred direction of simple spikes, assessed in the acceleration window and plotted relative to CS preferred direction. B, Preferred direction of simple spikes, assessed in the sustained window plotted relative to CS preferred directions.....	47

Figure 9: A, Example velocity in the learning direction during the 3rd and 150th learning trials. Dashed lines indicate an instruction interval used to assess the state of learning. B, The time course of learned changes in eye velocity in the pursuit (blue) and learning (direction) averaged across 75 learning sessions. C, Summary of differences between average eye velocity in a prelearning block and during the last 20 trials of learning, with pursuit direction eye velocity in blue and learning direction eye velocity in red.50

Figure 10: Representative tuning curve from one session of learning. For this session, we defined the pursuit direction of our learning trials as downward, and the learning direction rightward. This was to maximize the change in firing rate between the pursuit direction (in black) and the prediction direction (dark green and between pursuit and learning directions). This is an example of ON learning.52

Figure 11: A, Behavioral learning during an example session. In blue we illustrate eye velocity during a prelearning block where the target moved in the pursuit direction only. Compare this to eye velocity acquired after learning (in red). B, Firing rate in the prelearning block and after learning (blue and red curves respectively). C, Example session learning curve that shows changes in firing rate (relative to the pre-learning block) over the course of sets of 20 learning trials.54

Figure 12: A, Average instruction interval firing rate changes over the course of learning, relative to prelearning block firing rates, calculated separately across all ON (blue) and OFF (red) learning sessions. B, For individual sessions, average instruction interval firing rate in the prelearning block is plotted against the average instruction interval firing averaged over trials 140-160 in the learning block.....55

Figure 13: A, Peak complex spiking response during the first 20 learning trials, arranged according to the time of peak CS probability. B, Learning curve showing that on average CS activity is stable over the course of learning. C and D Plots of CS probability in the tuning block against complex spike probability in the learning block. CS probability in the tuning block separately assessed for trials requiring tracking targets in the pursuit direction (C) or tracking targets in the learning direction (D)57

Figure 14: Trials were separated according to whether the complex spike activity during eye movements in the pursuit direction exceeded complex spike activity during eye movements in the learning direction (A) or vice versa (B). C, D show the average firing rate across Purkinje cells in our population divided in this manner. Green curves illustrate the average response after learning, while blue curves illustrate the average response in the prelearning block.59

Figure 15: A, Average position (smooth line) and target position (dashed line) over time. B Average velocity (smooth line) and target velocity (dashed line) over time. C, Average acceleration over time. We mark two intervals that we analyzed in depth below, “f” is a fixation interval. “i” is the interval encompassing the initial acceleration of the eye.70

Figure 16: A, An example raster from a Purkinje cell recorded in the oculomotor vermis. Each tic mark corresponds to one spike during a trial arranged in rows. B, Voltage trace from one trial, with complex spike indicated below. C, Distribution of fixation interval firing rates between the floccular complex (FLc) and oculomotor vermis (OMV). D,E same but for CV and CV2 values.72

Figure 17: A, B Examples of linear regression fits to a Purkinje cells recorded in the floccular complex and OMV respectively. The closeness of the red and black lines indicates the excellent fits provided by the regression model to these cells. Other colors indicate the amount of average firing rate in each cell which is accounted for by the time varying changes in position, velocity, and positive acceleration. C, D distribution of R2 values for all neurons in each population.75

Figure 18: A, B, C regression coefficients for velocity, positive, and negative acceleration plotted against position. Each point signifies one neuron recorded in either the floccular complex (FLc) or oculomotor vermis (OMV). D-F, distribution of regression coefficients displayed independently using histograms.77

Figure 19: A, Trial by trial variations in eye speed during an example session. Thin traces signify eye speed on individual trials, black trace represents the average of the thin traces. B, Simultaneous trial-by-trial variations in firing rate that were recorded from a Purkinje cell during this session78

Figure 20: A, Trial-by-trial correlations between eye speed and firing rate. Each pixel indicates the size of a pearson correlation coefficient calculated between firing rate at time t on the x axis, and eye speed at time t on the y axis. Data are averaged across all floccular complex Purkinje cells. B, C same, but for OMV neurons separated according to whether they increased or decreased responses during the first 225 ms of pursuit80

Figure 21: A-C, Plots of pursuit speed in an example session, separated according to the upper and lower third percentiles of gain, latency, and direction respectively. D-F, Corresponding average firing rates in the same session, averaged across trials in A-C. .82

Figure 22: A, The correlation between an example FLc neuron’s firing rate with the trial-by-trial variations in gain, latency, and direction respectively. B, C Fraction of neurons in

in the FLc and OMV with significant correlations with gain, latency, and direction. Black horizontal lines indicate expected level of type I error.	83
Figure 23: A-C Example position, velocity, and acceleration traces during saccade trials. D-F, Example position, velocity, and acceleration traces during a rightward set of pursuit trials. Dashed lines indicate target position, smooth lines indicate eye position, velocity, or acceleration.	97
Figure 24: A, B Simple spikes recorded from an example Purkinje cell during both pursuit (A) or saccade (B) trials. Direction of the movement is indicated by the arrows on the left. Each tick mark represents one spike on one trial (arranged in rows). This particular neuron was inhibited during leftward (contralateral) pursuit, and rightward (ipsilateral) saccades.....	99
Figure 25: A, Distribution of preferred directions calculated separately from pursuit (red) and saccade (gray) trials. B, The same, but only for neurons that were significantly responsive to both saccade and pursuit. C, For jointly modulated neurons, the distribution of saccade preferred directions relative to pursuit preferred directions. D, The cumulative distribution describing the size of the dispersion ratio for the subpopulation of jointly modulated neurons.....	101
Figure 26: A, Population responses during saccade trials with neurons organized according to their saccade preferred direction. B, Population responses during pursuit trials with neurons organized according to their pursuit preferred direction. Arrows indicate direction of eye movements relative to the preferred direction (illustrated in red). C, D Firing rates across target directions assessed at dashed lines in panels A and B.	104
Figure 27: A, B Population response during pursuit trials when all trials are aligned pursuit and saccade preferred direction respectively. D, E same but for population response to saccade trials. C, F Population tuning curves, during pursuit and saccade trials, when neurons are organized along their saccade and pursuit preferred directions respectively.....	106
Figure 28: A, B Example median fits to firing rates using regression model. C distribution of R^2 values showing the percentage variance accounted for by the regression model in each neurons' preferred direction.	108

Figure 29: A-C Contribution of position (A), velocity (B), and acceleration (C) coefficients to firing rate in during movement initiation in saccade trials (horizontal axis) vs pursuit trials (vertical axis).....109

Figure 30: A, Regression fit to population average firing rate in pursuit trials (neurons aligned to pursuit PD). B, Regression fit to the population average firing rate with during saccade trials (neurons aligned to saccade PD).....110

Figure 31: A,B Average of 50 bootstrapped population responses for both pursuit and saccade trials. Gray shading is +/- 1 SEM. C, Peak firing rate of populations during pursuit trials contributed by acceleration vs peak actual firing rates (resting rate subtracted) D, Peak firing rate of pseudopopulations during saccade trials contributed by velocity vs peak actual firing rates (resting rate subtracted). Each point is generated from one pseudopopulation, that contributed to the average firing rates illustrated in figures A and B.....113

Acknowledgements

“I am who I am because somebody loved me, somebody cared for me” – Cornel West

I want to thank my mother and father, who put up with me during the PhD process and supported me throughout. Together with my sisters Tara and Deepa, who helped me move to Durham six years ago, none of this would be possible. I owe a tremendous deal to Steve Lisberger, who guided me through the work that is presented in these pages. He taught me how to think about problems, and I pray I never forget those lessons. Marc Sommer was another savior. He lifted me out the lowest point in my life, that I hit in my second year and gave me his lab to call a home. In that lab I learned to do deep structure electrophysiology, microstimulation, and most importantly present data. Within Steve’s and Marc’s labs many people played a critical role in my intellectual development. Vincent Prevosto in Marc’s lab taught me to record and the importance of neuroanatomy, and was a good shoulder to cry on. Kesh Rao, was my colleague, friend, and good late night work partner. Mati Joshua in Steve’s Lab helped me set up the experiments described below from nuts to bolts, and taught me how to work efficiently. Yan Yang in Steve’s lab taught me how to record Purkinje cells so she is now and forever my scientific sister. I worked for a year in Miguel Nicolelis’s lab, and in his lab Mikhail Lebedev in particular taught me a tremendous deal about motor physiology, somatosensory physiology, and most importantly forced me to think big.

I owe quite a bit to Stefanie Tokiyama in the Lisberger lab and Jessi Cruger in the Sommer lab. I wish I could put into words how critical they were to my thesis work. As lab managers they provided more than technical assistance, they were advisors in at multiple stages of my professional development, and helped me through any and all of my personal struggles in graduate school. To me they are family.

I had the luck of making some great friends over the last few years. Mark and Anders were always there to commiserate with me on life in neuroscience and in life in general. Hannah helped keep me sane, and was always up for interesting discussions on scientific philosophy, politics, history, and every other topic under the sun.

Finally, I want to thank the Neurobiology Department at Duke and the brave members of the admissions committee who decided to accept a student with no neuroscience background into the program. You took a chance on me and I hope I have lived up to your expectations.

1. Introduction: Why study eye movements?

Multiple types of eye movements act to place or stabilize the fovea of the retina on objects in our environment. These movements can be very precise and low-dimensional motor behaviors (Osborne, Lisberger et al. 2005) and this precision is the result of a diverse set of circuits that, with high fidelity, convert visual signals into the set of axial torques required to move the eyes.

Combined with several other simplifying features, the low dimensionality associated with eye movements have made the oculomotor circuitry amenable to systems level analysis. Research into the oculomotor system was inaugurated by the quantification of the signals carried by primary motoneurons innervating the eye muscles during various eye movements, and has since proceeded to systematically move backwards, synapse by synapse, attempting to form a similarly rigorous quantitative description of the transformations occurring at each premotoneuronal level with reference to its inputs and outputs. As a result, both the signals of primary motoneurons and premotoneuronal populations in the brainstem are well characterized for multiple types of voluntary eye movement (Robinson 1970, Sparks 2002, Joshua, Medina et al. 2013). Comparable work on other major motor systems, such as those governing locomotion and forelimb movements, has been hampered by technical difficulties associated with recording the signals of motoneuronal and premotoneuronal populations in the spinal cord simultaneously with a relevant behavior (Robinson 1986).

These facts make the oculomotor system an ideal model motor behavior for investigating questions of motor control and learning.

Using eye movements to investigate general principles underlying motor control and learning often overshadows two other reasons that make studying the oculomotor system so important. The first concerns the critical role the oculomotor system plays in guiding visual processing. Research suggests that primate vision relies on a sophisticated network of visual circuitry (Van Essen, Anderson et al. 1992), where each component plays a functional role in constructing the rich picture of the world primates perceive. However, this diversity in neural circuitry underlying the processing of visual scenes is paralleled by an equally impressive array of motor areas dedicated to the control of eye movements, distributed across cortical and subcortical structures (Krauzlis 2004). The fact that high acuity visual information necessary for visual analysis is conveyed by only 1% of retinal real estate (associated with the fovea) suggests that understanding the mechanisms by which the oculomotor system directs this “foveal spotlight” is important to understanding visual perception. Indeed, perception and eye movement mechanisms are inextricably linked, and eye movement systems are hypothesized to optimally sample the visual scene in a manner best suited to perceptual processing (Gegenfurtner 2016).

A second benefit to studying oculomotor system concerns the partially conserved structure of gaze stabilizing networks across multiple species. While there

are critical physiological, behavioral and anatomical differences that distinguish the primate oculomotor system from similar systems in the rodent, rabbit, cat, or zebrafish (Carpenter 1988), the systems are similar enough that they allow researchers to leverage the benefits of each model system (behavioral repertoire, physiological accessibility, tractability of manipulations) to come to a better understanding of the function of oculomotor control across systems (Joshua and Lisberger 2015).

The work contained within this thesis follows in the tradition of exploiting the simplifying features of the primate oculomotor system in order to investigate functional role played by the cerebellum in generating such movements. Eye movements have historically offered a unique window into the operation of cerebellar circuitry (Robinson and Fuchs 2001), and what follows builds on this work. Of the many questions the oculomotor researcher faces in studying the cerebellum, none is more pressing than the characterization of the functional roles played by apparently distinct regions of the cerebellum in coordinating eye movements. It is known that multiple substructures of the cerebellum play a role in voluntary eye movement control (Simon, Iain et al.). Arguably, the best understood of these regions is the floccular complex. Evolutionarily, the floccular complex is one of the oldest regions of the cerebellum and its role in the control of smooth pursuit eye movements is well-established (Robinson and Fuchs 2001). A less understood oculomotor subregion of the cerebellum is the oculomotor vermis, the chief subject of the following experimental work. While there is a rich history

describing its anatomical connectivity (Voogd, Schraa-Tam et al. 2012) and a number of its functional properties (Simon, Iain et al.), a number of questions regarding its role in voluntary eye movement control remain. It is these questions I attempt to address in the chapters presented below.

At a more conceptual level, I see what follows as an attempt to probe an assumption underlying a great deal of cerebellar research. This assumption rests on the fact that while the cerebellar cortex itself is a large place, its circuitry is relatively simple. If you were to take a small 100 square-micron cube of cerebellar cortical tissue, for example, it would be nearly impossible to determine from which lobule of the cerebellar cortex it came from. Drawing inspiration from this repeated architecture, most theories of cerebellar function suggest that the cerebellar cortex is performing some “canonical” computation with this circuitry, with different regions processing their inputs in exactly the same way before transmitting these signals via their output pathways. More specifically multiple lines of evidence have suggested that the cerebellar cortical microcircuitry acts as a timer, a predictive machine, a device for motor learning, or some combination of all three (Raymond, Lisberger et al. 1996, Mauk, Medina et al. 2000, Ivry and Spencer 2004, Bastian 2006). While provocative, there remain a few impediments to determining the validity of these claims. Most studies of the cerebellum pick one area like the ansiform lobule, the floccular complex, or the eyeblink conditioning regions of the paramedian lobule and study them in depth. But processing of any one motor

behavior is not so easily restricted to one site of the cerebellar cortices. That's clear for oculomotor control, as discussed above, but it seems to also be the case for forelimb control (Kelly and Strick 2003) and for simpler movements like eye blink conditioning (Green and Steinmetz 2005). However, almost no work has been undertaken to see what differentiates these areas, particularly in regards to the neural signals in these regions. One would like to know whether these regions process information in a similar way or not, and comparisons based solely on anatomy or the effects of lesions place limits on the inferences we can draw. Even when multiple sites of the cerebellar circuitry have been studied, they have typically been examined in different contexts. For example, restricting ourselves to the study of eye movements, studies of the floccular complex have almost entirely focused on its contribution to smooth pursuit eye movements or the vestibulo-ocular reflex, whereas those in the oculomotor vermis almost always focus on its contribution to saccadic eye movements. Without studying the contribution of both structures during the same behavior, however, one cannot test whether they are performing the same function.

The first two chapters of my thesis seek to address this overall conceptual limitation in cerebellar research, by providing a quantitative dataset of response properties in the oculomotor vermis during the execution of smooth pursuit eye movements that can be more easily compared to previously published work on the floccular complex.

With this goal in mind, I define smooth pursuit eye movements at a behavioral level below. This will help clarify the computations the brain needs to perform in order to correctly execute such movements. I then move on to describe current understanding of the brain circuitry implicated in driving pursuit eye movements, with a focus on the cerebellum. Finally, I present experiments and quantitative analysis aimed at understanding the role the oculomotor vermis plays in encoding parameters of smooth pursuit during movement execution and adaptation. These experiments were designed in order to contrast recorded responses to previously published data in the floccular complex, and whenever appropriate, I attempt to quantify these differences.

The last chapter of my thesis concerns a very different conceptual problem in cerebellar research, namely the capacity of the cerebellar circuitry to accommodate the large operating range of the eye speeds. As I will describe more in depth below, eye movements come in two forms, saccades and smooth pursuit. These two types of movements have a very different range of operating speeds, with saccades being ballistic (fast) movements, while pursuit movements being continuously controlled (slow) movements. However, there are multiple sites in the oculomotor system where these two behaviors seem to be driven by the same set of neurons (Krauzlis 2004). In the oculomotor vermis, for example, prior reports suggest that one can find neurons responsive to both pursuit and saccadic eye movements (Sato and Noda 1992). This is a useful context, therefore, to probe the capacity of single cerebellar neurons to

accommodate multiple types of movement profiles. This is an important question because eye movements are not the only instance in which an effector needs to accommodate a large range of operating speeds. Forelimb movements also are classifiable into ballistic or slow movements (Desmedt 1978), and therefore study of this problem in the context of eye movement control may provide general principles that can be applied to other regions of the cerebellar circuitry responsible for the control of forelimb movements. Because of this secondary goal of my thesis work, below I also detail the behavioral and anatomical architecture of the saccadic eye movement system in the same way I do for the smooth pursuit eye movement system.

1.1 Behavioral characteristics of voluntary eye movements

Psychophysically, one can identify five to six types of eye movement, but only two are subject to voluntary control. These are smooth pursuit eye movements, utilized to foveate moving objects, and saccadic eye movements, utilized to foveate stationary or moving objects (Krauzlis 2005). While both systems need to be coordinated during natural tracking behavior, their behavioral differences are stark enough to consider them separately (Lisberger, Morris et al. 1987).

1.1.1 Behavioral characteristics of smooth pursuit eye movements

Smooth pursuit eye movements are smooth rotations of the eye that occur when a primate attempts to track a moving target across its visual field. Motion is a necessary stimulus to evoke smooth pursuit eye movements, and smooth movements of the eyes

cannot be voluntarily initiated or sustained by most primates including humans (Lisberger, Morris et al. 1987). In the laboratory, a common procedure for eliciting smooth pursuit eye movements is called the *Rashbass paradigm*. In a typical variant of this paradigm, an individual or animal begins by fixating on a point of light. After a randomized interval the target steps away from the ultimate direction of pursuit and begins to move at a constant velocity. At a latency of between 65-130 ms (Lisberger, Morris et al. 1987) the eye accelerates and begins to track the moving target. In the absence of the target step, the eye first makes a fast a saccade in the direction of the moving object before switching to smooth pursuit. The Rashbass paradigm conveniently illustrates the types of sensory signals that drive smooth pursuit eye movements and saccadic eye movements. As the target steps away from its initial position, it creates a mismatch between two signals, the target position (which initially moves away from target motion direction) and target velocity (which moves in the target motion direction). The fact that this stimulus drives initiation of smooth pursuit as opposed to saccades, illustrates that the dominant sensory drive for pursuit is target velocity, which is capable of overwhelming concurrent target position signals (Rashbass 1961). Further research has shown that target position is not entirely without effect, but exhibits a more modulatory influence on pursuit eye movements initiated by this paradigm (Lisberger and Westbrook 1985, Orban de Xivry and Lefevre 2007).

In identifying the primary sensory drive to the pursuit system, research has settled on conceptualizing the pursuit system as a textbook example of negative feedback control. In this scheme of control, target motion, sensed and represented by the visual system, acts as an error signal that the movements of the eyes seek to counteract (Carpenter 1988). Often, researcher focuses on the first 65-130 ms of pursuit elicited by the rashbass paradigm, which occurs 165-230 ms after target motion onset. Not only is this period of time unlikely to have initial targeting saccades due to the nature of the rashbass paradigm, it represents a period of time when the eye is moving open loop relative to target motion and becomes a clearly defined sensorimotor transformation (Lisberger, Morris et al. 1987). As soon as this period ends, however, target motion sensed by the visual system is determined by the variable speed of the eye during “open loop interval,” and the experimenter loses control over the behavior, and is left to only characterize the global properties of the closed loop system being studied.

What has been presented thus far is a skeletal view of the pursuit systems’ rich psychophysics. A full discussion of pursuit psychophysics is the scope of the current work. However, one additional capability of the pursuit system needs to be mentioned, namely its capacity to adapt to visual contingencies. In the laboratory this can be demonstrated by having animals or humans pursue targets that undergo predictable changes in speed (Kahlon and Lisberger 1996) or direction (Medina, Carey et al. 2005).

The pursuit system learns to anticipate these changes and pursuit kinematics change in a way that improves subsequent target tracking.

1.1.2 Behavioral characteristics of saccadic eye movements

The second class of voluntary eye movements are fast (or ballistic) movements of the eye called saccades. The goal of saccades is to place the fovea of the eye at different locations in the visual periphery. They exhibit a greater degree of voluntary control than smooth pursuit eye movements as they can be executed volitionally in absence of any stimulus (Carpenter 1988). Saccades are believed to be driven by a central representation of target position error (Lisberger, Morris et al. 1987). Two sources of evidence suffice to illustrate this fact. The first is the relative ease by which saccades can be directed towards visual targets that undergo sudden steps from the point of fixation. The second comes from the rashbass paradigm, where it is possible to contrive a situation where the target lags the eye during the initiation of pursuit. In instances where pursuit is initiated in response to target motion in a manner that causes the eye to lead target position, subsequent corrective saccades are made which occur in the direction opposite to the direction of pursuit to correct for the resulting position error. A second relevant behavioral characteristic of saccades is their high speeds which can reach a peak velocity up to 1000 degrees per second (Keller 1974). This renders the duration of most saccadic eye movements less than their minimally observed latency, which is 80 ms for so called "express saccades" (Sparks, Rohrer et al. 2000). This

mismatch suggests that continuous control of saccades by sensory feedback is nearly impossible, implying that saccades must be executed in an open loop manner, in contrast to the smooth pursuit eye movements discussed above.

1.2 Anatomical substrates underlying voluntary eye movement control

A combination of single cell recordings, targeted lesions or inactivations, and clinical observations have charted many of the cortical and subcortical networks which implement the voluntary control of eye movements (Leigh and Zee 2006). Just as the two forms of oculomotor control, saccades and smooth pursuit eye movements, seem to share differing behavioral characteristics with some notable interactions, the oculomotor networks known to play a role in these two behaviors seem rather separate, with some notable interactions (Lisberger, Morris et al. 1987). Below I shall present an admittedly cerebello-centric view of the neuroanatomy of the pursuit and saccade systems. For pursuit, this description is fairly accurate, as the cerebellum serves as a critical bottleneck through which sensory and motor signals can initiate pursuit. By contrast, sensory and motor signals can influence saccade initiation via two parallel pathways, one through the cerebellum and the other through the superior colliculus.

1.2.1 Functional anatomy of the smooth pursuit eye movement system

As discussed above, the driving input to the pursuit system seems to be errors in target motion. In the visual system, evidence suggested that two regions of the dorsal

stream, the middle temporal (area MT) and medial superior temporal (area MST), provide the requisite target motion error signals required to drive the pursuit system (Lisberger 2010). These feedforward sensory signals seem to be subject to modulation or gain control, implemented by the pursuit subregions of the frontal eye fields and lateral intraparietal area (Lisberger 2010, O'Leary and Lisberger 2012).

These visual and visuomotor cortical signals are relayed via interneurons in the pontine nuclei, nucleus reticular tegmentis pontis (NRTP), or inferior olive to various regions of the cerebellar cortex and deep cerebellar nuclei (Voogd, Schraa-Tam et al. 2012). Ultimately the cerebellum acts as a critical final bottleneck in conveying efferent motor commands that drive pursuit. Evidence for this comes from the observation that cerebellectomized animals cannot produce smooth pursuit eye movements (Westheimer and Blair 1973).

The main efferent pathway for horizontal and vertical pursuit seems to involve neurons in the vestibular nuclei and Y group that receive input from the cerebellar cortices and project onto motoneurons that innervate the horizontal and vertical eye muscles respectively (Chubb and Fuchs 1982, Voogd, Schraa-Tam et al. 2012, Joshua, Medina et al. 2013). Complementary input is provided by two structures, the nucleus prepositus hypoglossi (NPH) and the interstitial nucleus of cajal (INc) (Fukushima 1991, Keller and Heinen 1991) that are connected in feedback loops with the vestibular nuclei and Y group respectively. Other sets of brainstem interneurons that receive cerebellar

input reside in the central mesencephalic reticular formation, superior colliculus, and subregions of the paramedian pontine reticular formation. While traditionally implicated in saccade control, these regions have also been implicated in modulating pursuit eye movements (Missal and Keller 2002, Krauzlis 2004, Ugolini, Klam et al. 2006).

1.2.2 Functional anatomy of the saccadic eye movement system

The basic anatomy of the networks of the brain that involve the cerebellum and influence saccadic eye movements parallel in many ways those that influence pursuit (Krauzlis 2004). Visual signals that carry target position information are found across multiple regions in the prestriate and striate cortex, as well as across the dorsal stream. Like their target motion analogues, target position signals are subject to modulation by networks in the frontal (Tehovnik, Sommer et al. 2000) and parietal lobe (Bisley and Goldberg 2003), and ultimately converge at the level of the pontine nuclei, NRTP, and inferior olive (Voogd, Schraa-Tam et al. 2012). Projections from these structures terminate across divisions of the cerebellum discussed below. From the cerebellum, two efferent pathways exist by which signals can ultimately reach the eye muscle. The first involved direct projections to premotoneurons in the vestibular nucleus, y group, paramedian pontine reticular formation, and central mesencephalic reticular formation (Ugolini, Klam et al. 2006) that together influence vertical and horizontal saccadic eye movements. An additional efferent pathway links many regions of the cerebellum in a

feedback loop with the superior colliculus (May, Hartwich-Young et al. 1990), a structure presynaptic to interneurons in the PPRF that is critically involved in saccade initiation (Sparks 2002). As discussed above, the colliculus is more than a simple relay for cerebellar efferent commands, but is capable of integrating information from diverse cortical areas, the basal ganglia, and the cerebellum and initiating saccadic eye movements via its access to oculomotor premotoneuronal populations. This may account for the fact that saccades can be initiated after cerebellectomy (Westheimer and Blair 1973).

1.3 The contribution of the cerebellum to voluntary eye movement control

Hereto, I have described the cerebellum as a single block of neurons which integrates visual and visuomotor inputs and drives premotoneuronal activity through its outputs. However, this view belies a more elaborate structure to the cerebellum that I have yet to introduce. For example, within the cerebellum, there exists a major division between the cerebellar cortex and deep cerebellar nuclei. The former is the predominant target of inputs from the pontine nucleus, NRTP, and inferior olive and sends inhibitory projections to the deep cerebellar nuclei via its output neurons, Purkinje cells. It is these target neurons, within the deep cerebellar nuclei, that ultimately project to premotoneurons or motoneurons innervating the eye muscles (along with a host of other targets). Moreover, there are four deep cerebellar nuclei that each receive unique input from separate regions of the cerebellar cortex. In this way the medial, intermediate,

hemispheric, and flocculonodular lobes of the cerebellar cortex project to the fastigial, interpositus, dentate, and vestibular nuclei respectively. Each deep cerebellar nucleus can in turn be defined by subregions that receive input from specific “lobules” that compose each division of the cerebellar cortex (Voogd, Schraa-Tam et al. 2012).

To describe the oculomotor cerebellum, therefore, is to revise the monolithic description offered beforehand and to describe a patchwork of areas across the cerebellar cortices and deep cerebellar nuclei, that integrate input emanating from visual and visuomotor areas across the rest of the oculomotor system and target brainstem nuclei that ultimately drive eye movements. There are multiple such oculomotor lobules of the cerebellum (Simon, Iain et al. , Voogd, Schraa-Tam et al. 2012). In the next two sections I describe the functional anatomy of two of these regions, the floccular complex and oculomotor vermis. Furthermore, I review the properties of input and output signals in these regions, as determined by prior studies, and end by describing a set of experiments performed in my thesis work aimed at filling gaps in our current knowledge of output signals conveyed by the oculomotor vermis.

1.3.1 Functional anatomy and physiology of the floccular complex

The floccular complex consists of one of the oldest regions of the cerebellar cortex, and targets brainstem neurons (also referred to as floccular target neurons) in the vestibular nucleus and γ group. Inputs to the floccular complex are provided by regions of the dorsolateral pontine nucleus (Langer, Fuchs et al. 1985) and the dorsal and rostral

caps of the inferior olive (Voogd, Schraa-Tam et al. 2012). Additional inputs are provided by the nucleus prepositus hypoglossi (Belknap and McCrea 1988). Lesions of the floccular complex (Zee, Yamazaki et al. 1981, Rambold, Churchland et al. 2002) strongly impair multiple parameters of pursuit, including the initial acceleration of the eye and its velocity during pursuit maintenance.

Physiologically, mossy fibers, the axons of neurons projecting to the floccular complex the NRTP, DLPN, or NPH, are driven by changes in eye position, initiation of saccades and pursuit (Lisberger and Fuchs 1978, Miles, Fuller et al. 1980), or visual motion (Noda 1981). Purkinje cell simple spikes closely match the kinematics of eye movements observed during pursuit (Shidara, Kawano et al. 1993, Lisberger 2009). Moreover, simple spikes in the floccular complex exhibits strict directional tuning, with increases in response frequency for movements occurring only in the horizontal or downward plane (Krauzlis and Lisberger 1996). Complex spikes, driven by input from the inferior olive, convey visual information related to the retinal slip of image motion across the eye (Stone and Lisberger 1986) and also share strict directional organization, in a manner opponent to tuning of simple spikes (Stone and Lisberger 1990). The directional organization of these signals is not simply a convenient statistical description of floccular output. Rather, it seems well aligned to the pulling direction of eye muscles and so seems to exist in a format well suited to drive motor output (Krauzlis and Lisberger 1996). Signals from the floccular complex are sent to premotoneuronal

populations in the vestibular nucleus or interstitial nucleus of cajal. Responses in these target structures have been studied in depth and are found to be very similar in character to what is found in the floccular complex (Fukushima 1991, Joshua, Medina et al. 2013).

1.3.2 Functional anatomy and physiology of the oculomotor vermis

The oculomotor vermis is defined as the region of the medial cerebellar cortex from which eye movements can be reliably evoked via microstimulation and where background neural activity is vigorously modulated by spontaneous eye movements (Noda and Fujikado 1987). It corresponds to lobules 6c, 7a, and 7b of the vermis and projects to the caudal edge of the fastigial nucleus (Voogd, Schraa-Tam et al. 2012). From the caudal fastigial nucleus two efferent pathways terminate on interneurons in the paramedian pontine reticular formation or in the intermediate layers of the superior colliculus (Voogd, Schraa-Tam et al. 2012). Additional output projections from the caudal fastigial nucleus terminate in the pontine nuclei, NRTP, and the cMRF (Noda, Sugita et al. 1990). Mossy fiber inputs to the oculomotor vermis arise from both the dorsomedial and dorsolateral pontine nuclei, as well as the NRTP and NPH. Climbing fiber inputs to the oculomotor vermis arise from subnucleus b of the caudal medial accessory olive (Voogd, Schraa-Tam et al. 2012). Lesions of the oculomotor vermis result in deficits in both smooth pursuit eye movements and saccades (Takagi, Zee et al. 1998, Takagi, Zee et al. 2000).

Physiologically, mossy fiber inputs to the OMV are quite similar to those in the floccular complex. They fire in relation to saccadic eye movements, position of the eye in orbit, and visual motion. This is not all that surprising considering the substantial overlap in pontine nuclear inputs between the oculomotor vermis and floccular complex. Purkinje cell activity in the OMV is known to be modulated by pursuit with some reports suggesting that this activity encodes movement kinematics during the initiation of pursuit (Dash, Catz et al. 2012). Climbing fiber inputs have been shown to respond to small position errors (Soetedjo, Kojima et al. 2008) and it is unknown whether they can be driven by visual motion errors.

A number of questions exist as to the directional organization of signals in the OMV. While prior reports suggest that the preferred direction of simple spikes in the OMV is uniformly distributed (Thier, Dicke et al. 2000), these same reports did not examine the responsivity or directionality of complex spikes nor did they characterize their relationship with simple spikes. It is likely that climbing fiber inputs to the OMV encode visual motion, given pretectal inputs to the caudal medial accessory olive (Gamlin 2006), but no studies have tested whether this is the case. Recent studies suggest peak population climbing fiber responses (in response to small saccadic motor errors) are inversely correlated with peak population simple spike rates (Herzfeld, Kojima et al. 2015) during saccades, so we may also hypothesize a similar relationship

holds between potential complex spike responses to target motion and simple spike responses to pursuit onset.

The OMV is not simply dedicated to pursuit control, indeed it has traditionally been studied as a region of the brain which plays a role in the execution and plasticity of saccadic eye movements (Robinson and Fuchs 2001). Beyond the fact that saccades are easily evoked by microstimulation of the OMV, it is known that Purkinje cell activity in the OMV is strongly modulated during saccades and covaries with the duration of saccadic eye movements and eye speed (Suzuki, Noda et al. 1981, Herzfeld, Kojima et al. 2015). While, prior reports suggest that Purkinje cell simple spike responses in the OMV can respond to both pursuit and saccades (Sato and Noda 1992), it remains very unclear what the directional relationship between these signals are. Moreover, at present it remains unknown what aspect of movement kinematics OMV Purkinje cells are modulated by, and whether this is the same irrespective of whether a saccade or pursuit eye movement is being executed. Two pieces of evidence suggest that the vermis is manipulating a kinematic variable that is common to both types of movements. The first is that very similar kinematic deficits in saccades and pursuit are observed following lesions of the OMV or pharmacological disruption of the caudal fastigial nucleus (Robinson, Straube et al. 1993, Robinson, Straube et al. 1997, Krauzlis and Miles 1998, Takagi, Zee et al. 1998, Takagi, Zee et al. 2000). This second line of evidence comes from experiments where microstimulation was applied to the OMV while animals pursued

targets moving ipsilateral or contralateral to the site of stimulation. In the case of pursuit contralateral to the site of stimulation, large smooth pursuit-like increases in eye velocity were evoked during stimulation. In the case of pursuit ipsilateral to the site of stimulation or during fixation, fast saccade like increases in eye velocity were evoked. From both of these findings we may hypothesize that a directional organization of pursuit and saccadic responses in the OMV exists whereby similar kinematic variables are controlled along opponent directional axes.

1.3.3 Major anatomical differences between the floccular complex and oculomotor vermis

As stated above, one key goal of my thesis work is to contrast the role played by the oculomotor vermis in pursuit with the role played by the floccular complex. The first two chapters of my thesis present experiments aimed at addressing this goal. With regards to input pathways, the clearest difference between structures involves an additional input to the oculomotor vermis that is provided by the dorsomedial pontine nucleus. This structure relays efferent signals from the superior colliculus to the oculomotor vermis (Voogd, Schraa-Tam et al. 2012). With regards to output pathways, differences are larger. Beyond the fact that the OMV and floccular complex target different deep cerebellar nuclei, the efferent pathways of these target nuclei are very different as well. Ultimately, floccular complex Purkinje cells are 2 synapses removed from the motoneurons that innervate the eye muscles. By contrast, Purkinje cells in the OMV are at least 3 synapses removed from the motor periphery. It remains unknown

whether these differences in the anatomical structure of cerebellar output have any functional consequence, but as a result of the experimental results I present below I argue that they might.

1.4 Outline of the chapters presented henceforth

As discussed above, the primary goal of my thesis work was to generate a quantitative dataset of Purkinje cell responses in the oculomotor vermis **during smooth pursuit eye movements** that could facilitate comparison with previous studies of the floccular complex. Chapters 2-3 summarize experiments aimed at addressing this goal. A secondary goal of my thesis work was to understand how smooth pursuit eye movements and saccadic eye movements could be jointly encoded by neurons in the oculomotor vermis. Chapter 4 summarizes an experiment aimed at addressing this goal. All experiments involved recording Purkinje cell responses in the oculomotor vermis of monkeys performing a variety of eye movement tasks. In each chapter that follows, I introduce the motivation for each experiment, discuss the specific details of my experimental design, and present the results of my work. Each experimental chapter is followed by a brief discussion. The final chapter of this thesis is a more in depth discussion aimed at summarizing the results of all my experiments as well as outlining future avenues of research.

2.The directional organization of pursuit eye movement signals in the oculomotor vermis and their consequences for motor learning

2.1 Introduction

Within many brain regions that contribute to motor control, neurons exhibit a pattern of selectivity for movement direction. This pattern of activity can manifest itself in different ways, for example during the preparation for movements (Cisek and Kalaska 2002, Bastian, Schoner et al. 2003) or during their execution (Georgopoulos, Schwartz et al. 1986, Roitman, Pasalar et al. 2005). During movement execution, in particular, firing rates can vary as a function of movement direction in a very precise mathematical way (Georgopoulos, Kalaska et al. 1982). Such organization does not merely serve as a descriptive convenience for physiologists, as the statistical structure of such directional tuning has downstream consequences (Salinas and Abbott 1994, Pouget, Deneve et al. 1999) and therefore constrains the precision with which movements are executed (Todorov 2002). One key feature of the motor system for which directional tuning matters concerns its remarkable capability to predict and adapt to directional contingencies imposed by the external environment (Shadmehr and Mussa-Ivaldi 1994, Medina, Carey et al. 2005). Directional responses in motor areas seem particularly useful in predicting the capacity of those circuits to serve as sites of plasticity during motor learning (Gandolfo, Li et al. 2000, Medina and Lisberger 2008, Yang and Lisberger 2014).

An excellent example of this comes from studies examining the role of the cerebellum in driving adaptation of smooth pursuit eye movements. Smooth pursuit eye movements allow primates to foveate moving targets in their environment. They have many simplifying features that make them amenable to studying the neural processes that drive motor learning (Medina, Carey et al. 2005, Lisberger 2010). For example, when targets animals are tracking undergo predictable changes in direction, the pursuit system learns to anticipate these changes and attempts to use its past experience to reduce tracking errors. Accumulating studies have implicated a region of the cerebellum, the floccular complex (FLC), in driving this directional adaptation (Medina and Lisberger 2008, Yang and Lisberger 2014). The role of the FLC in driving directional adaptation is supported, in part, by the unique structure of FLC Purkinje cell directional tuning. The activity of most FLC Purkinje cells is organized into two channels, encoding horizontal and vertical eye movements. Directional selectivity is strong, such that firing increases largely for rightward, leftward, or downward pursuit with decreases in the opposite directions (Krauzlis and Lisberger 1996). Complex spikes, which convey afferent signals from the inferior olive to Purkinje cells, are tuned 180 degrees away from the preferred direction of simple spikes (Stone and Lisberger 1990). This structure seems optimally suited to drive trial-over-trial depression or potentiation in simple spiking that covaries strongly with and presumably drives simultaneous trial-over-trial adaptation in pursuit eye velocity (Medina and Lisberger 2008).

Quantitative analysis of FLc responses suggests during the initial phases of learning, FLc Purkinje cells play a dominant role in driving expression of learned behavior (Medina and Lisberger 2009, Yang and Lisberger 2014). If true, this predicts that sites outside the FLc in the cerebellum are unlikely to express learning, despite playing an important role in controlling eye movements. A natural place to test this hypothesis are the other major cerebellar lobules believed to play a key role in pursuit eye movement control (Simon, Iain et al.). The best understood oculomotor area of the cerebellum, outside the FLc, is a structure along the midline of the posterior cerebellum called the oculomotor vermis (OMV). Comprising lobules 6c and 7a and b of the midline cerebellar cortex, the OMV has been long hypothesized to play a role in the control of pursuit eye movements and their adaptation (Robinson and Fuchs 2001). The OMV receives input from areas considered necessary to drive pursuit including motion processing areas like area MT and motor cortical areas like the frontal pursuit area (FPA). These are areas that also project to the floccular complex (Voogd, Schraa-Tam et al. 2012). Lesions of the OMV impair pursuit eye movement gain and speed adaptation (Takagi, Zee et al. 2000), and Purkinje cells in the OMV are modulated during pursuit initiation and track kinematic changes during speed adaptation (Dash, Catz et al. 2012, Dash, Dicke et al. 2013). These findings suggest that if plasticity in pursuit eye movements is being driven by a cerebellar structure outside the FLc, the oculomotor vermis the best candidate.

To evaluate the likelihood of this hypothesis and to test its predictions, however, we first need to address some current gaps in our knowledge about the directional tuning of Purkinje cells in the OMV. Only one prior study has examined the basic structure of directional tuning of Purkinje cells in this structure (Dash, Catz et al. 2012). This study was limited, however in simply documenting the existence of directional tuning in the OMV. It did not specifically evaluate whether the directional tuning in the OMV would be sufficient to drive directional pursuit adaptation in a manner akin to the FLc. Moreover, this prior study left open to what degree climbing fiber inputs were organized onto single Purkinje cells, and how they were oriented relative to simple spike tuning.

In a bid to determine the structure of directional tuning in the OMV, we recorded the activity of Purkinje cells in the oculomotor vermis of macaque monkeys as they performed smooth pursuit eye movements. We evaluated the tuning properties of both the simple and complex spike activity of these Purkinje cells and discovered that in contrast to the FLc, tuning of OMV Purkinje cell simple spikes is more likely to be organized in graded manner over uniformly distributed preferred directions. Moreover, the structure of climbing fiber tuning in the OMV is not organized a manner conducive to driving directional adaptation, with the preferred direction of simple spikes not falling into any clear relationship with the preferred direction of complex spikes at either the single neuron or population level. From these findings we predicted that Purkinje

cells in the OMV were unlikely to track changes in behavior that occur over the course of directional adaptation. We tested this prediction explicitly by recording Purkinje cell responses over the course of directional adaptation, in the same way FLc Purkinje cells have been tested. We found, as predicted, that neurons did not show modulations in activity consistent with the behavioral changes observed during adaptation. We conclude from this that the oculomotor vermis likely lies outside the learning loop responsible for directional adaptation of smooth pursuit eye movements.

2.2 Methods

2.2.1 Subjects

Data for these experiments were collected from two male rhesus macaque monkeys (*Macaca mulatta*). Animals were surgically implanted with scleral search coils to track the movements of the eyes and a titanium headpost to restrain the movement of the head. Details of the surgical procedures used have been published in prior reports (Ramachandran and Lisberger 2005). After a period of initial training, where the animal learned to fixate on and track visual stimuli, animals were surgically implanted with chambers aimed at the oculomotor vermis. Chambers were placed on a 27-degree angle and off the midline in order to access the oculomotor vermis (chamber coordinates ML 0 AP -16) in order to avoid the possibility of hitting the sagittal sinus during neural recording. All surgical and behavioral procedures used in this study were approved of in advance of these experiments by the Institutional Animal Care and Use Committee

(IACUC) at Duke University and were in accordance with the National Institute of Health's *Guide for the Care and Use of Laboratory Animals*.

2.2.2 Visual stimuli and Experimental Design

Visual stimuli were presented on a Sony Barco CRT monitor placed 30-45 centimeters away from the animals' eyes. Stimulus control and data acquisition relied on custom built acquisition software and hardware used in our laboratory. Signals related to eye position in the horizontal and vertical plane were measured via a field coil and stored at a resolution of 1 KHz. Stimuli consisted of small round white dots less than half a degree in diameter that the animal was trained to fixate on and track. Experiments were conducted in a block design and all began with a white dot appearing on the center of the screen upon which the animal had to maintain fixation, enforced using a 2x2 degree invisible window around the dot. In tuning blocks, after a variable delay of 400-600 ms, the target would displace 3 degrees away from the direction of the target motion and begin moving for 750 ms. Following a grace period of 200 ms, the eye was required to track the target within a 2x2 degree window centered on the target. After 750 ms of motion the target underwent a 1-degree step in the direction of target motion. Animals were reinforced with either water or juice for completing trials successfully. Target motion for each trial was randomly selected from one of eight radially spaced directions, at 0, 45, 90, 135, 180, 225, 270, and 315 degrees. During some behavioral sessions, we also ran a directional adaptation paradigm utilized in prior

studies (Medina, Carey et al. 2005) that followed the tuning block. The structure of these experiments began similarly to those used in the tuning block, with a small white dot appearing on the center of the monitor cueing the animal's fixation. After a variable delay of 400-600 ms, the target would begin to move in a direction we term *pursuit direction*. After 250 ms however, the target would undergo an additional 30-degree component of motion in a direction orthogonal to the initial pursuit direction, which we term the *learning direction*. Pursuit and learning directions were selected on a session-by-session basis using criterion described in section 2.2.3. Animals were required to repeatedly track the direction of motion in these trials using a 2x2 degree invisible window centered on the target before direction change, and a 4x4 degree invisible window centered on the target after direction change. The same target motion was presented repeatedly, between 160-1000 times in a row. Over time both monkeys displayed evidence of pursuit adaptation as we detail in our results section.

In most sessions, prior to starting our learning block we had our monkeys track a target that moved solely in the pursuit direction for at least 20 trials. This served as a baseline against which we could calculate behavioral and neural related changes over the course of learning. We refer to these trials subsequently as a prelearning block.

2.2.3 Neural Recording

In each daily experiment a microelectrode (Alpha Omega) was lowered into the oculomotor vermis (about 20 mm beneath the surface of the dura) using a hydraulic

microdrive (Narishige MO-97). Microelectrodes were lowered from a guide tube positioned 2 mm above the tentorium of the cerebellum. In many experiments electrodes were coated using a dalic iron solution to reduce impedance (Sisco AFC). Electrode impedances, measured daily using an impedance meter (Bak Electronics), could range between 150 kOHMs to 3 mOHMs. In our experience Purkinje cell isolation was best when electrode impedance was between 500-800 mOHMs. The oculomotor vermis was identified by the vigorous background swishing activity related to spontaneous eye movements as previously reported (Noda and Fujikado 1987) and the presence of short lead saccadic burst Purkinje cells. Action potentials were monitored online and Purkinje cells identified as having both simple and complex spikes. Extracellular signals were recorded using a conventional amplifier (Dagan), filtered between 300 Hz and 5 KHz and digitized at 25 KHz. During any given experiment, we could isolate simple spike activity from Purkinje cells using an online window discriminator (Bak Electronics) and could store threshold crossings of these spikes as digital timestamps for online analysis. Upon locating a Purkinje cell, we would assay its directional tuning using a directional tuning task (described above). Per each Purkinje cell we would then select a pair of orthogonally oriented initial pursuit and learning directions with the largest firing rate difference between them. These would define the directions used subsequently during the learning block. Across both monkeys, we recorded 130 Purkinje cells (55 monkey V, 75 monkey Y) on our directional tuning task,

with at least 10 repetitions of target motion in each direction. Of these, 75 Purkinje cells were also run on a directional adaptation paradigm. All learning block cells were held for at least 160 learning trial repetitions, a period of time sufficient to induce strong behavioral adaptation as detailed below in section 2.3.4. For all but 6 cells used in the tuning analysis and 2 used in learning analysis we could maintain isolation on both simple and complex spike activity throughout our trials. Leaving data without consistent complex spike activity out of our analyses did not change our results and so we opted to include them in the results presented below.

2.2.4 Data Analysis

All data analysis was done using Matlab (Mathworks). As mentioned above extracellular signals and behavioral data were stored using custom acquisition software and imported into matlab or a custom made software suite for data analysis. For behavioral processing, this software suite allowed us to manually mark catch up saccades that occurred during smooth pursuit. We then exported saccade start and stop times to matlab for further analysis. Eye position traces were smoothed using a second order Butterworth filter with a cutoff at 25 Hz. We then numerically differentiated these traces to obtain eye velocity signals. In behavioral analyses presented below, both position and velocity data during saccades were excised from these behavioral traces by replacing them with NaNs. For neural preprocessing, simple spikes and complex spikes were detected using Spike2 (CED microsystems). Any complex spikes missed by this

initial sorting were manually marked afterwards. All Purkinje cells, for which both complex and simple spike isolation could be maintained throughout our protocol, were confirmed to have a post-complex spike pause in simple spikes at least 10 ms in duration.

Firing rates of simple spike activity during trials was calculated by taking the inverse of the interspike interval (Lisberger and Pavelko 1986). In figure 1, presented below we smoothed these firing rates with a median filter (matlab command `medfilt1`) with a window size of 10 ms. This smoothing was only done for presentation purposes; all analyses were performed on non-smoothed firing rates. Complex spikes were displayed in terms of probability measured in a sliding 100 ms window slide across time.

Most of our analysis focuses on firing rates occurring in three 200 ms wide windows. The first was a fixation window (FW) centered on the time 100 ms preceding target motion onset, and during which the monkey was required to actively maintain fixation in our task. The second was an acceleration window (AW) centered on a time 175 ms after target motion onset, during which the monkey was typically accelerating their eyes to match target motion. The final window was a sustained window (SW) centered 375 ms after target motion onset, during which the monkey maintained active pursuit of the moving target with near zero acceleration.

Preferred directions were calculated by taking the circular mean of data, averaged across one of the relevant windows (FW, AW or SW) across 8 target direction

conditions. Directional sector widths were defined as 2 times the circular standard deviation of average firing rates in one of these windows across our 8 target direction conditions. (Fortier, Smith et al. 1993). Prior studies have shown that firing rates in the cerebellum can be divided into two components. An unmodulated component that is defined as the minimum average response across movement conditions, and a movement component that is defined as the range of responses observed across directions. The directional sector width is very sensitive to the size of the unmodulated component of firing rates, a problem in the cerebellum where minimum response frequency can range from 50-100 Hz. Therefore, we calculated directional sector widths on the movement related components of firing rates, taking average firing rates across 8 conditions and subtracting off the minimum response.

2.3 Results

2.3.1 Psychophysics of Pursuit

In figure 1A we illustrate the sequence of events that comprise a rightward pursuit eye movement trial. Initially an animal is fixating on a central target. After a period of time the target undergoes a step away from the cite of fixation (note step in dashed line occurring at time zero in figure 1A) and begins to move at a constant velocity rightward. The eye compensates for this target motion by smoothly tracking the target (compare smooth to dashed lines in figure 1A). We can also illustrate the movement of the eye in other kinematic coordinates, such as velocity (Figure 1B) and

acceleration (Figure 1C). This is useful as it allows us to divide the initial response of pursuit into time windows that we shall refer to subsequently. In our directional tuning task, animals are required to actively maintain fixation prior to target motion. We term this the fixation window (FW), illustrated by the gray shading in figure 1C. The positive acceleration of the eye, towards the direction of target motion, is mostly contained within a 200 ms window centered 175 ms after target motion. We term this the acceleration window (AW), illustrated by the green shading in in figure 1C. This is followed by a brief period of time where the eye moves at a sustained velocity without strong acceleration. This period of time is roughly contained within a 200 ms window centered 375 ms after target motion onset. We term this the sustained window (SW), and illustrated by the red shading in figure 1C.

Animals pursued targets moving in 8 radially spaced target directions. We recorded Purkinje cell activity in the oculomotor vermis as animals performed this task and analyzed the directional selectivity of their complex and simple spiking activity. The analysis presented below examines average simple spike firing rates calculated in one of the aforementioned analysis windows.

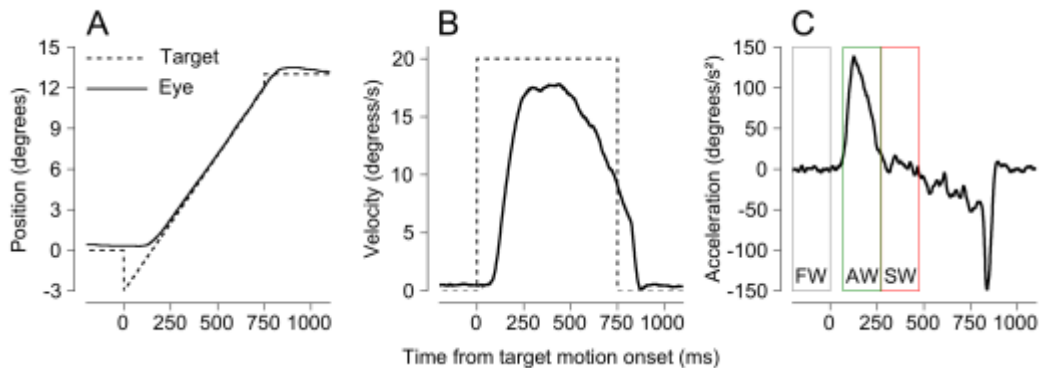


Figure 1: A, Eye position trace for rightward pursuit (smooth line) against target position (dashed line). B, Eye velocity trace for rightward pursuit (smooth line) against target velocity (dashed line). C, Eye acceleration trace for rightward pursuit with three relevant intervals highlighted. FW = fixation window (grey), AW = acceleration window (green), SW = sustained window (red).

2.3.2 Example response

Below, in Figure 2, is an example Purkinje cell recorded in the oculomotor vermis. More specifically, we show the average number of simple spike fired by this Purkinje cell over time and across 8 directions of pursuit. This example Purkinje cell's simple spikes responded maximally to pursuit eye movements executed towards the lower left quadrant of the screen, with a peak firing rate of 150 spikes/s in the acceleration window and a peak firing rate of 100 spikes/s second in the sustained window.

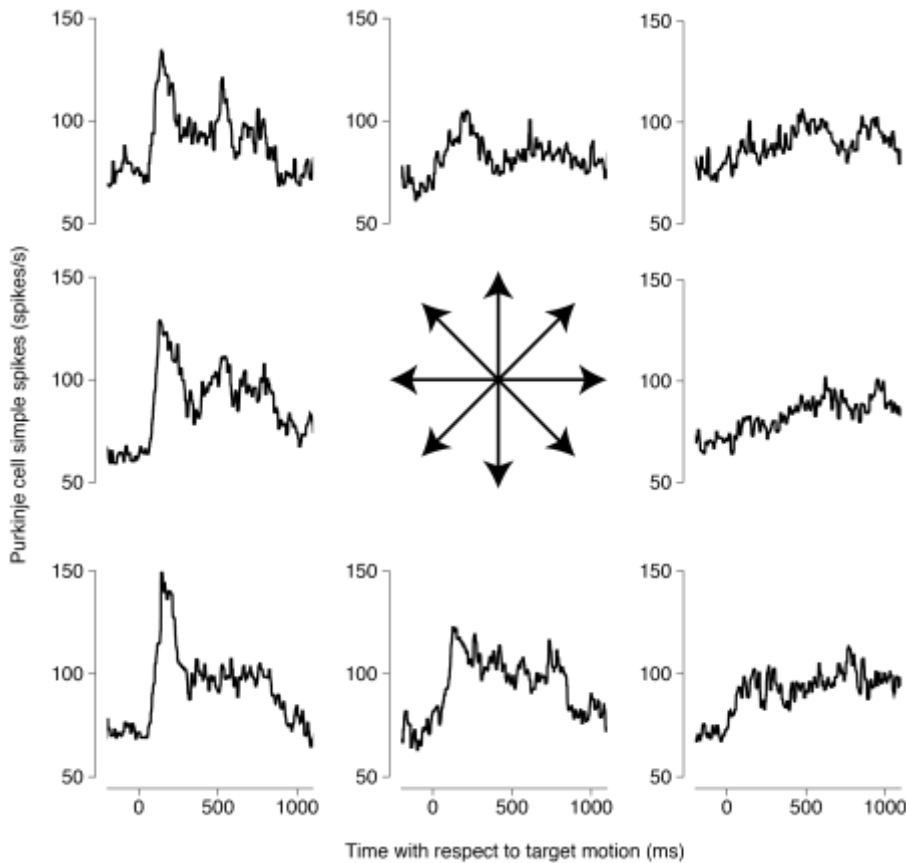


Figure 2: Firing rate of an example Purkinje cell for pursuit in eight directions. This example neuron preferred down-left pursuit reaching peak firing rate during the acceleration interval, before settling at a constant rate of firing rate during the sustained window.

For this neuron, a one-way analysis of variance (ANOVA) demonstrated that mean firing rates across target direction conditions were not significantly tuned during either the fixation window ($p=.62$) or the sustained window ($p = .1742$) but were strongly tuned during the acceleration window ($p = 7.83e-07$) confirming what is apparent by visual inspection. Apart from this basic statistical analysis to confirm firing rate differences as a function of target direction condition, we utilized a number of analyses to quantify the directional selectivity of each neuron in our population.

In figure 3A we plot the average firing rates, assessed in the acceleration window for the example neuron in figure 2, as a function of target direction. The dashed line illustrates the average firing rate during fixation. The smooth line is a tuning curve, fit to these average firing rates using a circular gaussian (von mises) function. For this neuron, the tuning curve could account for 90% of the variance in the firing rates ($R^2=.90$) suggesting this neuron varies its firing rate with respect to pursuit direction in an orderly simple manner.

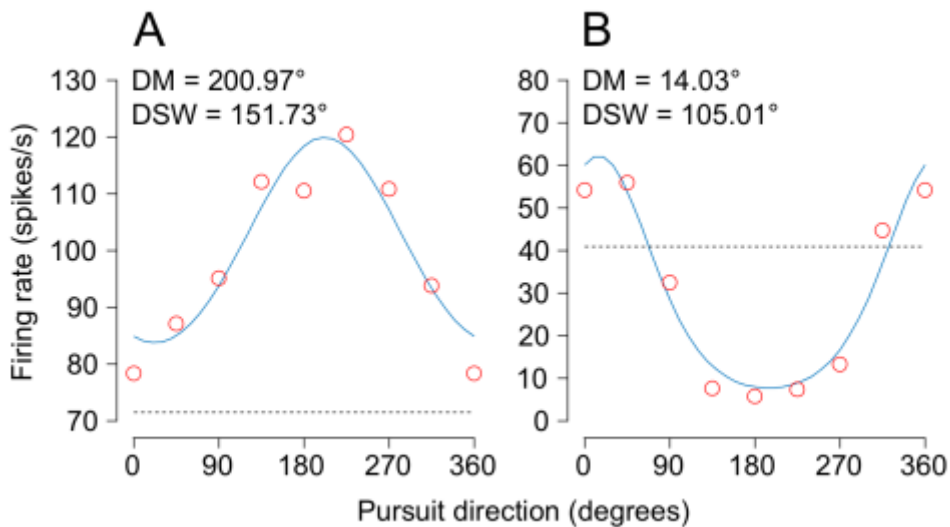


Figure 3: A, Average firing rates in the acceleration window of an example Purkinje cell as a function of pursuit direction. Smooth lines denote von mises tuning curve fits, dashed lines denote the average fixation interval firing rate. B, A second example of tuning, generated from a second Purkinje cell's simple spike response during the acceleration interval.

We also calculated, for this example neuron and neurons in our population, both the circular mean and the directional sector width (Fortier, Smith et al. 1993). The circular mean provides a secondary estimate of the preferred direction of the neuron

under question, independent of the quality of tuning curve fit. The directional sector width is defined as twice the circular standard deviation of the average firing rates and evaluates the sharpness in directional tuning independent of our tuning curve fits. For our example neuron with clear directional tuning in the acceleration window, the circular mean (preferred direction) was 200.97 degrees (very close to the value estimated from the tuning curve). The directional sector width was 151.73 degrees during the acceleration window, and 198.92 degrees during the sustained window.

In figure 3B we illustrate the tuning curve in the acceleration window for a second neuron. While this neuron also had significant directional selectivity it differed in some important ways. In our first example neuron, firing rates increased across all 8 directions of pursuit, relative to fixation window firing rate. By contrast, the second example neuron could either increase or decrease its firing rate relative to the fixation window firing rate. In keeping with prior studies, we would characterize the first cell as having a “graded” response to pursuit direction, while the second cell has a “reciprocal” response to target direction. In other cerebellar structures, such as the floccular complex, most neurons have a reciprocal responses (Krauzlis and Lisberger 1996). Below we test whether the same organization holds in the OMV. We also point out that the directional sector width is a good deal smaller for our second example neuron than our first. This confirms what you see by eye, namely, that the dispersion about the peak firing rate for

rightward eye movements, for example neuron 2, is much smaller than the dispersion about the peak firing rate for down-left eye movements for neuron 1.

2.3.3 Summary of population simple spiking directional selectivity

In table 1 we present the outcome of statistical tests for directional selectivity across our neural population. The majority of neurons in our population were sensitive to differences in pursuit direction during either the acceleration or sustained windows (82%) and just over half of these responses were unimodally tuned (55%) as assayed using a Rayleigh test. In general, firing rates in the sustained window were more directionally sensitive than firing rates in the acceleration window. Average firing rates in the fixation window did not vary, above chance levels, with changes in pursuit direction.

Table 1: Summary of statistical tests on firing rates across three intervals

	Fixation Window (FW)	Acceleration Window(AW)	Sustained Window (SW)	AW + SW
Anova (% p<.05)	5	64	73	55
Rayleigh (% p<.05)	2	37	44	25
Von Mises (% R ² >.70)	6	58	36	20

As can be seen from Table 1, just over half of the directionally sensitive neurons in our population could be fit well with a von mises tuning function. Therefore, we elected to quantify preferred direction and the degree of directional sensitivity by calculating the circular mean and directional sector width as described above. In figures 4A-D we

summarize the distribution of preferred directions and directional sector widths of firing rates in the acceleration and sustained windows.

Consistent with prior reports, we found that for those Purkinje cells that had significant directional selectivity, the preferred directions of their simple spikes did not seem to cluster into any apparent directional channels regardless of whether we looked at responses during the acceleration (figure 4A) or sustained windows (figure 4B). Data were not unimodally tuned during either the acceleration window and sustained windows ($p = .6839$ and $p=.4731$ respectively, Rayleigh test for unimodality). Analysis of directional sector widths revealed a surprising homogeneity in tuning curve bandwidth across the population during both acceleration and sustained windows (figures 4C and D respectively), with a mean directional sector width of 165.98 degrees during the acceleration window, and 167.46 degrees during the sustained window. These distributions were not significantly different from one another, as assessed by either a two sample t test ($p=.73$) or a wilcoxon ranksum test ($p=.62$).

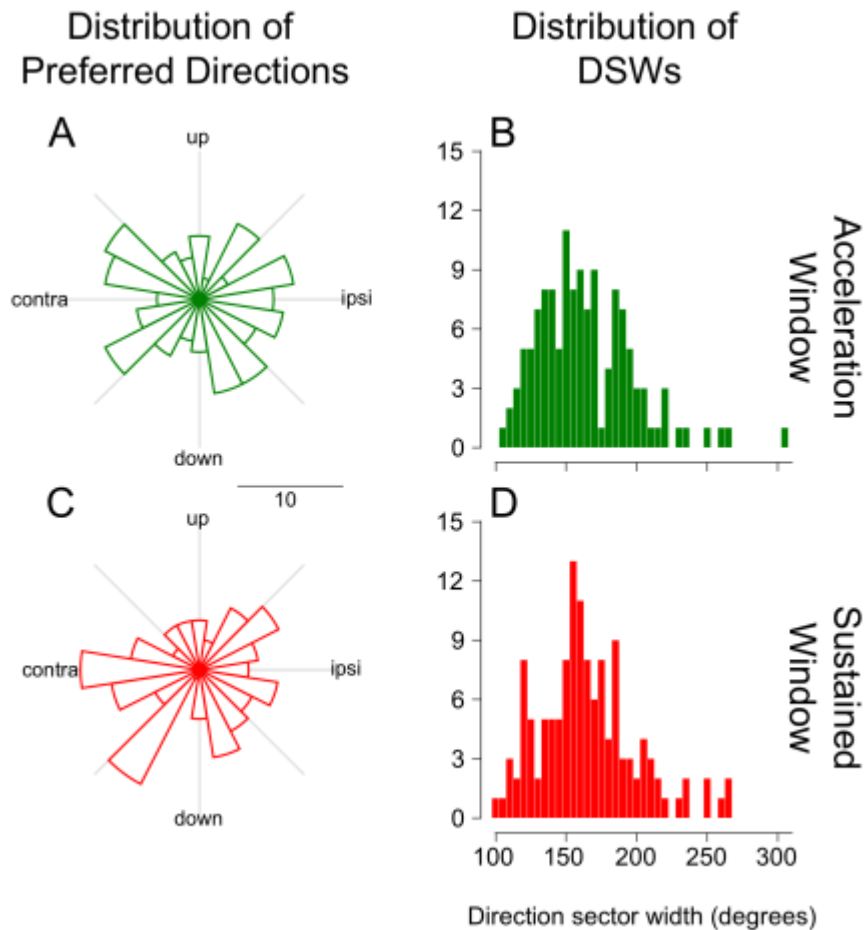


Figure 4: A,C The distribution of simple spike preferred directions as determined during the acceleration and sustained windows respectively, calibration bar indicates number of cells with tuning in a given direction. **B and D**, Directional sector widths for these same windows of time.

Given that the majority of our analyzed dataset (67%, see table 1) had significant directional tuning during both the acceleration window and the sustained window, we wanted to quantify the degree to which directional tuning changes across intervals. To investigate this, we calculated the preferred direction of each neuron during the acceleration window and looked at the preferred direction of firing rates in the sustained

window relative to this direction (Figure 5A). As is apparent by eye, the preferred direction of neurons calculated using the sustained window was very similar to the preferred direction of neurons calculated using the acceleration window. The strong unimodal bias of the population was confirmed using a Rayleigh test ($p = 2.88e-18$). We further confirmed that the mean of this distribution was 358.69 degrees with 95% confidence intervals of 12 degrees, confirming the distribution was not significantly different from zero. We also calculated the difference in directional sector width as assayed during the acceleration and sustained windows (figure 5B) respectively and found no difference between them ($p = .70$, one-sample t test).

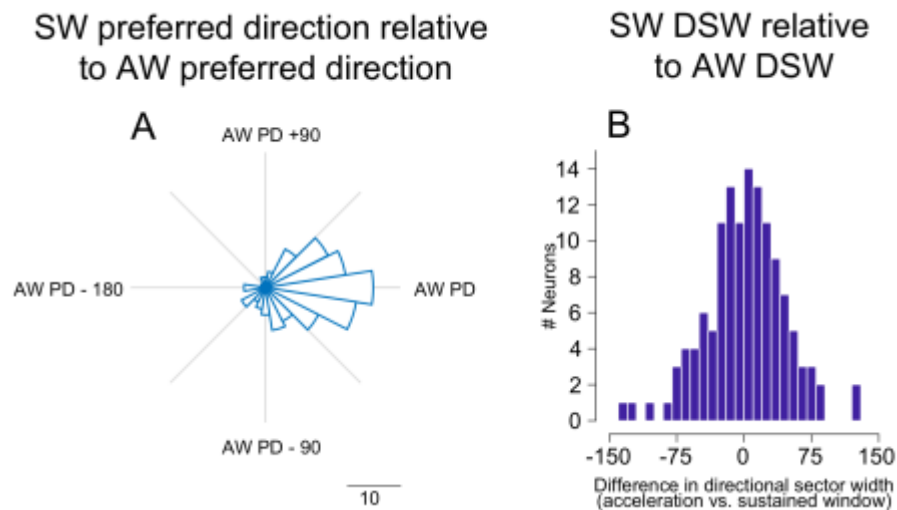


Figure 5: A, Preferred direction for all neurons, calculated in the acceleration window, relative to the preferred direction calculated from the firing rates in the sustained window. B, Difference in directional sector widths between the sustained and acceleration windows.

Finally, we wanted to see to what degree neurons could be easily categorized into reciprocal and graded cell types. We divided our data into three populations of

neurons, those with only significant tuning during their acceleration interval (Group I), those with only significant tuning during their sustained interval (Group II), and those with significant directional tuning during both intervals (Group III). For each neuron we selected two target conditions that were closest to its preferred and anti-preferred direction (preferred direction $- 180$). We call these the ON and OFF direction of each cell in question to avoid confusion. We calculated the preferred direction using firing rates in the acceleration window for group I neurons, and calculated the preferred direction using firing rates in the sustained window for groups II/III neurons. The firing rates in these two target conditions were then compared to the firing rates calculated in the fixation window. Neurons that increased their firing rate in their ON direction (relative to fixation window firing) and decreased their firing rate in their OFF (relative to fixation window firing) direction, were categorized as reciprocal neurons like the neuron in Figure 3B. We required at least a 5 spike per second increase and decrease in firing rates, to guard against false positives generated by random fluctuations expected about the fixation window firing rate. Of the remaining neurons that were not classified as reciprocal, neurons that had significant directional tuning, but decreased or increased their firing rate across at least 6 directions were considered graded neurons like the neuron in Figure 3A. We did not require that the firing rate increase or decrease across all 8 directions as this would be subject to small fluctuations in the average firing rate that may push it slightly above or below zero. We therefore settled on a threshold

criterion that matched what we observed by visual inspection of all tuning curves. Those neurons that did not fall neatly into these categories were considered unclassified. We display the results of this categorization process in the table presented below.

Table 2: Classification of Neurons on the basis of their firing rate during movement windows

	Reciprocal	Graded	Unclassified	Total
Group I	0	5	1	6
Group II	2	14	3	19
Group III	21	34	8	63
Total	23	53	12	88

As can be seen, the majority of directionally selectivity neurons in our population (60.23%) resembled our neuron from example 1, with responses that moved away in a graded manner from the average firing rate during fixation. By contrast, reciprocally responsive neurons (similar to our neuron in example 2) constituted 26.14% of directionally selective Purkinje cells. We should note that classification did not easily predict factors like the directional sector widths of the neurons in question, and when comparing these values, we could only find weak differences between the two populations ($p=.404$ two sample t test, $p = .008$ wilcoxon ranksum test).

2.3.4 Directional tuning of Purkinje cell complex spikes during pursuit in eight directions

We continued our analysis of directional tuning by studying the hereto uncharacterized organization of Purkinje cell complex spikes in the OMV. Our dataset consisted of 124

Purkinje cells for which isolation of complex spikes could be maintained throughout our tuning block. Below is an example of the complex spiking response recorded from our example Purkinje cell from Figure 1. Like the simple spiking response, it exhibits directional tuning (albeit a sharper directional tuning).

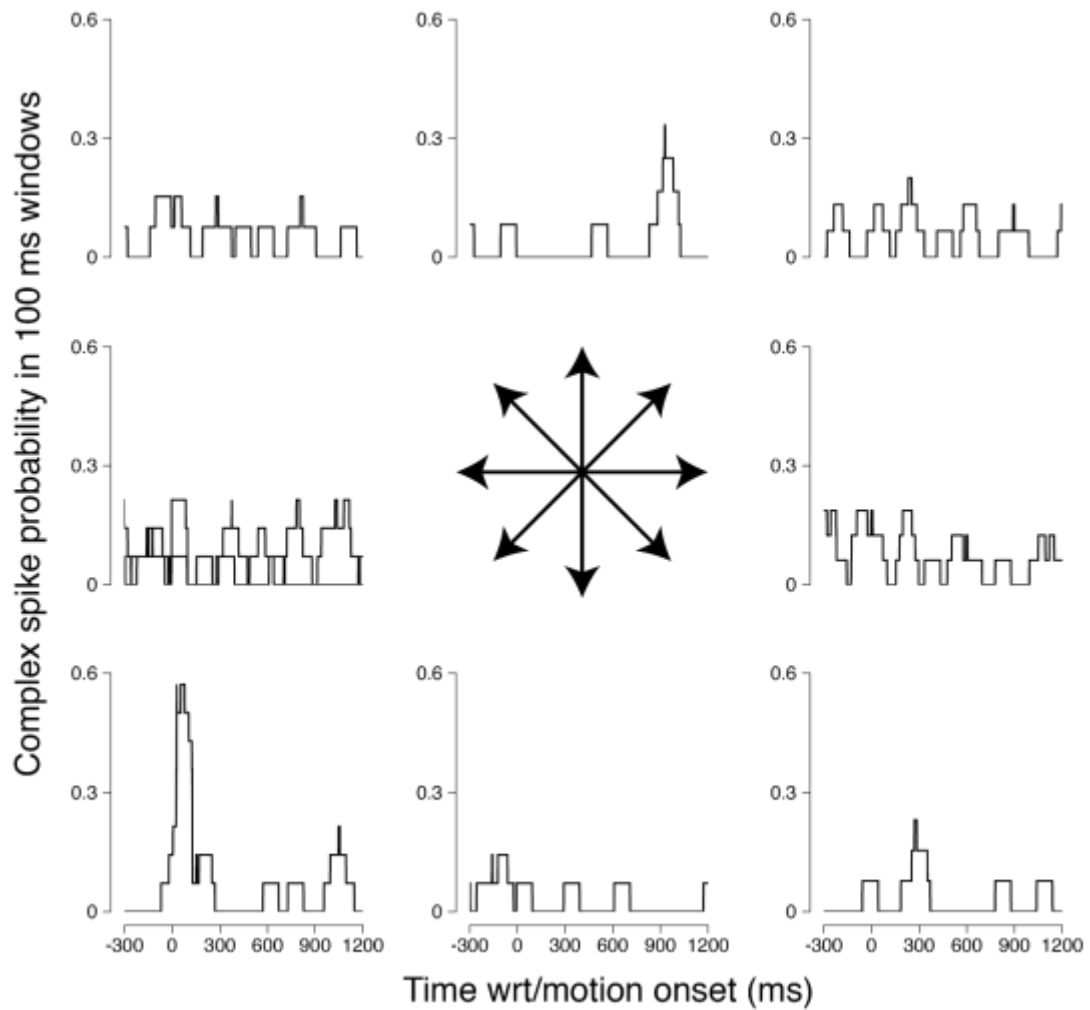


Figure 6: Complex spike tuning of Purkinje cell from Figure 1. Neuron responded with the highest spiking probability towards movements down and to the left.

This neuron responded most strongly to down-left pursuit just after target motion onset. We wanted to know how indicative this was of the population as a whole. To do this we considered the number of complex spikes occurring in a window 75 ms after target motion onset to 175 ms after target motion onset. Our choice of this window of time was motivated by two reasons. First, complex spikes in this window of time have been shown to occur at a high probability in the floccular complex during step ramp pursuit, and strongly covary with behavioral changes that occur over the course of directional adaptation. Secondly, we wanted to restrict our analysis to an interval of time that was relatively uncorrupted by saccadic eye movements, particularly given previously published results suggesting complex spikes in the oculomotor vermis are driven by saccadic eye movements (Soetedjo, Kojima et al. 2008).

Keeping in line with prior studies, strong complex spike responses in this window are expected to occur at a probability of .25. Only 45.38% of the neurons in our population reached this complex spike probability. They were usually strongly tuned for direction. In figure 7A we illustrate the distribution of preferred directions for only these strongly responsive neurons. Like the distribution of simple spike preferred directions, the distribution of complex spike preferred directions was only weakly unimodal (Rayleigh test for unimodality, $p = .0233$). In figure 7B, we illustrate the distribution of directional sector widths associated with these responses. We found that the average

directional sector width was 141.61 degrees. Ultimately this suggests complex spikes are more sharply directionally tuned than their simple spike counterparts.

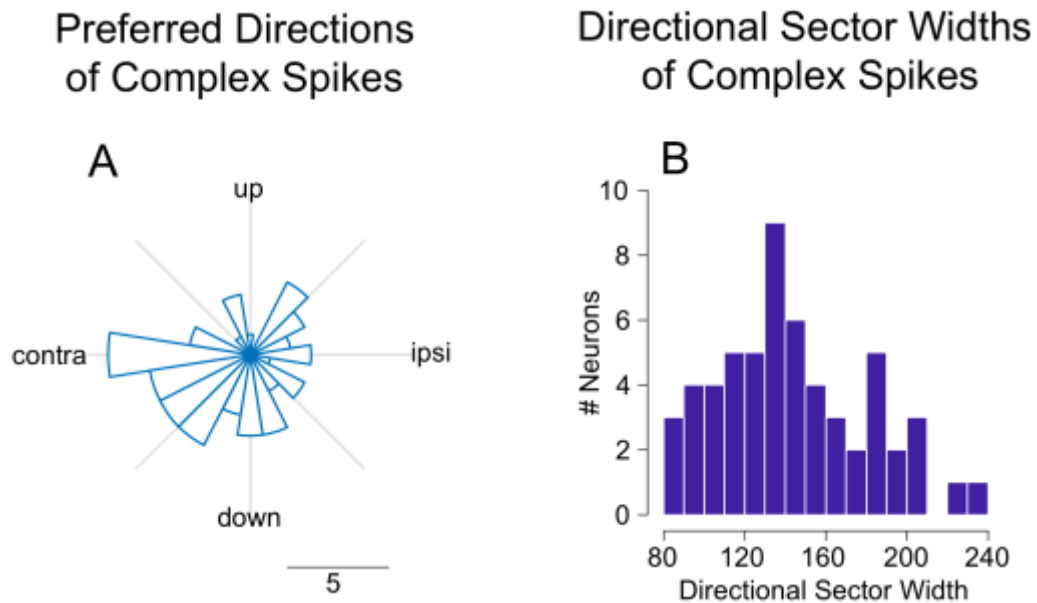


Figure 7: A, Distribution for preferred directions for Purkinje cell complex spikes assessed during the open loop interval of pursuit. B, Distribution of directional sector widths of Purkinje cell complex spikes.

Finally, we considered the relationship between the preferred directions of simple and complex spikes. We expected an opponent organization, similar to what has been demonstrated in the floccular complex (Krauzlis and Lisberger 1996). To test for this, we looked at the orientation of simple spike preferred direction relative to complex spike preferred direction. Since neurons with strong complex spiking responses could express directional tuning during either the acceleration or sustained windows, we calculated the preferred direction of simple spikes relative to complex spike preferred direction in both these windows. This is illustrated in Figure 8A. As in the case of simple

spikes and considered separately, complex and simple spikes were not organized into a clear relationship with respect to one another. During both the acceleration and sustained windows simple spike activity was consistent with being uniformly distributed relative to the complex spike preferred direction (Omnibus test, $p = .1852$ and $p = .8196$ respectively).

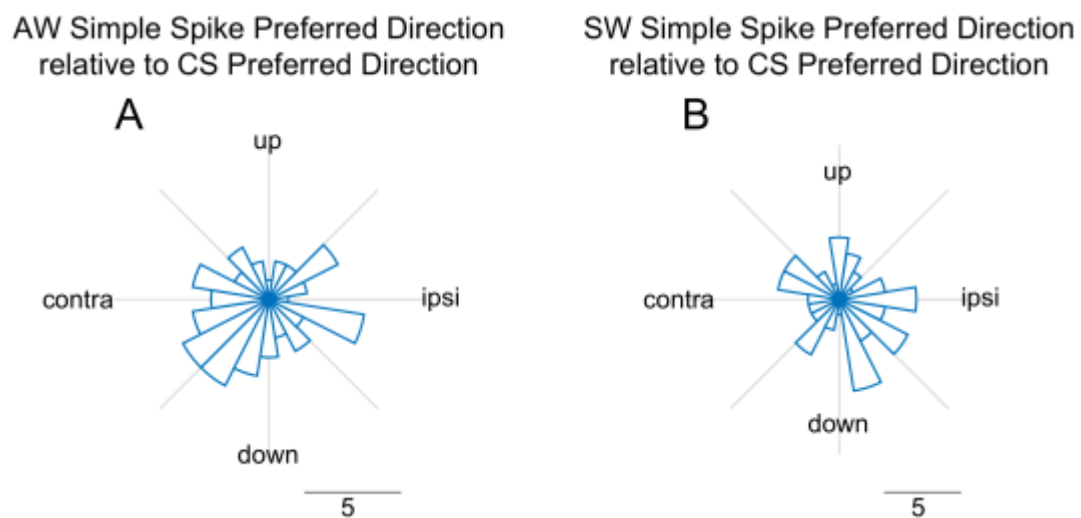


Figure 8: A, Preferred direction of simple spikes, assessed in the acceleration window and plotted relative to CS preferred direction. B, Preferred direction of simple spikes, assessed in the sustained window plotted relative to CS preferred directions

2.3.5 Summary of findings on tuning properties

The analyses of the prior two sections suggests that neurons within the oculomotor vermis are strongly directionally tuned during the periods of time encompassing the initial acceleration and sustained pursuit of the eye. However, no clear channels seem to exist for simple spike responses, and we found that directionality was more likely to manifest itself in a graded way. This is in contrast to neurons in the

floccular complex, whose directionality is more reciprocal in organization. Only a fraction of cells showed strong complex spike modulation following target motion onset. Moreover, we could not find evidence that complex spikes from responsive neurons showed clear evidence for channel-like organization. Finally, we did not find evidence for opponent organization of complex vs simple spike tuning as has been documented for floccular complex Purkinje cells. We next turned to the question of whether activity of these neurons changes over the course of directional adaptation. We hypothesized that given the graded representation of simple spike activity along with the weak complex spike responses, we were unlikely to find any changes over the course of pursuit adaptation. We confirm this hypothesis in sections presented henceforth.

2.3.6 Methods for studying directional adaptation

In figure 9A and B we illustrate the basic aspects of a task used to elicit directional adaptation of smooth pursuit eye movements. Typically, directional adaptation is induced when a target, initially moving in one direction, undergoes a predictable change in target trajectory. Over time, the pursuit system learns to anticipate such changes and begins to adapt behavioral trajectories to intercept the target. For example, in Figure 9A we illustrate one set of behavioral trials where the target is initially moving downward (called the pursuit direction) at 20 degrees/s. 250 ms after target motion onset, we introduce a 30 degree/s component of motion moving rightward. The direction of this component of motion is called the learning direction. As a monkey repeatedly tracks a

target like this, the eye begins to develop a component of velocity in the learning direction that precedes instruction onset. This is illustrated by the difference between the blue and red curves in figures 9A. The green trace is the horizontal component of eye velocity during the third learning trial. During the 150th trial, illustrated by the gray trace, the component of eye velocity in the learning becomes larger around the time of instruction onset. This window of time is indicated via dashed lines in figure 9A and we refer to it as an “instruction interval.”

Trials were always organized in this form, with the pursuit direction and learning direction being orthogonal. The result of this trial structure, irrespective of the exact direction of the pursuit and learning directions is that the eye acquires a large increase of eye velocity in the learning direction. This occurs alongside a slight decrease in eye velocity in the pursuit direction. This is illustrated in figures 9B where the blue and red curves show average eye velocity, averaged across learning trials, in pursuit and learning directions respectively. These values are calculated relative to the size of eye velocity in the instruction window as assessed during a prelearning block. We always quantify learning effects as average responses in this window, calculated over sets of 20

learning trials.

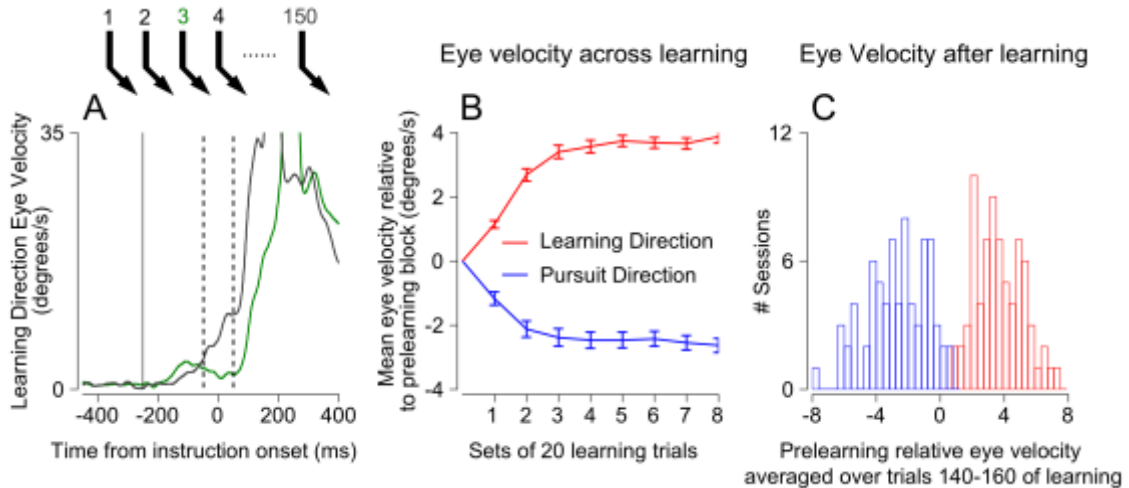


Figure 9: A, Example velocity in the learning direction during the 3rd and 150th learning trials. Dashed lines indicate an instruction interval used to assess the state of learning. B, The time course of learned changes in eye velocity in the pursuit (blue) and learning (direction) averaged across 75 learning sessions. C, Summary of differences between average eye velocity in a prelearning block and during the last 20 trials of learning, with pursuit direction eye velocity in blue and learning direction eye velocity in red.

2.3.7 Structure of our learning population, experimental setup

We were able to record a total of 75 Purkinje cells during our learning paradigm. For each cell, we would first assay its simple spike tuning and generate peristimulus time histograms for its responses across 8 directions of pursuit. Pursuit and learning directions for our learning paradigm were selected online on the basis of this tuning curve to maximize the chance of observing learned changes. We reasoned that as the eye learns a new trajectory to anticipate directional change, the initial direction of the eye achieves a trajectory commensurate with tracking target motion that is midway between the pursuit and learning components of target motion (we term this the prediction

direction, and define it as a direction of pursuit 45 degrees away from the pursuit direction towards the learning direction). For each neuron, therefore, we picked our learning trials based on the largest discernible difference possible between pursuit directions spaced radially 45 degrees apart. Figure 10 illustrates this with an example. We show the tuning curve for simple spike responses of an example Purkinje cell. The largest difference in tuning between two directions occurred between pursuit in the downward direction and down-right pursuit. This motivated us to set up learning trials where the pursuit direction was downwards, and the learning direction rightward. We assumed that as the pursuit system adapted, the firing rates of the neuron ought to resemble the firing rates associated with movement along the prediction direction (namely, the dark green firing rate in figure 10).

Tuning Curve of Representative Purkinje Cell studied during directional adaptation

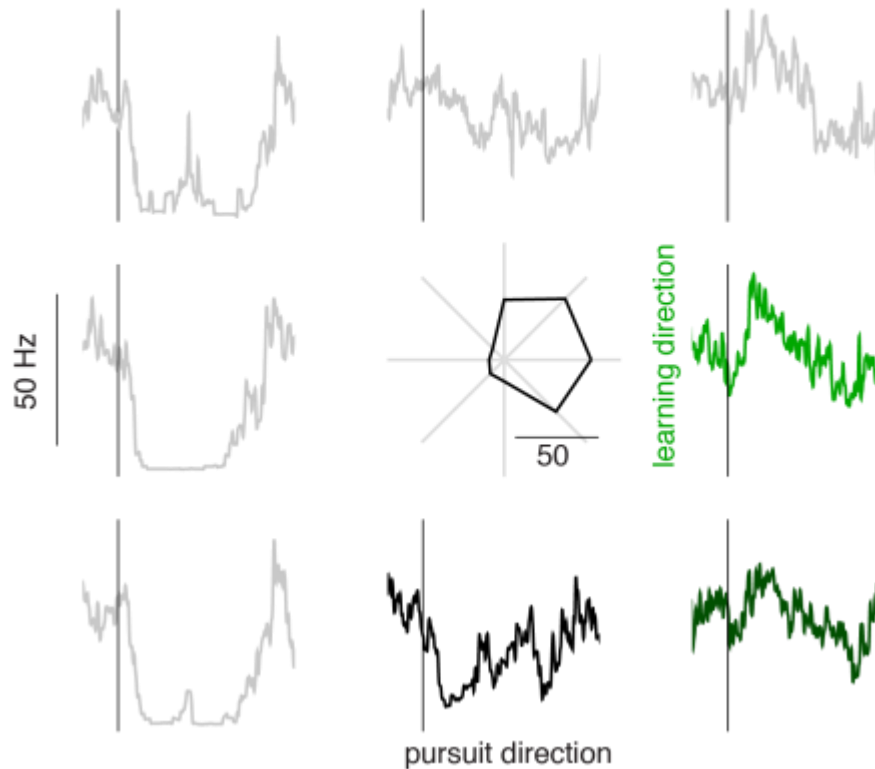


Figure 10: Representative tuning curve from one session of learning. For this session, we defined the pursuit direction of our learning trials as downward, and the learning direction rightward. This was to maximize the change in firing rate between the pursuit direction (in black) and the prediction direction (dark green and between pursuit and learning directions). This is an example of ON learning.

Our dataset consisted of 75 Purkinje cells which were held long enough to assay tuning and hold through at least 25-50 trials of target motion in the pursuit direction and at least 160 repetitions of learning trials. 160 learning trials was sufficient to induce large changes in eye velocity, as illustrated in figure 9D. Neurons that did not significantly change their activity between our fixation window and instruction window were not

considered. When the firing rate in the learning direction was larger than the firing rate in the pursuit direction, we termed these trials *ON trials*. When the firing rate in the learning direction was smaller than the firing rate in the pursuit direction, we termed these trials, *OFF trials*. The example in figure 10 illustrates a tuning curve for an ON learning session.

2.3.8 Simple spike changes over the course of learning

In figure 11 we illustrate an example session, where we assessed firing rate changes over the course of learning for one Purkinje cell. In figure 11A, we show the average eye velocity, in the learning direction, during the pre-learning block (blue curve), and the average eye velocity following learning (red curve). The red curve was calculated by averaging eye velocity over the last 20 learning trials. In figure 11B we illustrate changes in firing rate calculated at these same points in time. In blue are the firing rates during the prelearning block, while firing rates following learning are illustrated in red. Like eye velocity, we assessed firing rate changes over the course of learning in an instruction window marked via dashed lines 11B. In figure 11C, we show a neural learning curve that quantifies these firing rate changes, relative to prelearning firing rates assessed in the same window. As can be seen, during learning, firing rates initially rose rapidly, but settled back near zero by the time the animal had experienced 120 learning trials.

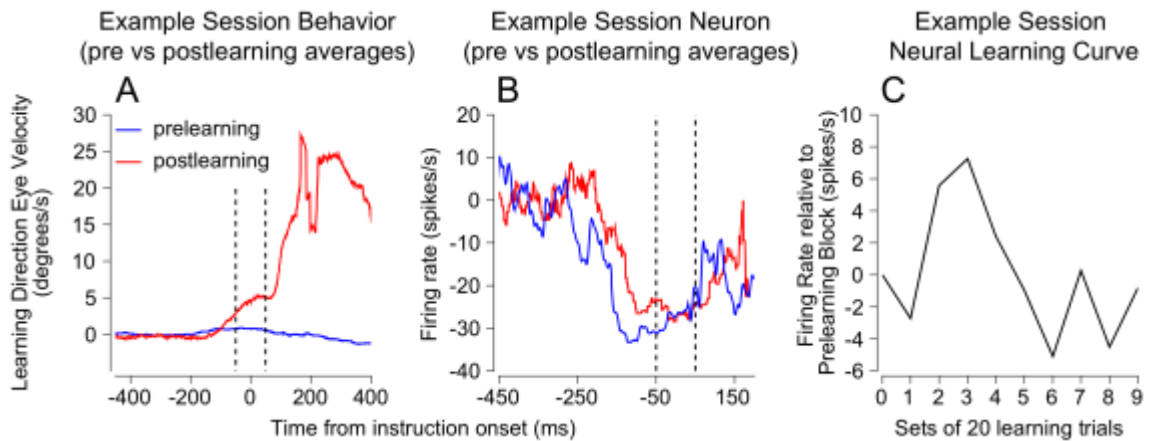


Figure 11: A, Behavioral learning during an example session. In blue we illustrate eye velocity during a prelearning block where the target moved in the pursuit direction only. Compare this to eye velocity acquired after learning (in red). B, Firing rate in the prelearning block and after learning (blue and red curves respectively). C, Example session learning curve that shows changes in firing rate (relative to the pre-learning block) over the course of sets of 20 learning trials.

We constructed learning curves like those shown in figure 11C for every neuron in our population. In figure 12A, we show what average learning curves look like during both ON and OFF learning. In both cases, firing rates begin near zero (as they are calculated relative to a pre-learning block). Throughout the learning trials they changed very little, shifting only slight upwards during ON learning. In figure 12CB we plot the firing rates assessed during the instruction interval in the pre-learning block against the firing rate in the instruction interval averaged over trials 140-160 in the learning block. A one-sample t test confirmed what is apparent by visual inspection, that the firing rates across the population did not change significantly in either the case of ON learning ($p = .1481$) or OFF learning ($p = .5659$).

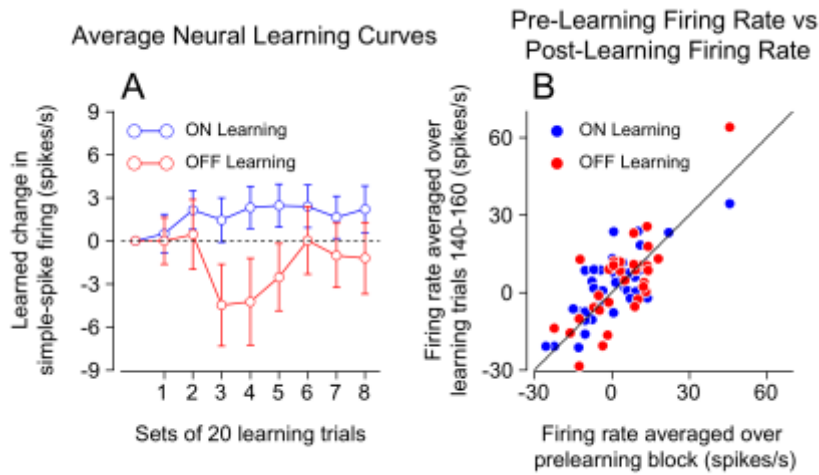


Figure 12: A, Average instruction interval firing rate changes over the course of learning, relative to prelearning block firing rates, calculated separately across all ON (blue) and OFF (red) learning sessions. B, For individual sessions, average instruction interval firing rate in the prelearning block is plotted against the average instruction interval firing rate averaged over trials 140-160 in the learning block.

2.3.9 Complex spiking changes over the course of learning

We next wanted to know if complex spike activity also remained unchanged over the course of learning. We hypothesized this would occur because simple spikes appeared relatively unchanged. We first tested whether there was any significant complex spike response at all during learning trials. For each learning session, we calculated the average complex spike modulation over time, in sets of 20 learning trials. In figure 13A, we have plotted the time course of complex spike probabilities, averaged over the first 20 trials, for each of our 75 learning sessions, and arranged according to the timing of peak CS probability. The strongest complex spike responses occurred shortly after instruction onset. This also appeared to be the most consistent time during which

complex spikes could be driven. Complex spike activity in this interval was, on average, highest during the beginning of the learning block (figure 13B) but remained stable throughout learning (figure 13B). A one-way analysis of variance confirmed this was an insignificant change over the course of learning ($p=.88$).

We wanted to know whether complex spike activity was more strongly modulated by trajectory changes during our learning trials than to pursuit outside the context of learning. To test this, we defined an open loop window of time, during which we would examine complex spike probability in tuning and learning blocks. In the tuning block this occurred 75-175 ms after target motion onset, while in the learning block this occurred 75-175 ms after instruction onset. We calculated complex spike probabilities for tuning block, restricting our analysis to trials where target motion occurred in the pursuit or learning direction. We also calculated complex spike probabilities during the first 20 trials of our learning block. In figures 13C and D we plot complex spike probabilities elicited by target motion in the pursuit or learning direction, against complex spike probabilities elicited by trajectory changes during learning trials. As can be seen visually, the magnitude of complex spike activity during the learning block did not exceed CS activity in either the pursuit direction or the learning direction (ranksum test, $p=.4948$ and $p = .2674$ respectively).

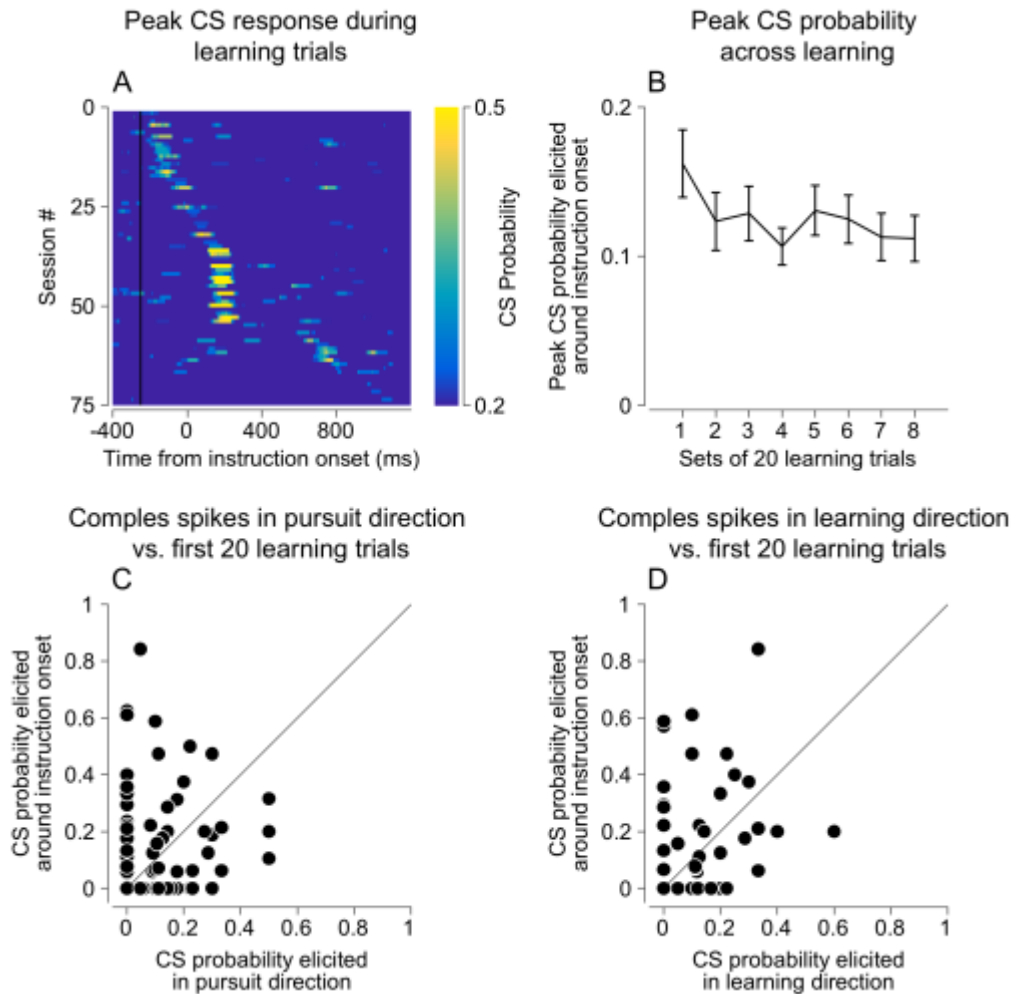


Figure 13: A, Peak complex spiking response during the first 20 learning trials, arranged according to the time of peak CS probability. B, Learning curve showing that on average CS activity is stable over the course of learning. C and D Plots of CS probability in the tuning block against complex spike probability in the learning block. CS probability in the tuning block separately assessed for trials requiring tracking targets in the pursuit direction (C) or tracking targets in the learning direction (D)

We finally tested whether complex spike tuning might be predictive of the capacity of Purkinje cell simple spikes to change over the course of pursuit adaptation, as it is in other cerebellar structures (Yang and Lisberger 2014). We divided our dataset

into situations where complex spike activity in the pursuit direction exceeded complex spike activity in the learning direction (during an interval 75-175 ms after target motion onset) and vice versa (figure 14A and B). We then compared the average firing rates of neurons during either the pre-learning block or following 140 learning trials (Figures 14C and D). We did not find strong changes in either case, with the largest observed changes occurring during a period of time when saccades were most likely to be initiated.

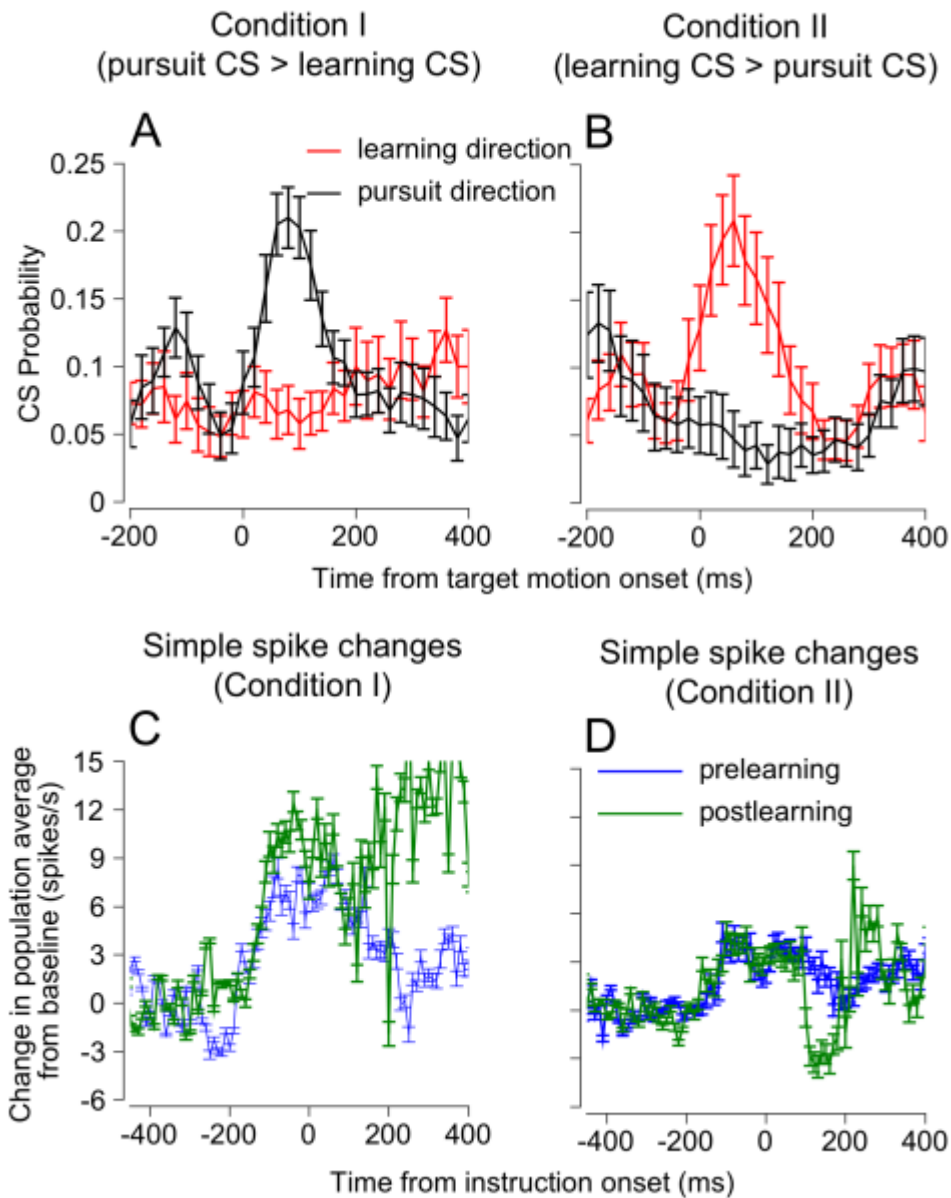


Figure 14: Trials were separated according to whether the complex spike activity during eye movements in the pursuit direction exceeded complex spike activity during eye movements in the learning direction (A) or vice versa (B). C, D show the average firing rate across Purkinje cells in our population divided in this manner. Green curves illustrate the average response after learning, while blue curves illustrate the average response in the prelearning block.

2.4 Discussion

Here I briefly summarize the findings above in the context of the introduction in section 2.1. An extended discussion of these results is presented in section 5. The main result I hope to have communicated is that pursuit tuning in the oculomotor vermis seems to fall outside the realm of clear channels of organization found in the floccular complex. While Purkinje cells were strongly directionally selective at an individual neuron level, this directional selectivity was very different from the directional selectivity of floccular complex Purkinje cells, as reported in the literature. Firstly, directional tuning was most likely to manifest itself in terms of graded responses, that were not organized in a reciprocal manner as has been found for nearly all floccular complex Purkinje cells. Moreover, the preferred directions of OMV simple spikes was distributed uniformly across all directions, suggesting that directional signals obey retinal as opposed to muscle coordinates.

Additionally, our results also suggest that Purkinje cells in the oculomotor vermis do not shift their responses over the course of pursuit adaptation. The exception is complex spike activity which seems modulated preceding and just after the trajectory change. But, this activity seems to remain unchanged over the course of the learning trials suggesting it is encoding aspects of our learning task that are unrelated to behavioral adaptation. At present it is unknown whether these responses are due to changes in retinal slip on the eye that occur as a result of learning, or to some other

factor like saccades that occur during pursuit. More careful experiments would need to be designed to answer these questions. Ultimately, our results suggest that the oculomotor vermis lies outside the behavioral loop that drives pursuit adaptation in this directional adaptation paradigm.

3. A quantitative comparison of the encoding of smooth pursuit eye movements by the oculomotor vermis and floccular complex

3.1 Introduction

The cerebellum plays an important role in the calibration and regulation of movements. In both the oculomotor (Simon, Iain et al.) and skeletomotor (Kelly and Strick 2003) systems, this role is believed to be implemented by a set of distinct subregions of the cerebellum, each with a different input-output topography. Prior studies that have investigated the role of the cerebellum in motor control, have traditionally focused on one subregion, without carefully considering the contributions of the others. An interesting case of this occurs in the oculomotor system when we examine the role played by the cerebellum in the control of voluntary smooth pursuit eye movements. Smooth pursuit eye movements are smooth rotations of the eyes that allow primates to foveate moving objects in their environment (Lisberger 2010). 40 years have passed since a classic lesion study demonstrated that an intact cerebellum is necessary for the execution of smooth pursuit eye movements (Westheimer and Blair 1973). Subsequent experiments have revealed that pursuit control emerges from the coordinated action of multiple domains of the oculomotor cerebellum, as lesioning any one oculomotor domain only impairs pursuit eye movements without abolishing them (Robinson and Fuchs 2001). Indeed, up to 4-5 anatomically distinct regions of the

cerebellar cortex may contribute to pursuit eye movement control (Simon, Iain et al.).

One persistent issue is that little data is available on what differentiates these areas.

Are these multiple regions of the oculomotor cerebellar cortex all performing the same function in driving smooth pursuit? Anatomy suggests many of these structures appear to have shared or overlapping inputs (Voogd, Schraa-Tam et al. 2012). Given the fact that the microcircuitry of the cerebellar cortex varies very little across these different subregions, a reasonable hypothesis would be to assume few functional differences between substructures. On the other hand, these regions differ strongly in terms of output projections, molecular constitution, and a host of other factors. Many of these factors are believed to contribute to the heterogeneity of basic firing properties one observes across the cerebellar cortex (Zhou, Lin et al. 2014). Adding to this quandary is the fact that different subregions of the cerebellum have typically been studied in the context of different behaviors.

For example, one well studied region of the oculomotor cerebellum is the floccular complex (FLC). Many studies have studied the role this structure plays in the control of the kinematics and adaptation of smooth pursuit eye movements (Zee, Yamazaki et al. 1981, Medina and Lisberger 2008, Lisberger 2009, Medina and Lisberger 2009). Several millimeters away is a second structure which is also believed to be critical to smooth pursuit eye movement control, the oculomotor vermis (OMV). Both the floccular complex and the oculomotor vermis receive visual and motor inputs that are

critical to the drive initiation and maintenance of pursuit (Voogd, Schraa-Tam et al. 2012). Neurons in both regions of the cerebellum have been shown to be responsive to pursuit eye movements (Sato and Noda 1992, Krauzlis and Lisberger 1996, Dash, Catz et al. 2012). Little comparative analysis has been done, however, to determine if these structures really are playing the same role.

To address these questions, we compared the simple spike activity of Purkinje cells recorded in the OMV and FLc during smooth pursuit eye movements. We investigated three aspects of these neural responses. The first were basic firing rate properties, including the coefficient of variation and baseline firing rate during fixation. We hypothesized that basic response properties like this were likely to differ between structures as has been demonstrated recently in the rodent cerebellum (Zhou, Lin et al. 2014). Secondly, we compared how simple spikes, in both regions, encoded features of smooth pursuit eye movements. We hypothesized that strength of the neural encoding of pursuit kinematics like velocity or acceleration would be significantly smaller in the OMV, as compared with the FLc. This is based on the fact that behavioral deficits following lesions of the FLc are greater than those following lesions of the OMV (Zee, Yamazaki et al. 1981, Robinson, Straube et al. 1997, Takagi, Zee et al. 2000, Rambold, Churchland et al. 2002). Finally, we compared trial-by-trial correlations (neuron-behavior correlations) between eye speed and simple spike firing rates. Given that the size of trial-by-trial correlations between single neuron firing rates and behavior is

believed to emerge as a result of shared variation between neurons (Medina and Lisberger 2007, Pitkow, Liu et al. 2015, Lee, Joshua et al. 2016), and given that the FLc and OMV share many of the common sources of visual and motor inputs (Voogd, Schraa-Tam et al. 2012), we hypothesized that these values ought to be equal.

Our findings indicate that at all levels of analysis, OMV Purkinje cells differ from FLc Purkinje cells. First, we found that these cells in the FLc were more regular, as assessed by their coefficient of variation, and had higher firing rates during fixation. Analysis of the CV2 values of each population showed that higher CV values in the OMV were likely driven by a systematic modulation in response frequency during fixation. Neurons in the OMV had lower kinematic sensitivity than their FLc counterparts and the values of these sensitivities was more broadly distributed. Finally, the size of trial-by-trial correlations between Purkinje cell firing rate and eye speed was nearly 2.5x higher (on average) in the FLc as compared with the OMV. Indeed, across our population of recorded OMV neurons we found chance-level correlations with eye speed. The only variable for which OMV neurons had above chance-level correlations was response latency.

3.2 Methods

Subjects, and methods for neural recording for the current set of experiments are covered in detail in Chapter 2. Here we will highlight some differences in both task or

trial structure and data analysis that are pertinent to understanding data presented below.

3.2.1 Visual stimuli and Experimental Design

All aspects of visual stimulus presentation were exactly the same as described in chapter 2, with very few modifications. A typical session began with a tuning block, where animals pursued step-ramp target motion (Rashbass 1961) moving along 8 radially spaced directions at a velocity of 20 degrees/s from a central fixation point. During the performance of this task, we would record individual Purkinje cells in the oculomotor vermis. Using a combination of an analog spike detection system (Bak instruments: Time Amplitude Window Discriminator) and custom analysis scripts written in Matlab (Mathworks) we determined the direction of pursuit in each neuron that yielded the largest change in firing rate relative to a fixation interval preceding target motion onset. We then proceeded to the next phase of our behavioral protocol, where we recorded from the same Purkinje cell as an animal pursued over 100 repetitions of target motion in its preferred direction. In Monkey V these trials were interleaved with motion in the anti-preferred direction (180 degrees away), while in Monkey Y these trials were interleaved with conditions where the target moved in the preferred direction at 2 other speeds (10,30 degrees/s).

3.2.2 Data Analysis

All analyses were performed Matlab (Mathworks). Much of our analysis focused on the analysis of properties of firing rate in two windows of time. The first interval was a fixation interval of length 150 ms long, preceding target motion onset during which a monkey was maintaining fixation on a target. The second interval was termed an open loop interval and was a 100 ms window of time, 75-175 ms after target motion onset. This interval was selected for two reasons. First, due to the nature of our Rashbass step ramp paradigm, it is the period of time when saccades are least likely to occur. The second was for the purpose of experimental control. From the moment the eye begins to move visual motion on the eye falls outside of an experimenter's control. However, the response latency of the pursuit system suggests there is a visual delay in the system. Pursuit eye movements in both of our monkeys during this step ramp paradigm were executed with a latency of roughly 100 ms on average. The fact that our window cuts off 75 ms after this feedback delay, therefore, allows us to relate pursuit responses solely to target motion that precedes movement onset.

Because we focused on this interval of time, we only analyzed neurons that had significant responses during this interval. Moreover, we discarded trials where saccades were made during this interval. Saccades were detected using a custom program. We were also able to mark larger amplitude saccades occurring later in pursuit by eye using software custom-built in our lab for this purpose. Latencies for pursuit eye movements

were calculated using a method previously described (Lee and Lisberger 2013). The method utilizes an iterative algorithm to estimate the gain and latency of individual pursuit trials relative to the average trajectory of pursuit. Coefficients of variation (CV) and fixation interval firing rates were calculated only from those trials where saccades did not occur during the 150 ms interval preceding target motion onset. This is critical as it insures that we are examining neural responses during identical behavioral conditions. Correlation values reported below are Pearson correlation coefficients, calculated using the matlab function corr.

For comparison with floccular data, we mined a set of data that was collected previously in the floccular complex of monkeys (Medina and Lisberger 2007). All analyses that were performed on neurons in the oculomotor vermis were also performed on data acquired from the floccular complex. The data collected in the floccular complex was from Purkinje cell simple spikes recorded while an animal pursued a target at 30 degrees/s. This is different from our analysis of oculomotor vermal Purkinje cells which were recorded as monkeys pursued targets moving at 20 degrees/s. We do not think difference in target speed will be a problem for two reasons. First, the analysis we report here for motion at 20 degrees per second in the oculomotor vermis has also been performed for floccular complex responses during pursuit of target motion at 20 degrees per second. We therefore reasoned that the differences in the results between floccular

responses for targets moving at 20 degrees per second and 30 degrees per second would be too small to impact the substance of our findings.

3.3 Results

3.3.1 Pursuit Kinematics

We begin with a brief overview of the schematics of our pursuit task and the parameters of pursuit eye movements that we analyzed in order to investigate differences across cerebellar structures. In our pursuit task, monkeys tracked repeated presentations of a target that underwent step ramp target motion at a velocity of 20 or 30 degrees per seconds

In figure 15A, we illustrate the trajectory of target position in a trial for rightward pursuit. The smooth and dashed black lines denote average eye position and target position over time respectively. In figures 15B and C, we converted this position trace to velocity and acceleration via numerical differentiation. These traces illustrate that pursuit can be characterized as a transition from a state of fixation to smooth acceleration that takes brings the eye to a sustained velocity maintained throughout the period of time the target is moving. In this current set of experiments, we were mainly interested in how the state of two different cerebellar cortical regions was modulated across two of these time periods, fixation (marked “f” in figure 15C) and the initial period of smooth acceleration of the eye (marked “i” in figure 15C).

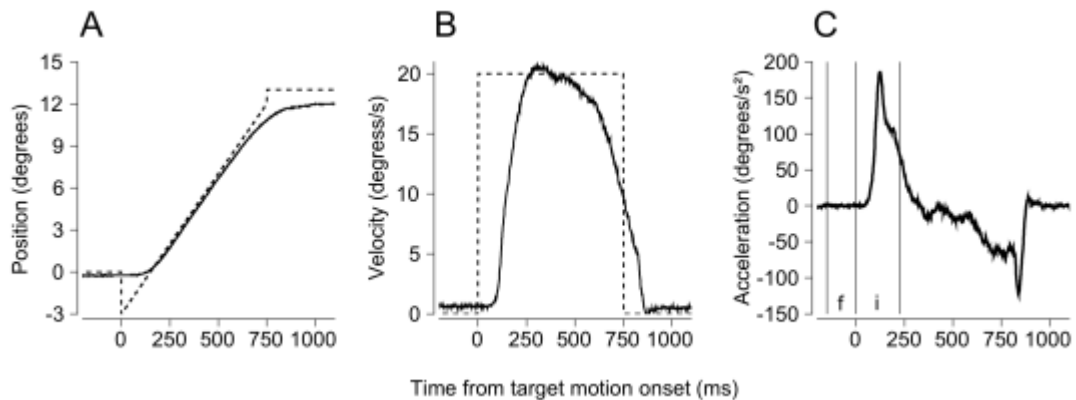


Figure 15: A, Average position (smooth line) and target position (dashed line) over time. B Average velocity (smooth line) and target velocity (dashed line) over time. C, Average acceleration over time. We mark two intervals that we analyzed in depth below, “f” is a fixation interval. “i” is the interval encompassing the initial acceleration of the eye.

3.3.2 Properties of Purkinje cell responses in the oculomotor vermis and floccular complex during fixation

We studied Purkinje cell responses in the oculomotor vermis (OMV) or floccular complex (FLC) as animals performed this task. In figure 16A and B, we illustrate an example neural response during the execution of a pursuit eye movement down and to the left. The graph in figure B indicates a raw voltage trace, with the presence of low-frequency complex spikes (marked CS in the dashed box) that allowed us to confirm our analysis was restricted to cerebellar Purkinje cells. We began our analysis by investigating the responses of neurons in the FLC and OMV during a period of behavioral fixation preceding target motion onset. We first calculated average firing rate in this fixation interval. Data in figure 16C demonstrates that fixation interval firing rates were slightly higher in the FLC by comparison to the OMV (two-sample t test, $p = .0133$;

ranksum test, $p = .0204$). We also calculated the coefficient of variation (CV) in an effort to quantify spike variability during this fixation interval. CV was strongly different between OMV and FLc populations, with a larger degree of spike variability in OMV responses as demonstrated in figure 16D (t-sample t test, $p = 1.23e-9$; ranksum test, $p = 8.65e-9$). We also calculated CV2, a measure which is far less susceptible to firing rate modulations (Holt, Softky et al. 1996). CV2 values were lower than CV values in both the floccular complex (two-sample t-test, $p = 2.62e-7$; ranksum test = .04) as well as the oculomotor vermis (t-sample t-test, $p = 2.78e-31$; ranksum test = $3.60e-16$). However, the differences were larger in the case of the OMV. Therefore, when we calculated CV2 for both populations, they were not significantly different from one another, as illustrated in figure 16F (two-sample t-test = .11; ranksum test, $p = .21$). Given that CV2 measures are more resistant to firing rate variations (Holt, Softky et al. 1996), these results suggest that modulation in firing rates preceding target motion onset is higher in the OMV than in the FLc.

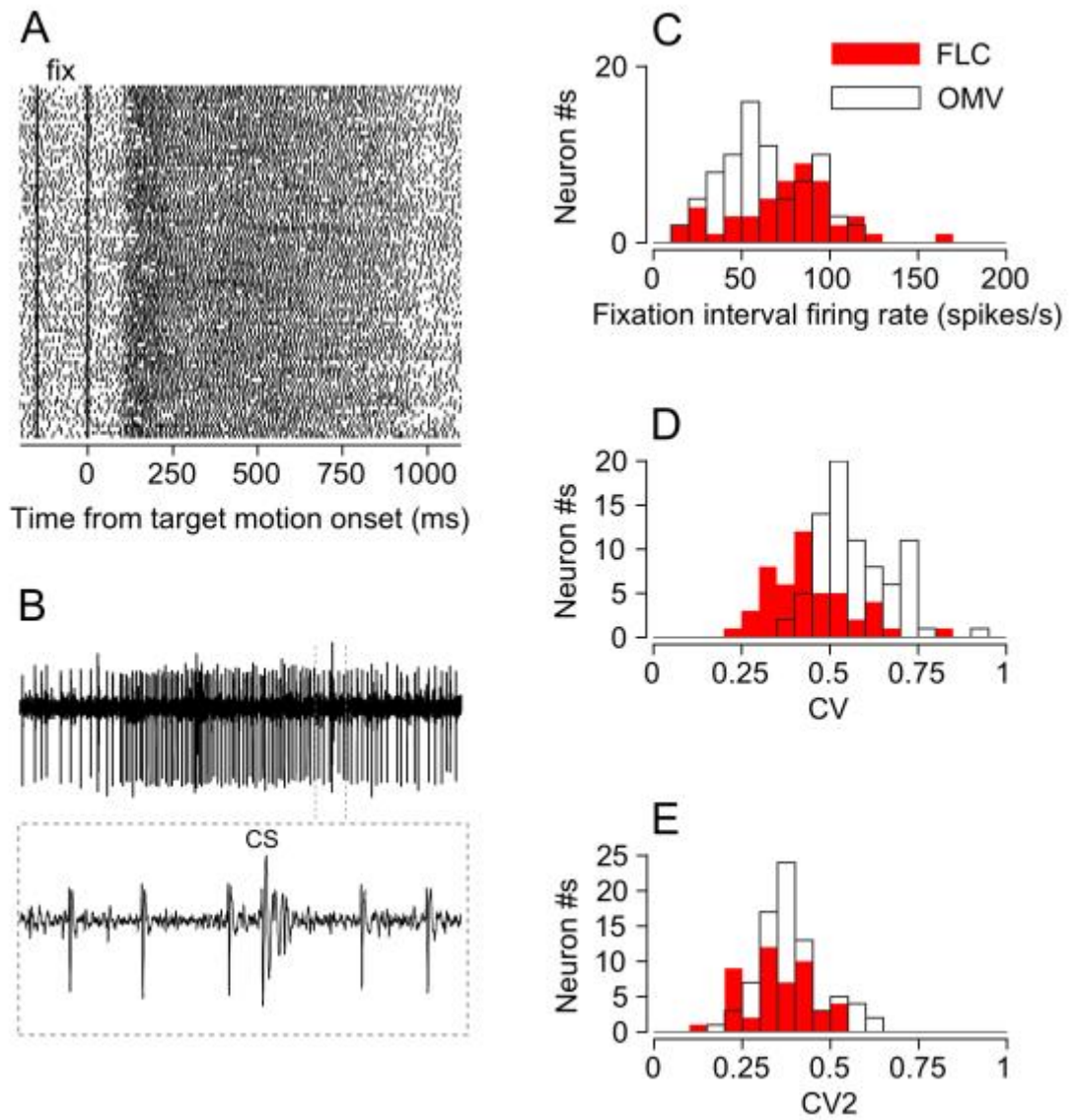


Figure 16: A, An example raster from a Purkinje cell recorded in the oculomotor vermis. Each tic mark corresponds to one spike during a trial arranged in rows. B, Voltage trace from one trial, with complex spike indicated below. C, Distribution of fixation interval firing rates between the floccular complex (FLC) and oculomotor vermis (OMV). D,E same but for CV and CV2 values.

3.3.3 Kinematic sensitivity of pursuit responses as compared between the Oculomotor Vermis and Floccular Complex

We next wanted to test the hypothesis that the activity of OMV Purkinje cells have weaker kinematic sensitivity than the activity of FLc Purkinje cells. To do this we took advantage of prior studies that show that the activity of FLc Purkinje cells can be well described as a linear combination of three variables, eye position, eye velocity, and eye acceleration during pursuit (Shidara, Kawano et al. 1993). This linear model usually accounts for greater than 75% of the variance in FLc Purkinje cell firing rates, with neurons typically having strong velocity and/or acceleration sensitivities (Medina and Lisberger 2009). If our hypothesis that OMV neurons have weaker sensitivity is true, this might manifest in two ways in this linear model, lower amounts of variance in Purkinje cell firing rate accounted for by kinematic variables, or lower valued regression coefficients. To test if any of these possibilities were true, we fit a simple linear model to each Purkinje cell in our neural populations, of the following form:

$$FR(t) = aE(t + \Delta t) + b\dot{E}(t + \Delta t) + c\ddot{E}_p(t + \Delta t) + d\ddot{E}_n(t + \Delta t) + rr$$

Here $FR(t)$ indicates the average simple spike firing rate of a Purkinje cell over time, while $E(t)$ and $\dot{E}(t)$ indicate average eye position and average eye velocity. $\ddot{E}_p(t)$ and $\ddot{E}_n(t)$ indicate the positive and negative components of average acceleration (with the values of opposite signs replaced with zeros). The regression coefficients a , b , c , and d quantify the sensitivity of each Purkinje cell to each of these components of pursuit while rr quantifies the mean firing rate of these neurons during the fixation period.

Position, and velocity averages were calculated after excising saccades from individual trials, and multiplying the horizontal and vertical components of these averages by a rotation matrix to examine the magnitude of each variable along the direction of target motion. Acceleration was calculated by numerically differentiating this rotated average velocity. This model has been previously shown to produce high quality fits to neural data recorded in the floccular complex (Medina and Lisberger 2009)

Below we illustrate two Purkinje cells, one recorded in the floccular complex (figure 17A) and one recorded in the oculomotor vermis (figure 17B). Smooth black lines in both figures illustrate the average simple spike firing rate over the course of the trial. The red lines exemplify high quality fits that can be achieved by this model. We also illustrate the proportion of this regression fit which is accounted for by position, velocity, and the positive component of acceleration individually, as illustrated by the green, blue, and purple lines respectively. Below each figure is the distribution of R^2 values quantifying the quality of fits across each population (figures 17C-D). While across both populations the fits of these linear regression models were significant, the model did a far better job in capturing responses recorded in the floccular complex. Indeed, confirming prior studies, we demonstrate that this simple linear model accounts for greater than 80% of the variance in 97.92% of floccular complex Purkinje cells, while the same model accounts for greater than 80% of the variance in only 63.29% of the Purkinje cells we recorded in the oculomotor vermis. Statistical tests confirmed that

values differed significantly between both populations of neurons (two-sample t test $p = 1.14e-9$; ranksum test $p = 1.87e-10$).

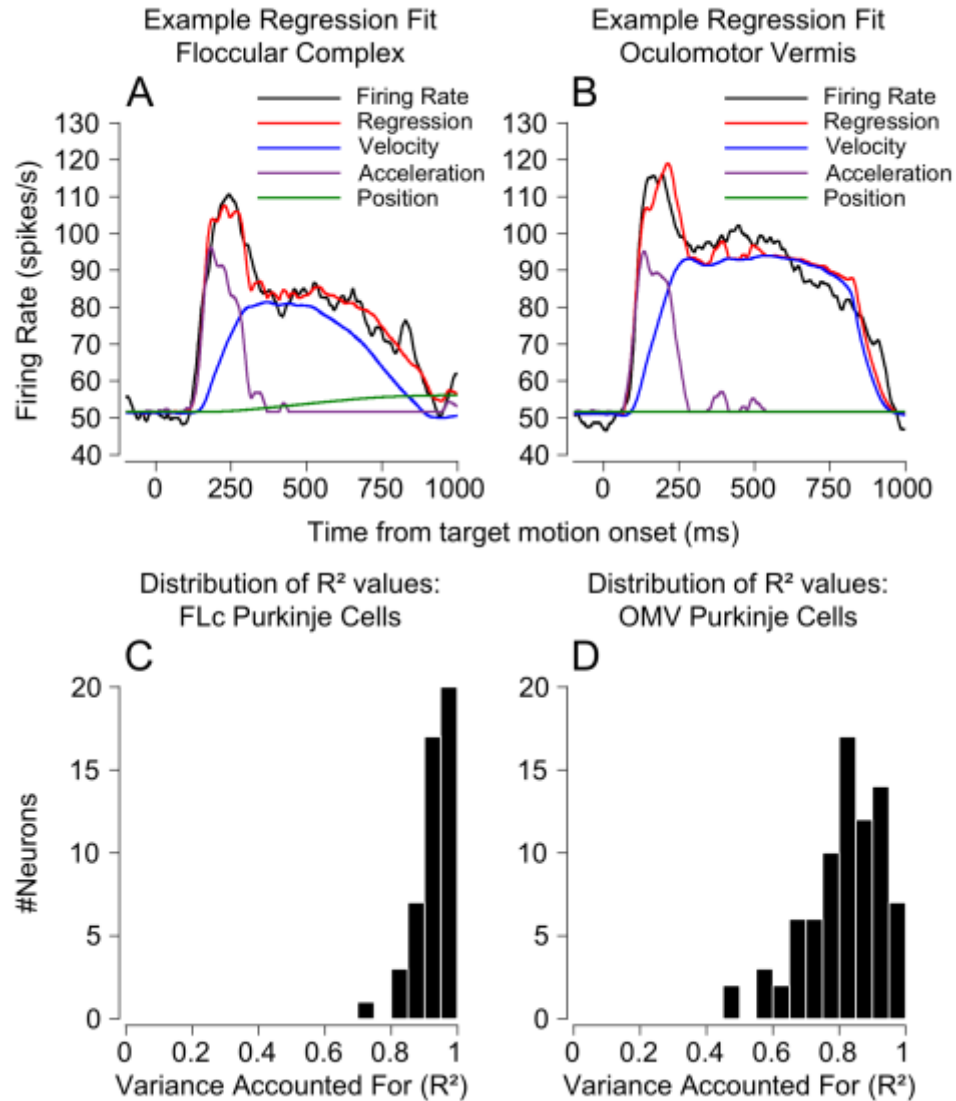


Figure 17: A, B Examples of linear regression fits to a Purkinje cells recorded in the floccular complex and OMV respectively. The closeness of the red and black lines indicates the excellent fits provided by the regression model to these cells. Other colors indicate the amount of average firing rate in each cell which is accounted for by the time varying changes in position, velocity, and positive acceleration. C, D distribution of R² values for all neurons in each population.

We next compared the regression coefficient values obtained from both populations. In figures 18A-C we plot the regression coefficients for positive and negative acceleration or velocity against the regression coefficients for position. Both populations fell into different clusters, but this is partially explained by the fact that in the OMV, the direction of pursuit which leads to the largest change in firing rate from fixation (which defined our trialset) could be decreases in activity. This is in contrast to the floccular complex, where increases in activity always define the largest change in firing rate from fixation. Therefore, there is a higher predominance of negative velocity and positive acceleration sensitivities in our OMV population. To objectively compare the degree to which the firing rates in each population were modulated by these kinematic variables, we compared absolute values of these coefficients in both populations against one another. This is illustrated in figures 18D-F. We found no differences in terms of position coefficients between populations (two-sample t test, $p = .79$, ranksum test, $p = .95$). Similarly, we found slight differences in terms of negative acceleration coefficients (two-sample t test, $p = .01$, ranksum test, $p = .01$). Differences were far larger in the case of velocity coefficients (two-sample t test, $p = 1.06e-6$; ranksum test, $p = 4.65e-6$). These differences were still larger when comparing positive acceleration coefficients (two-sample t test, $p = 1.35e-12$, ranksum test, $p = 1.85e-13$). This confirms that the separation of the clusters in figures 18A-C is not simply a function of the sign of the response profiles but is a genuine reflection of the strength of responses

themselves. By comparison to the activity of OMV Purkinje cells, FLc Purkinje cells fire over 2x (2.1926) the number of spikes per degree shift in eye velocity, and fire well over 3x (3.8760) the number of spikes per degree/s² shift in the initial positive acceleration of the eye.

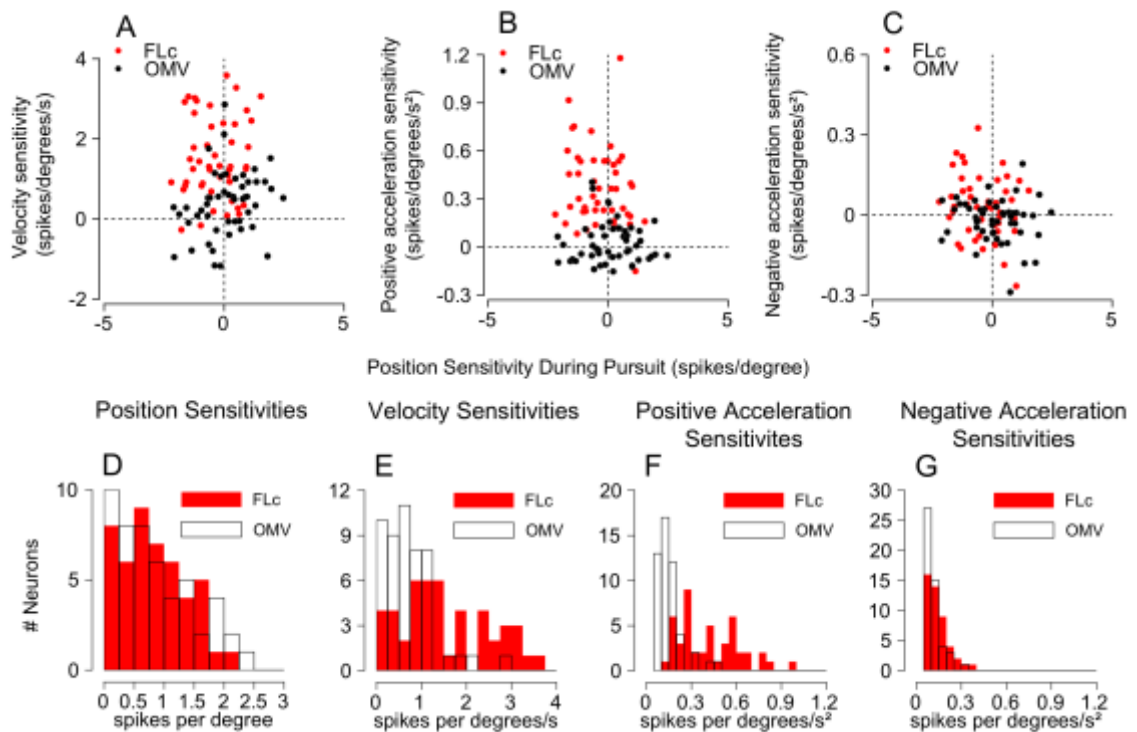


Figure 18: A, B, C regression coefficients for velocity, positive, and negative acceleration plotted against position. Each point signifies one neuron recorded in either the floccular complex (FLc) or oculomotor vermis (OMV). D-F, distribution of regression coefficients displayed independently using histograms.

3.3.4 Neuron-Behavior correlations during fixation and the open loop of pursuit: comparing the Oculomotor Vermis and Floccular Complex

We were next interested in seeing how responses in the OMV and FLc might encode changes in eye speed. To do this we took advantage of the natural variations in eye speed that occur from trial to trial. In figure 19A and B, we illustrate these trial to trial

variations for an example session, together with the trial to trial variations that occurred in a Purkinje cell which was recorded during these same trials. We focused on the period of time immediately following motion onset (during the initiation of pursuit), and only considered trials where saccades did not occur during this interval (extending up to 225 ms after target motion onset).

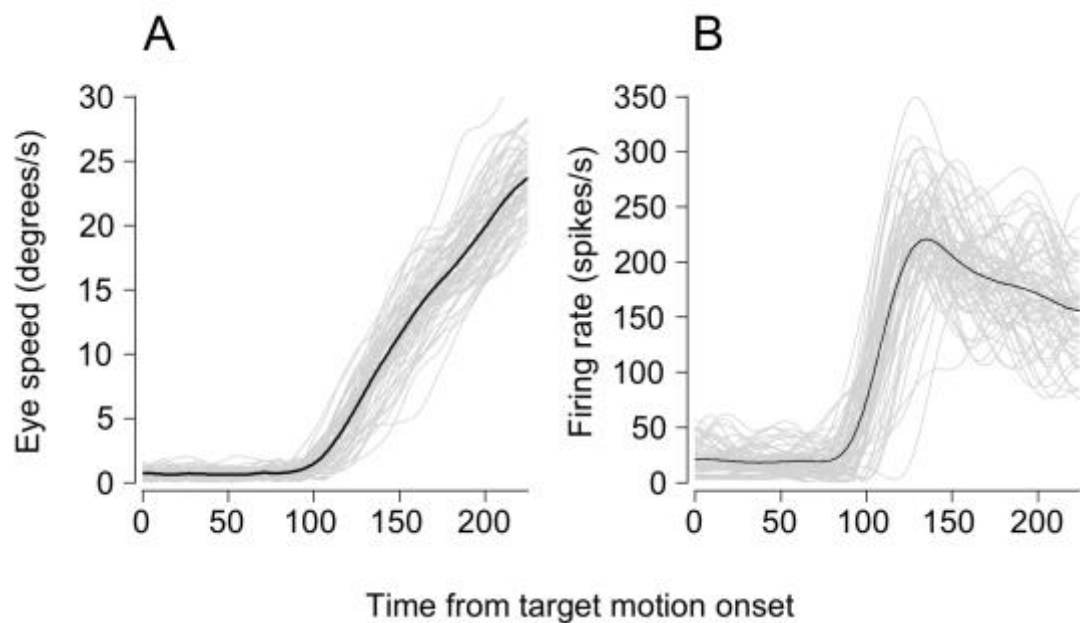


Figure 19: A, Trial by trial variations in eye speed during an example session. Thin traces signify eye speed on individual trials, black trace represents the average of the thin traces. B, Simultaneous trial-by-trial variations in firing rate that were recorded from a Purkinje cell during this session

We considered only neurons which had significant increases or decreases in firing rates during the initiation of pursuit as assessed using a two sample t-test between average firing rates during initiation (75 to 175 ms after target motion onset) and fixation (-150 ms to 0 ms before target motion onset). 61/79 neurons in the OMV passed this criterion.

All neurons in the FLc passed this criterion. We also divided neurons into those that increased and decreased their firing rate during the initiation of pursuit. As explained above, all FLc neurons increased their firing rate relative to fixation interval during the initiation of pursuit. Dividing our neurons in this way allows us to do a proper comparison between increasing FLc neurons and increasing OMV Neurons. Figure 20 illustrates clear evidence of correlations between the trial by trial variations of firing rate in floccular complex (FLc) neurons and concurrent trial-by-trial variations in eye speed that during the initiation of pursuit. The heatmap in figure 20A show average FLc-eye speed correlations across the entire population. Each pixel represents the correlation across all trials observed at a particular pair of time points. For example, time point 150,150 is the correlation between firing rates 150 ms after target motion onset with eye speed 150 ms after target motion onset. We calculated correlations for all combinations of times in eye speed and firing rate to account for the fact that firing rate changes may lead or lag eye speed changes. As can be seen, on average, the simple spikes from FLc Purkinje cells reached a peak correlation with eye speed between 100-150 ms after pursuit initiation. The same was true of both OMV increasing and decreasing cells, but the size of the correlation was much smaller (figures 20B and 6C respectively). OMV neuron peak correlations were nearly 2.5 times lower in magnitude, for either increasing or decreasing cells as opposed to their FLc counterparts. While this suggests clear differences in population structure between the FLc and OMV, it also averages away a

lot of the individual variation in our populations that we believe to be very important. For example, most FLc neurons on a per neuron basis actually reach peak correlations of .6 during pursuit initiation (Medina and Lisberger 2007). Small differences in the timing of peak correlation across our population of neurons are averaged away by this technique therefore. This technique also ignores other factors like latency that vary during the initiation of pursuit (Osborne, Lisberger et al. 2005).

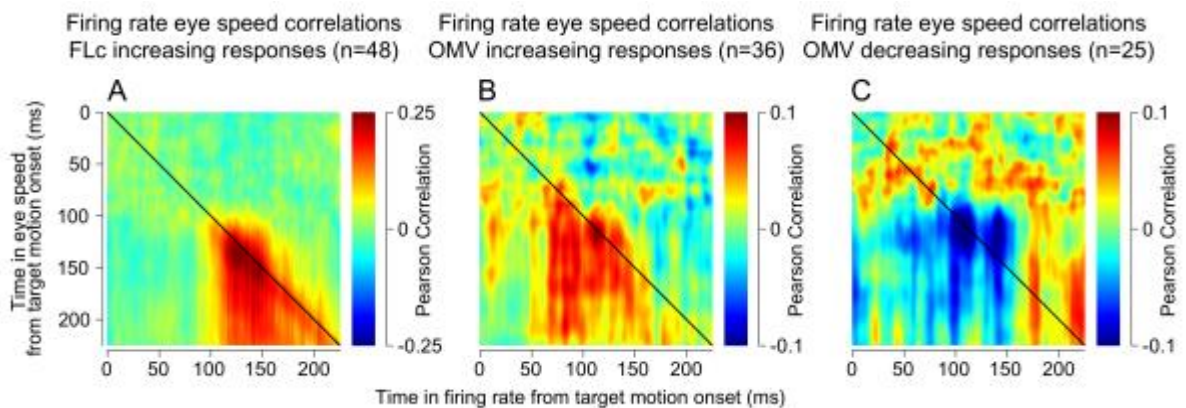


Figure 20: A, Trial-by-trial correlations between eye speed and firing rate. Each pixel indicates the size of a pearson correlation coefficient calculated between firing rate at time t on the x axis, and eye speed at time t on the y axis. Data are averaged across all floccular complex Purkinje cells. B, C same, but for OMV neurons separated according to whether they increased or decreased responses during the first 225 ms of pursuit

To deal with these issues we utilized a recently developed quantitative method that allows us to decompose the initial variations in pursuit into three components: eye speed gain, direction, and latency (Lee and Lisberger 2013). We illustrate the results of our methods below in an example session. Figure 21A illustrates the application of this technique using an example session recorded in the floccular complex. We calculated

the gain associated with eye movements on each trial and have plotted eye speeds associated with the top third of gains (fast trials) against eye speeds associated with the lower third of gains (slow trials). The clear separation in curves demonstrates the effectiveness of our algorithm in calculating these values. In figure 21B we show a similar division for latency, showing early and late trials. In figure 21C we show a similar division for direction by showing the component of velocity we calculate for trials along the direction orthogonal to target motion. We can divide trials into those that are biased positively or negatively biased away from the direction of target motion. Below each division of trials, we have also divided the firing rate between these conditions (figures 21D-F). This demonstrates the degree to which this particular FLc Purkinje cell's simple spikes are modulated by these three separable parameters of pursuit.

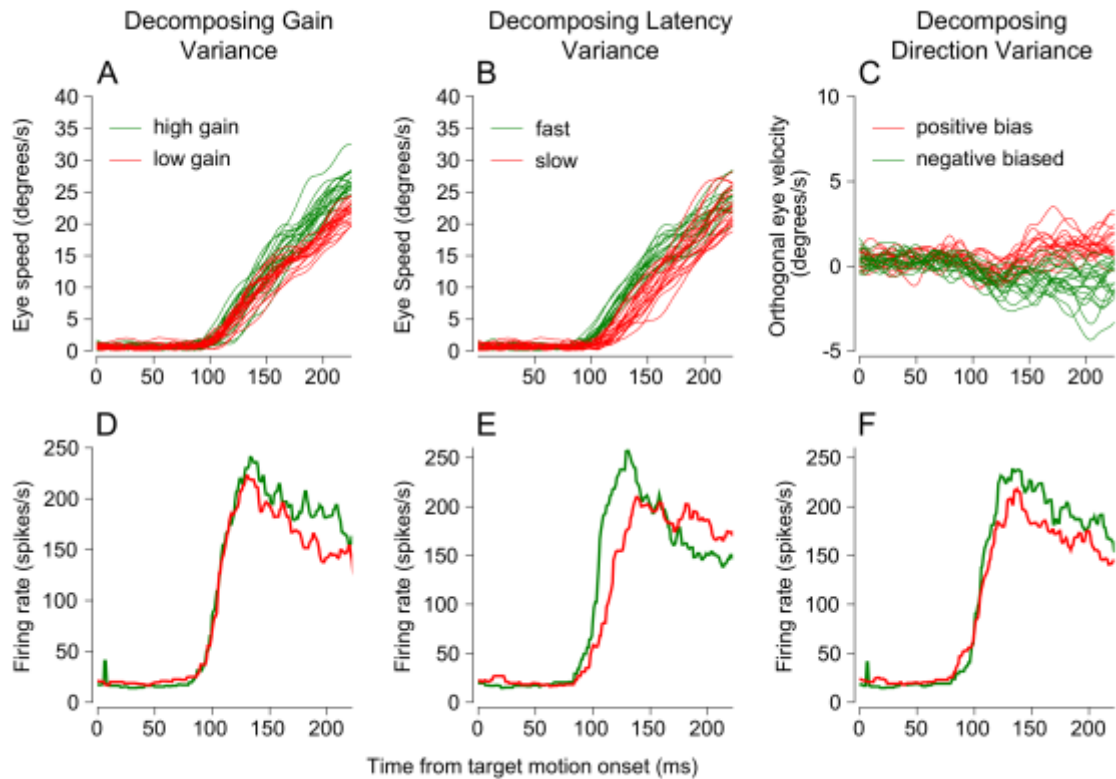


Figure 21: A-C, Plots of pursuit speed in an example session, separated according to the upper and lower third percentiles of gain, latency, and direction respectively. D-F, Corresponding average firing rates in the same session, averaged across trials in A-C.

In figure 22A we extend this approach to calculate the moment by moment correlation a neuron's firing rate had with pursuit gain, pursuit direction, and pursuit latency. This confirms more clearly what you see in figures 21D-F, that the firing rate of this neuron reaches its maximal correlation with latency and direction shortly after the initiation of pursuit, and ramps up to a peak correlation with speed gain later on during the initial pursuit interval. It also more accurately quantifies the size of peak neuron-behavior correlations with speed, which reaches a maximum of .5. We calculated time varying

correlations like this for all neurons within our FLC and OMV populations and calculated the number of neurons that had a significant neuron-behavior correlation at any particular point in time. The results are plotted in figure 22B for all neurons in the FLC and figure 22C for all neurons in the OMV.

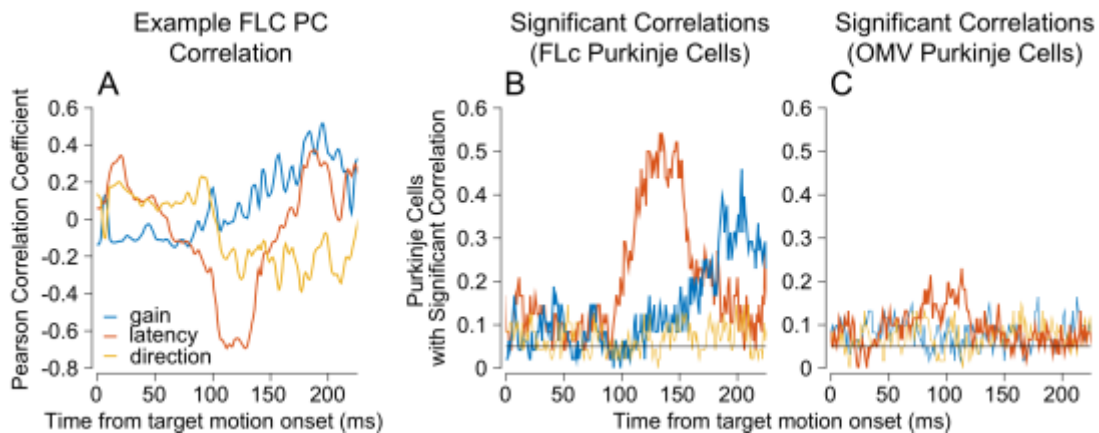


Figure 22: A, The correlation between an example FLC neuron’s firing rate with the trial-by-trial variations in gain, latency, and direction respectively. B, C Fraction of neurons in in the FLC and OMV with significant correlations with gain, latency, and direction. Black horizontal lines indicate expected level of type I error.

As is apparent by eye, the proportion of FLC neurons with significant trial by trial correlations between firing rate and both eye speed and latency was significant, but at different points in time. By contrast, firing rates in the OMV rarely reached strong correlations with any aspect of pursuit, with the exception of latency, where 122 ms after target motion onset just over 20% of neurons showed a significant correlation with latency. It’s clear therefore that the FLC population is more homogenous than the OMV population, in terms of the timing of peak correlations across all neurons. We also

determined that fixation related activity (not shown) was not strongly correlated with the parameters of movement during the initial period of movement.

3.3.5 Discussion

We recorded Purkinje cell activity in the oculomotor vermis (OMV) of monkeys performing smooth pursuit eye movements and compared the response properties of these neurons to the activity of Purkinje cells recorded in the floccular complex (FLc). We found that the two populations were strongly different, at all levels of analysis.

First, our analysis demonstrated that fixation related activity in the OMV is more variable from trial to trial than in the FLc, as assayed using the coefficient of variation. The equivalence of CV2 between populations suggests that this difference in CV does not arise from differences in the biophysical properties of both populations of Purkinje cells. However, it is commensurate that idea that OMV Purkinje cells have greater modulations in firing rate during the fixation interval. We did not find strong evidence that such activity was correlated to the parameters of pursuit that define behavior during the open loop. It is possible that the source of these modulations may be some slow trial to trial modulation in activity, related to global factors like attention or reward that we did not control for.

Our findings confirmed that the sensitivity of OMV Purkinje cells to kinematic aspects of pursuit is very different from Purkinje cells in the FLc. Response properties in the OMV were less accounted for by the time varying changes in average position,

velocity, and acceleration. Moreover, regression coefficient values were lower. We believe this is evidence that the OMV makes a smaller contribution to pursuit eye movements than hereto hypothesized (Krauzlis 2004). We also believe it could explain the smaller deficits that are known to occur following OMV lesions as opposed to FLc lesions.

We also examined the trial-by-trial correlations that occur between simple spikes and variations in speed gain, latency, and direction. We found that these correlations were larger in the FLc (specifically for speed and latency) than in the OMV. We caution the reader not to assume that this suggests that OMV neurons do not drive pursuit responses. Such correlations are more a statement of the structure of the neural population than of its role in the control of behavior, per say (Medina and Lisberger 2007). For example, if neurons in our OMV population were independent in terms of their responses, then we would expect integration of their responses by structures downstream of the OMV to average away the size of any individual's Purkinje cells contribution to pursuit. Therefore, the conclusion that one should draw from our analysis of neuron-behavior correlations is that floccular complex neurons are more homogenous, or have higher sources of shared variation that cannot be averaged away downstream. These data also suggest that OMV neurons are an unlikely source of trial-by-trial variation in eye speed. Why is the structure of neuron-behavior correlations so different between our populations of OMV neurons and FLc neurons? Computational

analysis suggests that trial by trial correlations between simple spikes and pursuit are influenced by the signal-to-noise ratio of neurons under consideration (Chaisanguanthum, Joshua et al. 2014). The fact that regression coefficients are typically far lower in our OMV population implies that signal-to-noise ratio is lower in this population. Further analysis is required to see whether neuron-behavior correlations in our population of OMV neurons are actually commensurate with what would be expected, given their signal amplitude. Regardless of their origin, we find the small values of neuron-behavior correlations very interesting however. Prior studies have clearly shown that correlations between firing rates in neural populations increase as one proceeds from the sensory periphery to the motor periphery. The size of neuron-behavior correlations we observed in the OMV is close to values found in cortical regions far removed from the motor periphery, like areas MT, FEF, or LIP. This would suggest that OMV neurons are further functionally removed from the motor periphery than their FLc counterparts. This is somewhat expected, given that OMV Purkinje cells are hypothesized to be at least 3 synapses removed from the motor periphery. This is in contrast to FLc Purkinje cells which are 2 synapses removed from primary motoneurons innervating the eye muscles. While we did find correlations between firing rates in the OMV and pursuit latency, these need to be more carefully examined. A limitation in correlating firing rate with behavioral latency during movement initiation is that it cannot take into account changes in neural latency that can occur during the same

period of time. Future studies and analyses will need to be done to more carefully examine this issue, therefore.

Prior studies have often assumed that the fact that pursuit remains after lesioning of the floccular complex implicates the OMV in providing residual drive to the pursuit system (Robinson and Fuchs 2001). While still possible, the nature of the responses we have recorded in the OMV suggest to us that it is quite possible that cerebellar areas outside the OMV are providing the compensatory drive witnessed after floccular complex. In section 5 we highlight other candidate structures in the cerebellar cortex that might provide stronger drive to the pursuit system.

4. A quantitative comparison of the encoding of smooth pursuit eye movements and saccadic eye movements by Purkinje cells in the oculomotor vermis

4.1 Introduction

Voluntary eye movements fall into two categories, smooth pursuit eye movements that are elicited when a primate attempts to foveate a moving target, and saccadic eye movements that orient the fovea of the eye towards different locations in the visual periphery (Robinson and Fuchs 2001). Several important differences exist between the saccadic and smooth eye movement systems. Firstly, in terms of behavioral output, saccades are ballistic. They reach peak speeds of over 600 visual degrees per second and occur within 50 ms (Harris and Wolpert 2006). Like fast movements of the arm they occur too quickly to be influenced by feedback from the periphery, and must be programmed entirely in advance. Moreover, unlike smooth pursuit eye movements, saccadic eye movements can be executed at will, and under a larger variety of conditions (Krauzlis 2005). By contrast smooth pursuit eye movements slower, reaching peak velocities of perhaps 60 degrees per second and are typically longer in duration than saccades (Lisberger and Westbrook 1985). These movements are also continuous or “closed loop” and are continuously adjusted by feedback from the periphery. Psychophysical analysis also indicates that the driving sensory information that elicits both types of movements is different, with target position instructing the initiation of saccadic eye movements and target velocity instructing the initiation of smooth pursuit

eye movements (Rashbass 1961). There are multiple instances in which these two systems interact, however. First, both movements are coordinated when tracking moving targets (Gardner and Lisberger 2002, Missal and Keller 2002). Second both of these types of movements seem to be controlled by partially overlapping neural structures that are presynaptic to the motoneuronal pools in the brainstem that move the eye (Krauzlis 2004).

The capacity of any neural structure to encode both types of movements is nonetheless surprising, however. While both pursuit and saccadic eye movements can be executed over a range of speeds, it is generally accepted that peak speed for pursuit occurs around a maximum of about 60 degrees per second, while peak saccade velocity can reach well over 10 times this rate. Excluding small fixational saccades, this suggests roughly 100 times more force is exerted on the eye during a saccadic eye movement than during a pursuit eye movement. However, both behaviors display a remarkable range of sensitivity to target properties. Pursuit thresholds during the open loop period usually fall within 11-15% of target speed (Osborne, Hohl et al. 2007) . For visually guided saccades accuracy is even higher, usually falling within 2.5% of average eccentricity (Kowler and Blaser 1995). What this implies is that the oculomotor system needs to maintain a large range of values over which acceleration and eye velocity must be controlled. There is a problem however, namely that neurons have a limited firing rate to encode the forces necessary to generate both types of eye movements. If a neuron can

sustain a maximum firing rate of say, 300 spikes/s within the average time window for the initial acceleration of the eye which is 100 ms, the brain only has roughly 30 spikes with which it can encode changes in eye speed or acceleration. A key question that arises is how this response range can account for the behavioral accuracy that is observed. One solution is to encode both movements separately. For example, in many structures it is possible to localize subpopulations of neurons that are sensitive to either slow or fast eye movements (Tanaka and Lisberger 2002). This suggests that both movements can be programmed or controlled separately, taking advantage of each neural populations respective bandwidth, and combined later downstream. However, this may be the exception rather than the rule. In plenty of oculomotor brain structures neurons seem sensitive to both types of movements (Krauzlis 2004). At present very few studies have examined how this latter encoding scheme can obey the constraints imposed by both types of movements.

While the problem of encoding both ballistic and continuous movements is not unique to the eye movement system, eye movements have traditionally provided a rich context within which to investigate such issues (Kornhuber 1971, Lisberger 2010). Moreover, multiple parallels exist between how these problems are dealt with in the oculomotor system and skeletomotor system (Robinson 1986). Indeed a classic problem in skeletomotor control also considers how fast and slow movements of the arm can be independently controlled by the brain (Desmedt 1978). Therefore, we believe that

analysis of this problem in the context of eye movement control might shed light on how this problem is solved in the context of other forms of movements.

Here, we analyze the response properties of one structure that is believed to contribute to both fast and slow eye movements, the oculomotor vermis (OMV). The OMV is hypothesized to drive the acceleration of the eye during both saccadic and smooth pursuit eye movements. This hypothesis has been made on the basis of lesion and pharmacological inactivation studies (Robinson, Straube et al. 1993, Robinson, Straube et al. 1997, Robinson and Fuchs 2001). Microstimulation experiments have also suggested a role of the OMV in controlling both types of eye movements, but along separate direction axes. In a classic study, (Krauzlis and Miles 1998), researchers discovered that microstimulation of the OMV evokes saccadic eye movements ipsilateral to the site of microstimulation and smooth pursuit eye movements contralateral to the site of microstimulation. Finally, recordings in the OMV have indicated a large number of neurons fire during the execution of both saccades and pursuit (Sato and Noda 1992). On the basis of these findings, we hypothesized that the signals emanating from the OMV were likely to encode acceleration of saccadic and smooth pursuit eye movements along a contralateral-ipsilateral axis separately. This would allow downstream structures to easily decode the responses of these neurons. We recorded Purkinje cells in the OMV as monkeys executed visually guided saccadic eye movements or tracked moving targets. We found a large proportion of neurons that were modulated by both

saccadic and pursuit eye movements. Analysis of our neural populations suggests that despite the overlap of tuning for saccades and pursuit, neurons were on average less likely to respond to pursuit in the direction that elicited maximal firing rate for saccades and vice versa. Indeed, at a population level we find that neurons are very sharply tuned, and encode pursuit and saccades along different axes (both not necessarily a contralateral-ipsilateral axis). Finally, while individual neurons were weakly sensitive to kinematics of eye movements, we found that at a population level neurons encoded a combination of acceleration and velocity signals for both saccades and pursuit but in a strongly non-linear manner.

4.2 Methods

Subjects, and methods for neural recording for the current set of experiments are covered in detail in Chapter 2. We briefly review the unique details of our experiments below

4.2.1 Visual stimuli and Experimental Design

In this work we analyze data from monkeys performing two types of trials. Both trial type began with the animal fixating on the center of the screen. In one block of trials the target would undergo step-ramp target motion along one of eight radially spaced directions at 20 degrees per second for 750 ms. This would cue the animal to smoothly track the target. In a second block of trials the target would undergo a sudden 10-degree step away from the center of the screen, cueing the monkey to elicit a visually guided

saccade towards the target in question. Targets jumped along the same 8 radially spaced directions that target motion occurred along in pursuit trials. The interval between fixation and target motion was randomized (400-600 ms) to prevent anticipatory pursuit and was fixed (500 ms) for visually guided saccades. After foveating the target in saccade trials, animals were required to hold fixation for an additional 500 ms to receive reward. Following target motion in pursuit trials, the target would step forward 1 degree and the animal was required to hold fixation on the target for 600 ms in order to receive reward. During the performance of these tasks, we would record individual Purkinje cells in the oculomotor vermis. Many of these experiments were performed alongside the experiments presented in prior chapters.

4.2.2 Data Analysis

All analyses were performed Matlab (Mathworks). Much of our analysis focused on the analysis of firing during the acceleration of the eye in saccade and pursuit trials. Because of the differences in saccade and pursuit latencies, this window was slightly different for each trial. For saccades it occurred from 100-300 ms after target step, while for pursuit it occurred 75-225 ms after target motion. We excluded pursuit trials with saccades happening between 0-225 ms after target motion onset. This ensured that we could analyze Purkinje cell responses related to the sensorimotor transformations occurring in the open loop of both saccade and pursuit trials. We excluded saccadic trials where fixational saccades occurred 100 ms before saccade onset, as well as saccade trials where

blinks occurred during saccade initiation. Trials were discarded using a custom program.

We recorded a total of 84 Purkinje cells in the OMV (41 from monkey V, 43 from monkey Y). We had relatively simple criterion for what would count as a significant response, using a two sample t-test to compare the firing rates in the fixation window vs the acceleration window in pursuit and saccade trials. Firing rates were estimated as in prior chapters, using the reciprocal of the interspike interval (Lisberger and Pavelko 1986). So long as the neuron responded significantly towards one direction of either pursuit or saccades it was considered to be eye movement related. 77/84 neurons were categorized as eye movement responsive in this manner. In analysis presented below we did not find that excluding our 7 non-eye movement responsive neurons changed results substantially, and so we elected to include all neurons in our analysis presented below.

Directionality was assessed slightly differently as the data were aligned on peak eye acceleration. Firing rates were either calculated in a 50 ms window centered on peak eye acceleration in both pursuit and saccade tasks. Tuning curves were fit to the simple spike firing rates of both sets of neurons using a von mises tuning function, which also allowed us to calculate how directionally selective neurons were. Directional sector width was calculated as 2 times the circular standard deviation of the neurons average response along the eight radially spaced directions of pursuit or saccades.

Population responses were estimated in two ways. The first was simply averaging the responses of all Purkinje cell simple spikes together. We also estimated firing rates and confidence intervals on the population response using a simple bootstrapping procedure. We drew, from our population of 70 neurons, sets of 50 neurons with replacement (roughly the number of Purkinje cells that synapse onto a deep cerebellar nuclear neurons). We averaged these neurons together, and calculated mean +/- 1 standard error of the mean for these pseudopopulations 50 times. We took this as an estimate of responses we would expect in the caudal fastigial nucleus, downstream of the OMV.

We fit a simple model to each set of neural responses in in the OMV during saccade and pursuit trials. This model was very similar to the model used to describe neural responses in chapter 3. We list it below.

$$FR(t) = aE(t + \Delta t) + b\dot{E}(t + \Delta t) + c\ddot{E}(t + \Delta t) \quad (1)$$

Here $FR(t)$ indicates the average simple spike firing rate of a Purkinje cell over time, while $E(t)$ and $\dot{E}(t)$ indicate average eye position and average eye velocity over time. $\ddot{E}(t)$ is average acceleration over time. The regression coefficients a , b , c , and d quantify the sensitivity of each Purkinje cell to each of these components of pursuit while rr quantifies the mean firing rate of the neuron during the fixation interval preceding target motion onset or target step.

4.3 Results

4.3.1 Task Differences

In figure 23 we illustrate the key behavioral differences between saccades and pursuit made towards a target that moved or jumped to right (ipsilateral). Animals were asked to repeatedly saccade to a target that underwent a sudden step in position (dashed line in figure 23A) or to repeatedly track a target that underwent step-ramp target motion (dashed line in figure 23B). These stimuli elicited pursuit or saccadic eye movements at an average latency of 100 ms for pursuit and 200 ms for saccades. The peak velocity of the eye during saccade trials (figure 23B) reaches well over 10x that of the eye during pursuit trials (figure 23E). Consequently, the peak acceleration of the eye is 100x larger during saccade trials (figure 23C) than during pursuit trials (figure 23F). While there were some anisotropies in saccades and pursuit made in different directions, eye velocity and acceleration during pursuit were always one log order smaller than these values during saccades.

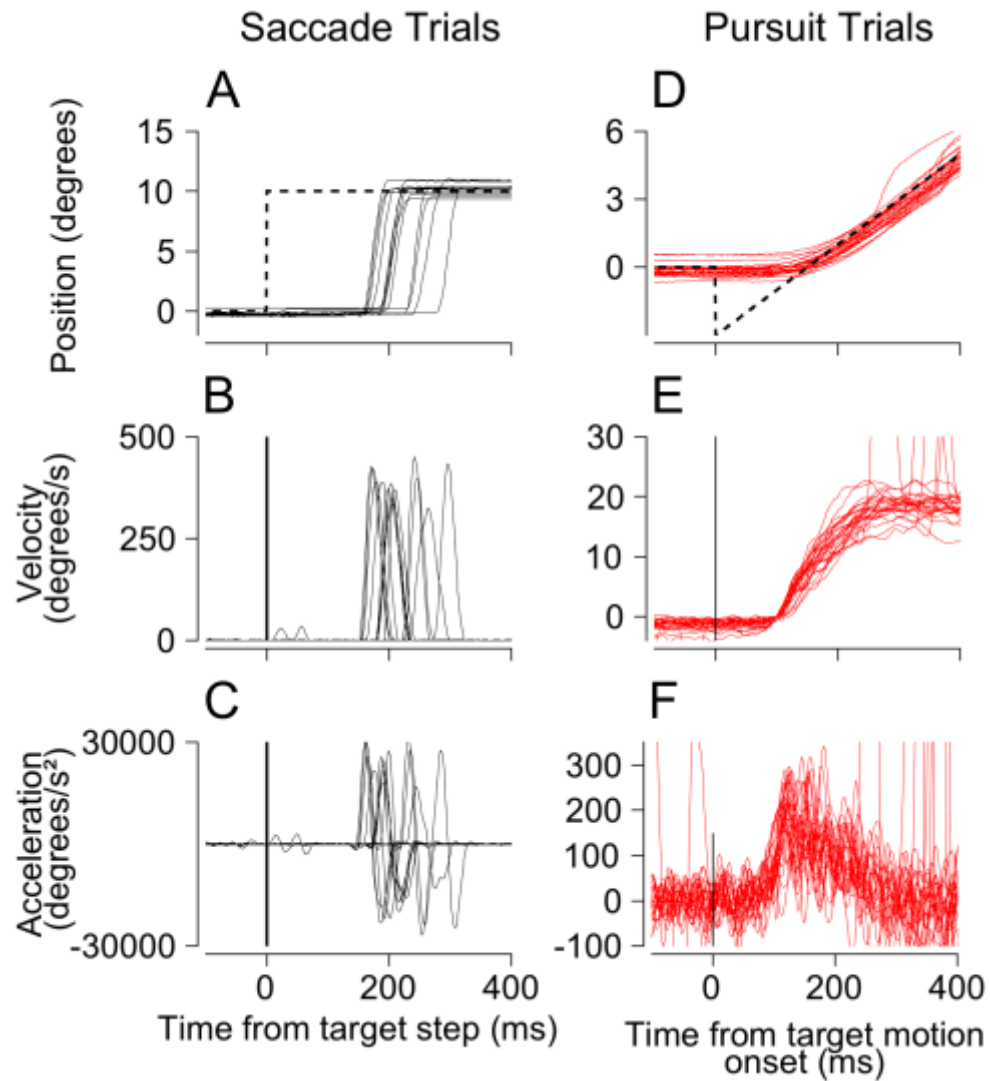


Figure 23: A-C Example position, velocity, and acceleration traces during saccade trials. D-F, Example position, velocity, and acceleration traces during a rightward set of pursuit trials. Dashed lines indicate target position, smooth lines indicate eye position, velocity, or acceleration.

4.3.2 Directional Selectivity of Individual Purkinje Cells During Pursuit and Saccades

While animals performed these two tasks, we recorded the activity of Purkinje cells in the Oculomotor Vermis (OMV) of two monkeys. Purkinje cells were identified by their

characteristic “complex” spike as illustrated in section 3.2.2. Our analysis only considers change in simple spikes that occurred during the performance of these task. Of the 84 Purkinje cells we recorded, 77 had significant task related activity (see methods for our criterion for determining significance). In figure 24, we illustrate a raster plot which shows the response of one Purkinje cell’s simple spikes along 8 different directions of pursuit (figure 24A) and saccades (figure 24B). Many cells in our population were modulated by saccade and pursuit direction like this one. We next ran a one-way anova on average firing rates within a 50 ms window centered on peak eye acceleration during either pursuit or saccade trials and across target direction conditions. 39/84 Purkinje cells in our population exhibited directional modulation during pursuit trials, while 61/84 Purkinje cells in our population exhibited directional modulation during saccade trials. 33/84 Purkinje cells exhibited directional modulation during both saccade and pursuit trials. Based on prior studies outlined in our introduction, we hypothesized that neurons in the OMV should have anti-parallel directional tuning for pursuit and saccades. More specifically, we hypothesized that neurons would be tuned ipsilateral to the site of recording during saccade trials and contralateral to the site of recording during pursuit trials. To test this hypothesis, we calculated the preferred directions for

each neuron during pursuit and saccade trials.

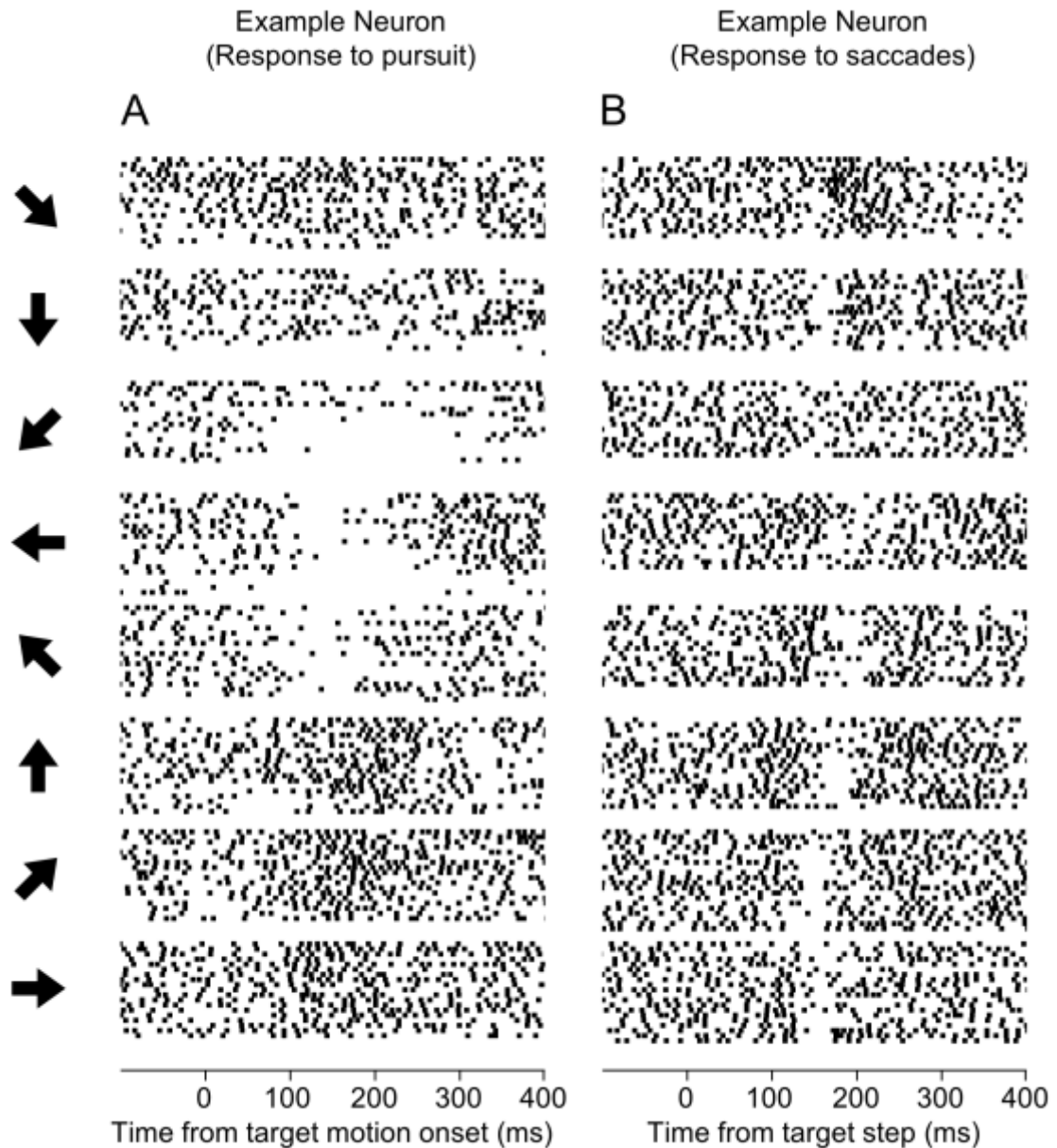


Figure 24: A, B Simple spikes recorded from an example Purkinje cell during both pursuit (A) or saccade (B) trials. Direction of the movement is indicated by the arrows on the left. Each tick mark represents one spike on one trial (arranged in rows). This particular neuron was inhibited during leftward (contralateral) pursuit, and rightward (ipsilateral) saccades.

To calculate preferred directions, we averaged firing rates during pursuit or saccade trials in a 50 ms window centered 25 ms before peak eye acceleration during pursuit or saccade trials. This was the same window used to test for significant directional selectivity. This yields two, 8x1 vectors which described the firing rate of each neuron across 8 directions of pursuit or saccades. The circular mean of each vector provides an estimate of the preferred direction for each neuron during pursuit and saccade trials independently. We analyzed data for neurons with only significant directional tuning first, as assessed by a one-way anova above, and found the results were not qualitatively different from the distribution of the rest of our data, so we elected to include all neurons in subsequent analysis. In figure 25, we illustrate the distribution of these preferred directions as calculated during each set of trials. Figure 25A illustrates the distribution of preferred directions calculated separately from saccade and pursuit trials for any neuron that was modulated by eye movements. Figure 25B is similar, but restricted to neurons which are modulated by both pursuit and saccadic eye movements. The distribution of preferred directions during saccade trials was consistent with coming from a uniform circular distribution ($p = .4733$ or $p = .2439$ for all neurons and jointly modulated neurons respectively, omnibus test for non-uniformity). The same held for directional tuning assessed during pursuit ($p = .6328$ and $p = .9188$ for all neurons and jointly modulated neurons respectively, omnibus test for non-uniformity).

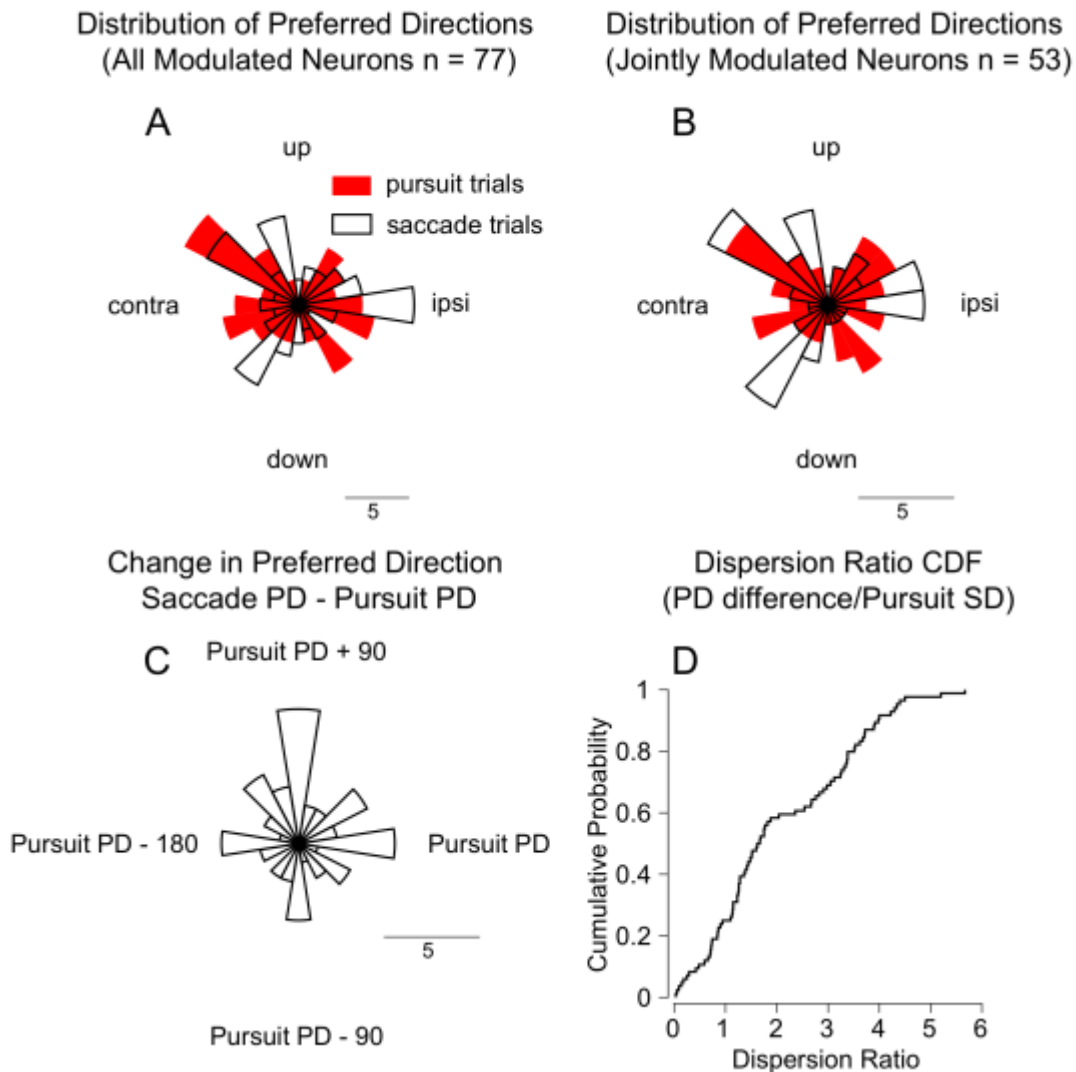


Figure 25: A, Distribution of preferred directions calculated separately from pursuit (red) and saccade (gray) trials. B, The same, but only for neurons that were significantly responsive to both saccade and pursuit. C, For jointly modulated neurons, the distribution of saccade preferred directions relative to pursuit preferred directions. D, The cumulative distribution describing the size of the dispersion ratio for the subpopulation of jointly modulated neurons.

This strongly rejects our hypothesis that neurons would be preferentially selective to ipsilateral saccadic eye movements and contralateral pursuit eye

movements. We also tested whether neurons might be organized in an opponent manner, with the preferred directions for saccade trials being 180 degrees opposite to the preferred direction of pursuit trials. We reasoned that this also might account for the effects of microstimulation outlined in the introduction. We calculated the preferred direction of each Purkinje cell during saccade and pursuit trials and looked at the distribution of preferred directions calculated from saccade trials when they were rotated *relative to* the distribution of preferred directions calculated from pursuit trials (figure 25C). We divided preferred direction differences by the circular standard deviation of firing rates during pursuit tuning trials. We call this a dispersion ratio, and it is simply a measure of how many standard deviations away from the pursuit preferred direction the saccade preferred direction lies. Figure 26D makes it apparent that over 80% of our population have saccade preferred directions that are within one standard deviation of pursuit preferred direction. This suggests that tuning curves, assessed separately on pursuit and saccade trials, overlap to a substantial degree. In the next section, we wondered what the consequences of this individual neuron tuning structure might be upon population responses.

4.3.3 Directional selectivity at a population level during pursuit and saccade trials

We wanted to test whether there may be some directional organization to our population that was not accounted for by tuning at the single neuron level. Prior work has suggested that population responses can be more sharply tuned to movement

direction than individual neurons in the cerebellum (Herzfeld, Kojima et al. 2015) . We first considered whether there may be some organization in the population response as a function of target direction. We calculated average firing rates for each Purkinje cell across each set of 8 target conditions during both pursuit and saccade trials. We next calculated the mean firing rates during the initial acceleration of the eye in both saccade and pursuit trials. Ultimately we were left with two, 84x8 matrices that describe the average acceleration interval firing rate organized by target direction, across our population during both sets of trials. We did a one-way analysis of variance on these matrices and found no effect of direction during either saccade (one-way analysis of variance, $p=.809$) or pursuit trials (one-way analysis of variance, $p=.9794$).

This situation became very different if we aligned each neuron to its preferred direction. For each neuron, we calculated the target condition that led to the largest increase in firing rate during pursuit and saccade trials separately. We then rearranged each neuron's firing rates relative to this direction. When we averaged our neural populations together in this way, strong population level directionality emerged. In figure 26A and B we show the population averages in 8 directions for pursuit and saccades. The red curves illustrate the results of averaging together Purkinje cells along their preferred directions during pursuit and saccade trials considered separately. Other colors illustrate what happens to population averages as one moves away from each neuron's preferred direction in 45 degree intervals. In figures 26C and D we illustrate

the tuning curves of population vector that result from this organization. A one-way analysis of variance confirmed what is apparent visually, that aligning our data on simple spike preferred direction yielded a population vector that was sharply sensitive to direction during saccade trials ($p = 4.22e-5$) and pursuit trials ($p=3.86e-5$).

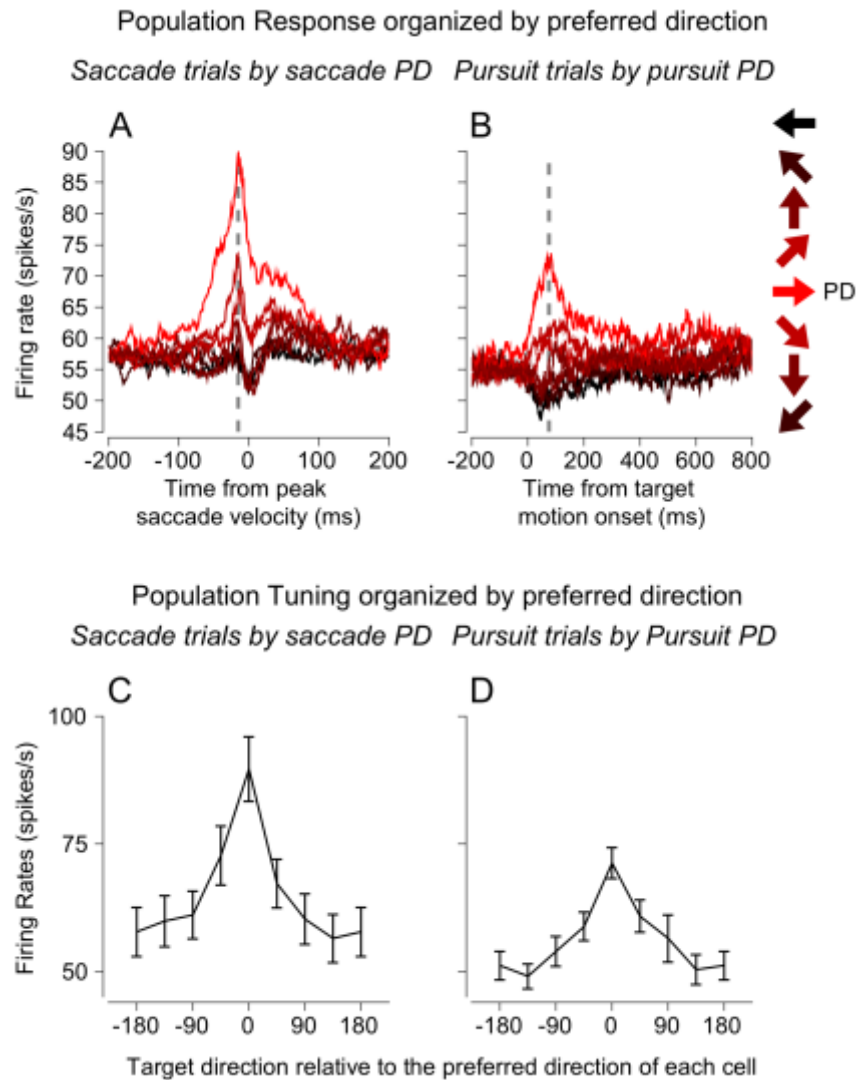


Figure 26: A, Population responses during saccade trials with neurons organized according to their saccade preferred direction. B, Population responses during pursuit trials with neurons organized according to their pursuit preferred

direction. Arrows indicate direction of eye movements relative to the preferred direction (illustrated in red). C, D Firing rates across target directions assessed at dashed lines in panels A and B.

Even more interestingly, when we aligned saccade trials to pursuit preferred direction or vice versa, responses in the opposite condition were suppressed (figures 27A-D). In figure 27D we show the population response, during pursuit trials, averaged along each neurons saccade preferred direction. In figure 27D we show the population response, during saccade trials, averaged along each neurons pursuit preferred direction. Ultimately, the directional sensitivity of the population to pursuit eye movements was lost if each neuron was aligned to its saccade preferred direction and vice versa (one-way analysis of variance $p > .95$).

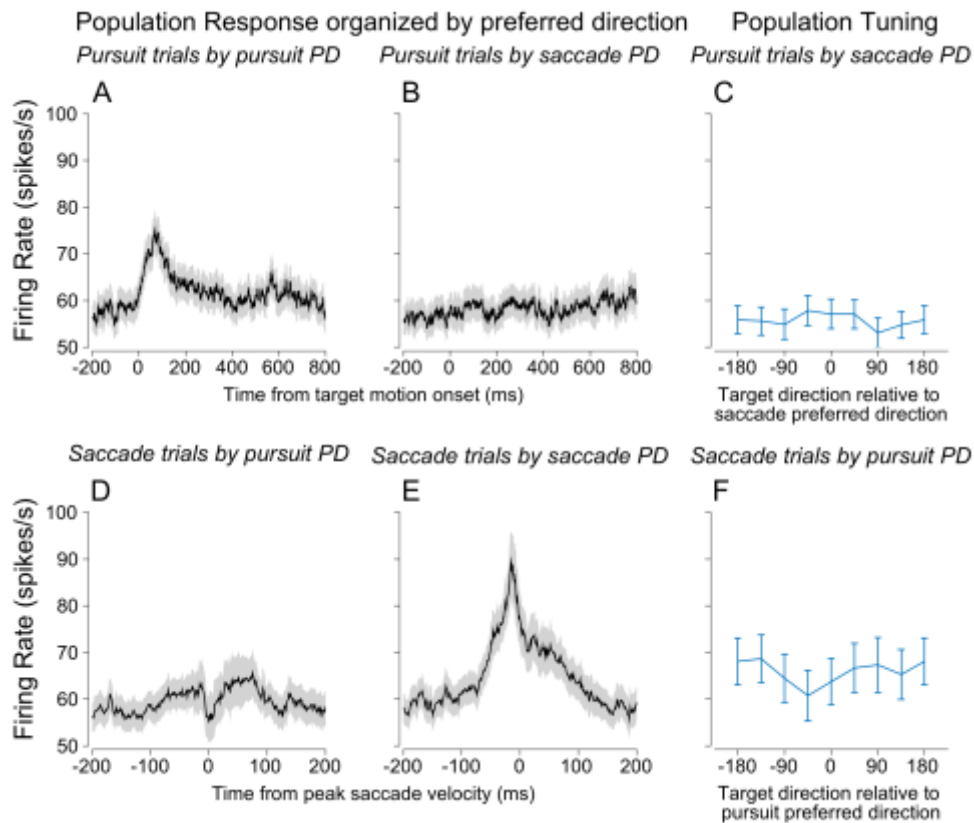


Figure 27: A, B Population response during pursuit trials when all trials are aligned pursuit and saccade preferred direction respectively. D, E same but for population response to saccade trials. C, F Population tuning curves, during pursuit and saccade trials, when neurons are organized along their saccade and pursuit preferred directions respectively.

4.3.4 Kinematic sensitivity of Individual Purkinje Cells during Pursuit and Saccade Trials

We next wanted to test the hypothesis that neurons in the OMV share sensitivity to some common kinematic variable that describes pursuit or saccades. Prior research has suggested that the OMV might be responsible for the acceleration of the eye during the initiation of both saccades and pursuit (Robinson, Straube et al. 1997, Takagi, Zee et al. 2000). Therefore, we hypothesized that regressing firing rate against position,

velocity, and acceleration would demonstrate our populations to be dominated by similarly valued acceleration sensitivities. We first needed to develop an objective criterion that would allow us to compare each neuron's sensitivity to the main kinematic aspects of pursuit and saccadic eye movements. To do this we took the direction of responses for each neuron that led to the maximal increase in firing rate for pursuit and saccadic eye movements (separately). We aligned neurons to movement initiation and considered responses in a time window that encompassed movement duration. For pursuit, this interval started 100 ms before pursuit onset to 700 ms after. For saccades, this interval was started 100 ms before peak saccade speed to 100 ms after. We regressed average firing rates in these time windows against the average eye position, velocity, and acceleration during these same time windows (see equation 1 in methods section). This allowed us to quantify the selectivity individual neurons had for each kinematic variable. In figure 28A and B we illustrate an example of the median quality of fits that were achieved by this process. While this model does a poor job in capturing the higher frequency fluctuations in simple spikes across these time windows, it does capture the major transients in firing rate that covary with the kinematics of eye movement. In figures 28C and D we illustrate the distribution of R^2 values achieved by model fits to both sets of data. Saccade fits were better as a whole, but this is most likely due to the fact that we regressed firing rate against more data points in the case of pursuit trials.

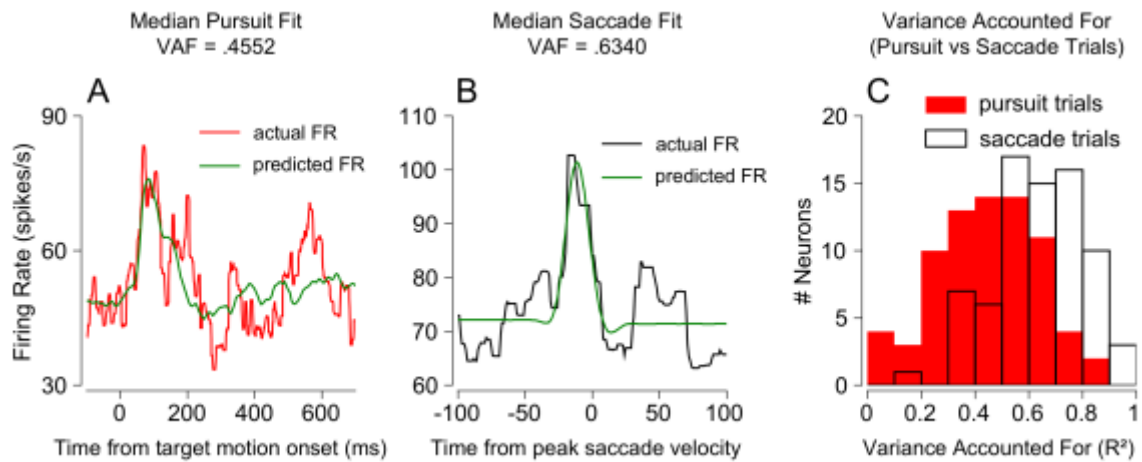


Figure 28: A, B Example median fits to firing rates using regression model. C distribution of R^2 values showing the percentage variance accounted for by the regression model in each neurons' preferred direction.

The output of each regression model yields a set of coefficients that describe the sensitivity of each Purkinje cell's firing rate to position, velocity, and acceleration. We can multiply these regression coefficients by average position, velocity, and acceleration traces to get an estimate of how much the total predicted firing rate is contributed by each variable. In figures 29A-C we illustrate how many spikes/s each variable contributed during movement initiation, comparing pursuit trials to saccade trials. For example, in figure 29A, we show the peak firing rate contributed by position in saccade trials vs. the peak firing rate contributed by position in pursuit trials. These were not significantly different across our population (ranksum test, $p = .6581$). By contrast both velocity (figure 29B) and acceleration (figure 29C) sensitivities differed strongly when contrasting pursuit and saccade trials. Velocity of eye movements contributed far more strongly to firing rate changes during saccades than it did during pursuit (ranksum test,

$p = 8.72e-07$). By contrast acceleration contributed more strongly to peak firing rates during pursuit as opposed to saccades (ranksum test, $6.37e-9$). This suggests that the sensitivity of an individual Purkinje cell to velocity and acceleration varies as a function of the peak speed of the eye movement. While this is not inconsistent with the hypothesis that the OMV drives some shared kinematic feature of saccadic and pursuit eye movements, like acceleration or velocity, it suggests that this occurs in a highly non-linear manner.

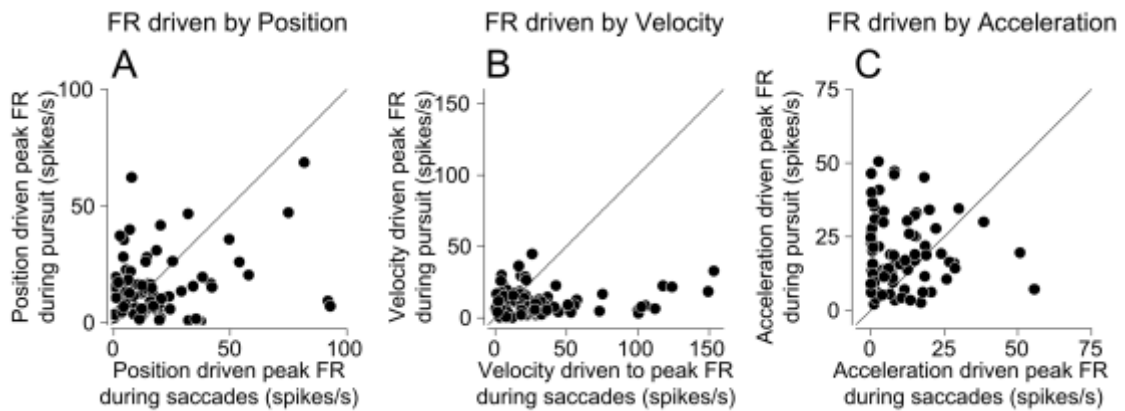


Figure 29: A-C Contribution of position (A), velocity (B), and acceleration (C) coefficients to firing rate in during movement initiation in saccade trials (horizontal axis) vs pursuit trials (vertical axis).

4.3.5 Kinematic sensitivity at a population level during pursuit and saccade Trials

In section 4.3 3, we discussed how population activity can take on a different structure than individual neurons considered independently. This motivated us to test the hypothesis that population firing rates were better related to movement kinematics than single neurons considered alone. We considered two population representations.

The first, was the population response averaged across neurons aligned on their preferred saccade direction. The second, was the population response averaged across neurons aligned on their preferred pursuit direction. We fit the same linear model we introduced in the prior section to these population responses. In figure 30A and B we illustrate these fits. Our data show that our model performs very well in the case of pursuit, with the dynamics of firing rates being almost entirely captured by our simple linear model ($R^2 = .81$). By contrast our model to poorly fit ($R^2 = .58$) the time varying dynamics of the population firing rates during saccades.

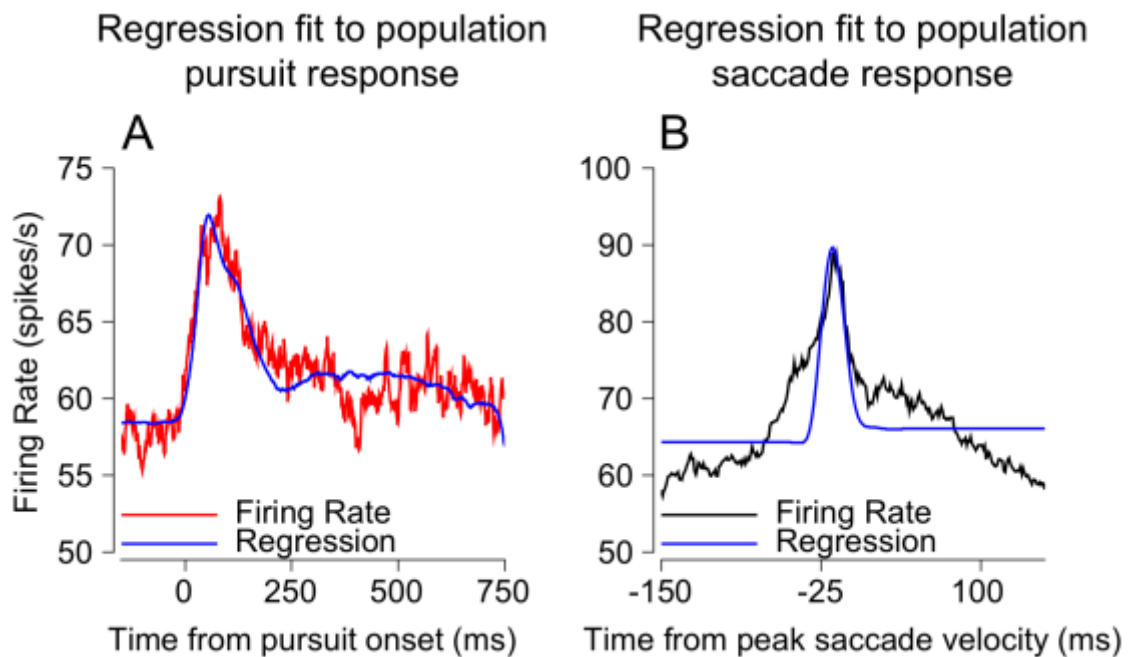


Figure 30: A, Regression fit to population average firing rate in pursuit trials (neurons aligned to pursuit PD). B, Regression fit to the population average firing rate with during saccade trials (neurons aligned to saccade PD).

Both models accounted for some substantial variance in firing rates, nonetheless. The time course of the initial rise of firing rates during saccade trials paralleled the time course of saccade velocity, for example. We wanted to see if this was simply a function of a small number of neurons in our population dominating firing rate. We tested next if these finds would hold for subpopulations of neurons. To answer this, we adopted an approach from prior publications (Herzfeld, Kojima et al. 2015). We generated, from our population of 84 Purkinje cells, pseudo-populations composed of 50 Purkinje cells each. This is roughly the number of Purkinje cells that are believed to synapse onto a deep cerebellar nuclear neuron. This allowed us to accomplish three things. First, it allowed us to determine errors in our estimate of mean population firing rates. Second, it allowed us to estimate the range of fits our model could achieve. Finally, it allowed us to see whether responses during saccades and pursuit truly tracked eye velocity and acceleration respectively, as opposed to being an effect of one or two cells in our population.

In figures 31A and B we illustrate mean firing rates + 1 sem across our pseudo-populations. This suggests that our estimates of mean firing rates across our population was relatively well founded. R² values during saccade trials could range from .39-.82 across each of our pseudo-populations, while R² values during pursuit trials could range from .47-.84. These two distributions were significantly different (ranksum test, $p=1.72e-12$). We then tested the ratio of peak firing rates (during the initiation of pursuit

or saccades) that could be accounted for by velocity for our pursuit pseudopopulations and our saccade pseudopopulations. The proportion of peak firing rates during saccades that could be accounted for by acceleration was essentially zero, and was strongly different from the proportion of peak firing rates that could be accounted for by acceleration during pursuit (two sample t test, $1.78e-58$). The reverse held true for velocity during saccades (two sample t test, $4.40e-45$). Finally, we found that the proportion of peak firing rates that could be accounted for by position was greater during pursuit than during saccades (two sample t test, $3.14e-8$), though less significantly. In figure 31C, we illustrate the peak firing rate contributed by acceleration during pursuit trials against peak baseline subtracted firing rates from those trials. Most of this data lies consistent above the unity line (one sample t test, $p = 1.43e-18$), suggesting that the largest proportion of peak firing rates during pursuit are accounted for by acceleration, with position accounting for the residuals. In figure 31D, we illustrate the peak firing rate contributed by velocity during saccade trials against peak baseline subtracted firing rates from those trials. As is apparent visually, points are balanced about the unity line. Overall, the data lied just below the unity line, but very weakly (one sample t test, $p=.002$), suggesting that the largest proportion of peak firing rates during saccades are accounted for by velocity, with position accounting for the residuals. We note this parallels our findings on individual neurons.

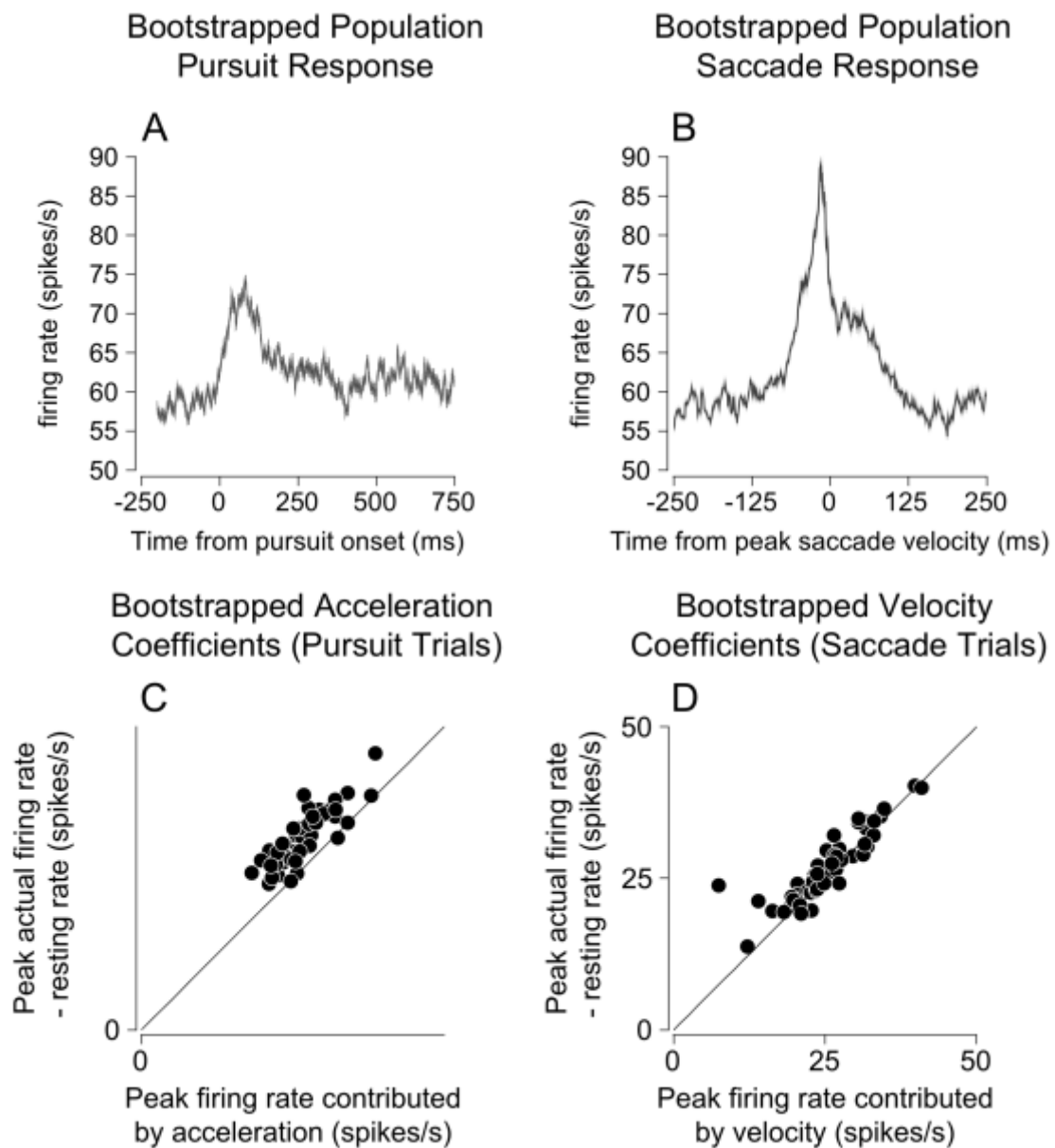


Figure 31: A,B Average of 50 bootstrapped population responses for both pursuit and saccade trials. Gray shading is ± 1 SEM. C, Peak firing rate of populations during pursuit trials contributed by acceleration vs peak actual firing rates (resting rate subtracted) D, Peak firing rate of pseudopopulations during saccade trials contributed by velocity vs peak actual firing rates (resting rate subtracted). Each point is generated from one pseudopopulation, that contributed to the average firing rates illustrated in figures A and B.

4.3.6 Discussion

We have studied the directional tuning and kinematic sensitivity of neurons recorded in the oculomotor vermis during the execution of pursuit and saccade tasks. At a single neuron level, we found responses could not easily be related to directional or kinematic aspects of behavior. Tuning curves in the OMV are broad, whether one is examining pursuit trials or saccade trials. The preferred directions for neurons are distributed uniformly regardless of whether one is analyzing pursuit or saccade trials. Moreover, within our population a neuron's preferred direction for pursuit usually lay within one standard deviation of its preferred direction for saccades.

Similarly, analysis of the kinematic sensitivity of OMV neurons during pursuit and saccades showed that individual neurons appear to have a special relationship to the kinematics of pursuit or saccades. The most important finding we report is that velocity sensitivity seems to be far greater for Purkinje cells during saccade trials than during pursuit trials and vice versa for acceleration. This is particularly puzzling as it suggests neurons covary with these variables in a highly non-linear manner. We do not think this is an effect of low variance accounted for by our regression model, as we verified even for poor quality fits, our model captures the firing rate transients that are best related to behavior.

The second major finding in this work is to show that population level responses in the OMV are more structured than individual neural responses. Firstly, neurons at a

population level are sharply tuned if organized according to their preferred direction regardless of whether one is studying saccades or pursuit trials. Secondly, we found that if you aligned all neurons to their pursuit preferred direction, the mean population response for saccades in the same directions was very small. This was paralleled by the fact that if you aligned all neurons to their saccade preferred direction, the mean response for pursuit in the same directions was very small. We speak at length about how we interpret these results in the discussion section that follows.

We found that at a population level, firing rates tracked eye movement kinematics well during pursuit when all cells were organized according to their preferred simple spike direction. By contrast, population level responses did not faithfully track movement kinematics during saccade trials, though they seem to clearly covary with eye velocity (Herzfeld, Kojima et al. 2015)

5. Discussion

Here, I first review the core findings of the work presented in the preceding three chapters. I discuss those aspects of the findings that I believe are core to understanding the function of the oculomotor vermis. I end with a discussion of future work that needs to be completed in order to move forwards.

5.1 Core Findings

Perhaps the core goal of this thesis was to construct, for the OMV, a quantitative dataset documenting responses to pursuit eye movements that places it on par with

prior studies of the floccular complex. With this in mind, I designed, executed, and analyzed Purkinje cell data gathered from the OMV. I performed multiple experiments that sought to determine the tuning structure of OMV Purkinje cells, document their responses over the course of pursuit adaptation, and determine the structure of their trial-by-trial correlations with pursuit metrics.

In terms of directional tuning, we can say with certainty that the structure of responses in the OMV is very different from the FLc. Directional tuning of OMV Purkinje cell simple spikes mostly manifests itself as graded responses that occur in retinal coordinates, as opposed to reciprocal or push-pull type responses that occur in muscle coordinates in the floccular complex. Complex spikes are not driven solely by retinal slip, like they are in the floccular complex, but are more complicated. It was already known that complex spikes were responsive to positional errors conveyed by the colliculus during the execution of saccades (Soetedjo, Kojima et al. 2008), but I have also shown that roughly 50% of neurons can also be strongly driven by target motion during the initiation of pursuit. While not explicitly covered in the chapters above, I found a fraction of cells could have complex spike activity during both target steps preceding saccades and target motion preceding pursuit. These results suggest that climbing fiber inputs to the OMV are more diverse than previously hypothesized. Complex spike tuning was sharp but not organized in an opponent manner to simple spike tuning, as shown in the floccular complex.

These two factors, the lower incidence of motion sensitive complex spikes and their poor relationship to simple spike activity are a parsimonious account for the lack of changes in these same cells that we observe over the course of pursuit adaptation. In the floccular complex, opponent tuning of complex and simple spikes is conducive to the sort of trial-over-trial plasticity that is believed to underlie its role in pursuit adaptation (Medina and Lisberger 2008). The OMV lacks the structure of complex and simple spike signals required to drive directional adaptation. This does not preclude the role of the OMV in driving other forms of pursuit adaptation, however. Prior studies have shown that OMV lesions impair pursuit speed adaptation (Takagi, Zee et al. 2000) substantially. We did not test pursuit speed adaptation in the above studies, and speed changes very little over the course of directional adaptation. Future studies would need to be performed to confirm whether the structure of target motion responsive complex spikes and related responses during pursuit at different speeds is sufficient to support speed adaptation. The fact that only a fraction of Purkinje cells in the floccular complex are modulated during speed adaptation (Kahlon and Lisberger 2000), and that inputs to the vermis are known to show strong changes over the course of pursuit speed adaptation (Chou and Lisberger 2004, Ono and Mustari 2012) suggests that future studies should test the hypothesis that the OMV serves as a site for speed adaptation.

A caveat to this point is raised by the second set of experiments where I more carefully considered the differences in response properties between the floccular

complex and the OMV. I found strong differences in the sensitivity Purkinje cell firing rates in the OMV have to different kinematic variables. We also found that trial-to-trial correlations between firing rate and pursuit metrics were much smaller in the vermis (by comparison to the floccular complex). We stress that low values between trial-to-trial variations in firing rate and behavior do not necessarily imply a brain region does not play a role in driving that behavior (Medina and Lisberger 2007, Pitkow, Liu et al. 2015). These values are more likely related to both the inputs to a particular region as well as the downstream decoding of its output. Indeed, similar values of neuron-behavior correlations have been shown in cortical structures that are believed to also play an important role in pursuit control (Schoppik, Nagel et al. 2008, Hohl, Chaisanguanthum et al. 2013).

In the final chapter of my thesis, I considered how a population of OMV Purkinje cells responded during the execution of both pursuit and saccadic eye movements. This comparison is important, as the role of the OMV in saccades is well established (Robinson, Straube et al. 1993, Takagi, Zee et al. 1998). In this set of experiments, I found that acceleration sensitivities of individual Purkinje cells were usually higher during pursuit than during saccades. Moreover, I found that while, at an individual neuron level, directional tuning curves were largely overlapping during saccade and pursuit trials, at a population level saccade and pursuit responses could be greatly suppressed depending on whether cells were organized according to pursuit or saccade preferred

directions. Finally, I used a procedure that estimates the potential responses expected from caudal fastigial nucleus neurons (cFN) to which the OMV projects and found that this putative response strongly tracks changes in kinematics that occur over the course of pursuit. Moreover, I found that the expected cFN response tracked moment by moment changes in pursuit kinematics better than saccade kinematics (as assessed by a simple linear model). The expected cFN population response during saccades that was predicted by this procedure and using the population of neurons I gathered in the OMV, strongly resembles the results of a recently published study investigating responses OMV responses during saccades (Herzfeld, Kojima et al. 2015). The replication of these results suggests that my study and this prior study recorded very similar neural populations, and to a certain extent validates the population prediction of cFN activity that I made. In the next section I state some conclusions that can be made on the basis of these findings and suggest several hypotheses that have been generated by these findings. I then highlight critical gaps in our current understanding of the OMV, the cFN, and their role in pursuit that I believe are critical to testing these hypotheses and honing in on the functional role of the OMV.

5.2 Conclusions and future lines of research

I think the main take home story of my findings is that the OMV, at least in the context of pursuit control, is further removed from the motor periphery than initial reports and anatomy suggest. First, the fact that the recorded population of Purkinje

cells in the OMV expressed their directional tuning in retinal coordinates suggests that OMV output activity is not packaged and ready to drive motor responses in the way Floc output activity is. Second the fact that neuron-behavior correlations in the OMV are more commensurate with values one finds in cortical areas like area MT, FEF and LIP (Schoppik, Nagel et al. 2008, O'Leary and Lisberger 2012, Hohl, Chaisanguanthum et al. 2013) suggests the OMV is far upstream from primary motoneurons. Finally, the lower kinematic sensitivity of our neurons suggest they are less intricately linked to the moment by moment control of behavior. These findings lead me to conclude that the OMV either plays a modulatory role in pursuit control, or receives pursuit related inputs for reasons unrelated to pursuit control.

Ultimately, it is hard on the basis of these findings to conclude that the OMV itself is responsible residual pursuit control following flocculectomy. I would suggest, however, on the basis of the population representations constructed in chapter 4 that the caudal fastigial nucleus (cFN) could serve as a potential site of residual pursuit control. Responses in the cFN are known to be strongly modulated by pursuit (Fuchs, Robinson et al. 1994) and bilateral injections of muscimol into the cFN impair pursuit acceleration and sustained velocity components (Robinson, Straube et al. 1997). If the predictions made about cFN population responses on the basis of OMV responses I have made hold, one might also predict signals in the cFN are better related to pursuit kinematics than in the OMV.

There are several problems with evaluating the role of the cFN however. Whereas we are perfectly aware of the efferent pathways emanating from the OMV (they are entirely localized to the cFN), the same cannot be said about the cFN. The only efferent pathways from the cFN that have been studied closely, concern projections from the cFN to the superior colliculus and saccade burst generator networks in the paramedian pontine reticular formation (Ugolini, Klam et al. 2006). Unfortunately, neither of these structures is known to play more than a large role in pursuit control, leaving open the problem of how signals from the cFN ultimately drive eye muscles during pursuit eye movements. The fact that there is no well-defined output pathway from the cFN that is known to influence pursuit eye movements also hampers investigation into the OMV. Indeed, part of the success in relating floccular complex responses to pursuit comes from the understanding that cells in the floccular complex exist within a well-defined pathway 2 synapses removed from motoneurons (Joshua, Medina et al. 2013). This points to a need not only to investigate cFN activity during pursuit, but to better understand brainstem premotoneuronal networks that are responsible for pursuit control. This, in turn, will likely inform how we understand the OMV's role in modulating cFN activity. One particular region, downstream from the cFN, that might mediate its role in pursuit eye movement control is the central mesencephalic reticular formation (cMRF). The cMRF receives input from the cFN and preferentially innervates the "slow" motoneurons hypothesized to control pursuit and

vergence eye movements (Ugolini, Klam et al. 2006). Responses in this structure have not been characterized during pursuit, but is the best current estimate as to the source of interneurons that link cFN pursuit responses to motoneuron activation in a way that explains why inactivation of the cFN influences pursuit eye movements. Therefore, I suggest a goal of future work should be to characterize pursuit responses in the cMRF, and perhaps even characterize the signals conveyed along the pathway from the cFN to the cMRF.

A side finding in the current work which is particularly interesting concerns the nature of population tuning in the OMV. I found that population tuning during pursuit and saccade trials was sharper than when I considered neurons individually. While I did not find opponent pursuit saccade tuning as hypothesized, I discovered a manner in which the OMV might still encode pursuit and saccadic eye movements independently of one another at a population level. By organizing cells according to pursuit or saccade preferred direction, I found that responses to the opposite sort of movement were strongly suppressed at the population level. Therefore, while OMV responses during pursuit are not consistent with it playing a strong role in driving these eye movements, the analysis of these responses might still provide insight into the question of how ballistic and continuous movements can be simultaneously encoded. I hypothesize that this response structure is a clear example of “null-space” dynamics. This refers to a hypothesis about the organization of neural responses in the motor cortex that is

believed to allow it to support different response dynamics during the preparation for movements and execution of movements without the two processes interfering with one another (Kaufman, Churchland et al. 2014, Li, Daie et al. 2016). While I did not explicitly test whether responses in the OMV during saccadic eye movements lie in the null space of responses during pursuit eye movements, it points to an interesting exciting future avenue of research.

One point which is worth stressing is that our results do indicate that OMV activity is more strongly driven by saccades than pursuit, at a population and individual neuron level. One hypothesis that is possible, therefore, is that activity in the OMV may be more related to catch up saccades that occur during pursuit eye movement than to pursuit eye movements themselves. This would provide the most parsimonious explanation for the findings reported above. First, it would explain why activity in the OMV seems so removed from the pursuit system. Second, the inability to execute these catch up saccades would explain many of the pursuit deficits following OMV lesions. Finally, it would explain why the vermis receives input from cortical structures related to visual motion or pursuit eye movements like areas MT or FEF. Saccades that occur during pursuit are different, in character, from those that occur to stationary targets. They typically land on target suggesting they take into account the motion of the target during the saccadic eye movement itself (Orban de Xivry and Lefevre 2007). Therefore, any structure that is responsible for fine control of saccades, like the OMV, needs access

to the state of the pursuit system and the motion of the target, but necessarily in a manner required to finely control trial-by-trial variation in pursuit.

A final caveat is that the work in the preceding chapters concentrated on the two best understood areas of the oculomotor cerebellum. These are but a fraction of the total regions that are believed to contribute to eye movement control, however (Simon, Iain et al.). Large regions of the cerebellar hemispheres, the dorsal paraflocculus, the nodulus, the uvula, and paraoculomotor regions that surround the oculomotor vermis are yet to be investigated. These areas all need to be characterized quantitatively in the same manner that I have done for the oculomotor vermis. Doing so will likely show how diverse sets of the cerebellum contribute to eye movement control, lessons that are likely to be important for understanding the role of the cerebellum in motor control in general.

References

Bastian, A., G. Schoner and A. Riehle (2003). "Preshaping and continuous evolution of motor cortical representations during movement preparation." Eur J Neurosci **18**(7): 2047-2058.

Bastian, A. J. (2006). "Learning to predict the future: the cerebellum adapts feedforward movement control." Curr Opin Neurobiol **16**(6): 645-649.

Belknap, D. B. and R. A. McCrea (1988). "Anatomical connections of the prepositus and abducens nuclei in the squirrel monkey." J Comp Neurol **268**(1): 13-28.

Bisley, J. W. and M. E. Goldberg (2003). "The role of the parietal cortex in the neural processing of saccadic eye movements." Adv Neurol **93**: 141-157.

Carpenter, R. H. S. (1988). Movements of the eyes. London, Pion.

Chaisanguanthum, K. S., M. Joshua, J. F. Medina, W. Bialek and S. G. Lisberger (2014). "The Neural Code for Motor Control in the Cerebellum and Oculomotor Brainstem." eNeuro **1**(1).

Chou, I. H. and S. G. Lisberger (2004). "The role of the frontal pursuit area in learning in smooth pursuit eye movements." J Neurosci **24**(17): 4124-4133.

Chubb, M. C. and A. F. Fuchs (1982). "Contribution of y group of vestibular nuclei and dentate nucleus of cerebellum to generation of vertical smooth eye movements." J Neurophysiol **48**(1): 75-99.

Cisek, P. and J. F. Kalaska (2002). "Simultaneous encoding of multiple potential reach directions in dorsal premotor cortex." J Neurophysiol **87**(2): 1149-1154.

Dash, S., N. Catz, P. W. Dicke and P. Thier (2012). "Encoding of smooth-pursuit eye movement initiation by a population of vermal Purkinje cells." Cereb Cortex **22**(4): 877-891.

Dash, S., P. W. Dicke and P. Thier (2013). "A vermal Purkinje cell simple spike population response encodes the changes in eye movement kinematics due to smooth pursuit adaptation." Front Syst Neurosci 7: 3.

Desmedt, J. E. (1978). Cerebral motor control in man : long loop mechanisms. Basel ; New York, S. Karger.

Fortier, P. A., A. M. Smith and J. F. Kalaska (1993). "Comparison of cerebellar and motor cortex activity during reaching: directional tuning and response variability." J Neurophysiol 69(4): 1136-1149.

Fuchs, A. F., F. R. Robinson and A. Straube (1994). "Participation of the caudal fastigial nucleus in smooth-pursuit eye movements. I. Neuronal activity." J Neurophysiol 72(6): 2714-2728.

Fukushima, K. (1991). "The interstitial nucleus of Cajal in the midbrain reticular formation and vertical eye movement." Neurosci Res 10(3): 159-187.

Gamlin, P. D. (2006). "The pretectum: connections and oculomotor-related roles." Prog Brain Res 151: 379-405.

Gandolfo, F., C. Li, B. J. Benda, C. P. Schioppa and E. Bizzi (2000). "Cortical correlates of learning in monkeys adapting to a new dynamical environment." Proc Natl Acad Sci U S A 97(5): 2259-2263.

Gardner, J. L. and S. G. Lisberger (2002). "Serial linkage of target selection for orienting and tracking eye movements." Nat Neurosci 5(9): 892-899.

Gegenfurtner, K. R. (2016). "The Interaction Between Vision and Eye Movements." Perception.

Georgopoulos, A. P., J. F. Kalaska, R. Caminiti and J. T. Massey (1982). "On the relations between the direction of two-dimensional arm movements and cell discharge in primate motor cortex." J Neurosci 2(11): 1527-1537.

Georgopoulos, A. P., A. B. Schwartz and R. E. Kettner (1986). "Neuronal population coding of movement direction." Science **233**(4771): 1416-1419.

Green, J. T. and J. E. Steinmetz (2005). "Purkinje cell activity in the cerebellar anterior lobe after rabbit eyeblink conditioning." Learn Mem **12**(3): 260-269.

Harris, C. M. and D. M. Wolpert (2006). "The main sequence of saccades optimizes speed-accuracy trade-off." Biol Cybern **95**(1): 21-29.

Herzfeld, D. J., Y. Kojima, R. Soetedjo and R. Shadmehr (2015). "Encoding of action by the Purkinje cells of the cerebellum." Nature **526**(7573): 439-442.

Hohl, S. S., K. S. Chaisanguanthum and S. G. Lisberger (2013). "Sensory population decoding for visually guided movements." Neuron **79**(1): 167-179.

Holt, G. R., W. R. Softky, C. Koch and R. J. Douglas (1996). "Comparison of discharge variability in vitro and in vivo in cat visual cortex neurons." J Neurophysiol **75**(5): 1806-1814.

Ivry, R. B. and R. M. Spencer (2004). "The neural representation of time." Curr Opin Neurobiol **14**(2): 225-232.

Joshua, M. and S. G. Lisberger (2015). "A tale of two species: Neural integration in zebrafish and monkeys." Neuroscience **296**: 80-91.

Joshua, M., J. F. Medina and S. G. Lisberger (2013). "Diversity of neural responses in the brainstem during smooth pursuit eye movements constrains the circuit mechanisms of neural integration." J Neurosci **33**(15): 6633-6647.

Kahlon, M. and S. G. Lisberger (1996). "Coordinate system for learning in the smooth pursuit eye movements of monkeys." J Neurosci **16**(22): 7270-7283.

Kahlon, M. and S. G. Lisberger (2000). "Changes in the responses of Purkinje cells in the floccular complex of monkeys after motor learning in smooth pursuit eye movements." J Neurophysiol **84**(6): 2945-2960.

Kaufman, M. T., M. M. Churchland, S. I. Ryu and K. V. Shenoy (2014). "Cortical activity in the null space: permitting preparation without movement." Nat Neurosci **17**(3): 440-448.

Keller, E. L. (1974). "Participation of medial pontine reticular formation in eye movement generation in monkey." J Neurophysiol **37**(2): 316-332.

Keller, E. L. and S. J. Heinen (1991). "Generation of smooth-pursuit eye movements: neuronal mechanisms and pathways." Neurosci Res **11**(2): 79-107.

Kelly, R. M. and P. L. Strick (2003). "Cerebellar loops with motor cortex and prefrontal cortex of a nonhuman primate." J Neurosci **23**(23): 8432-8444.

Kornhuber, H. H. (1971). "Motor functions of cerebellum and basal ganglia: the cerebellocortical saccadic (ballistic) clock, the cerebellonuclear hold regulator, and the basal ganglia ramp (voluntary speed smooth movement) generator." Kybernetik **8**(4): 157-162.

Kowler, E. and E. Blaser (1995). "The accuracy and precision of saccades to small and large targets." Vision Res **35**(12): 1741-1754.

Krauzlis, R. J. (2004). "Recasting the smooth pursuit eye movement system." J Neurophysiol **91**(2): 591-603.

Krauzlis, R. J. (2005). "The control of voluntary eye movements: new perspectives." Neuroscientist **11**(2): 124-137.

Krauzlis, R. J. and S. G. Lisberger (1996). "Directional organization of eye movement and visual signals in the floccular lobe of the monkey cerebellum." Exp Brain Res **109**(2): 289-302.

- Krauzlis, R. J. and F. A. Miles (1998). "Role of the oculomotor vermis in generating pursuit and saccades: effects of microstimulation." J Neurophysiol **80**(4): 2046-2062.
- Langer, T., A. F. Fuchs, C. A. Scudder and M. C. Chubb (1985). "Afferents to the flocculus of the cerebellum in the rhesus macaque as revealed by retrograde transport of horseradish peroxidase." J Comp Neurol **235**(1): 1-25.
- Lee, J., M. Joshua, J. F. Medina and S. G. Lisberger (2016). "Signal, Noise, and Variation in Neural and Sensory-Motor Latency." Neuron **90**(1): 165-176.
- Lee, J. and S. G. Lisberger (2013). "Gamma synchrony predicts neuron-neuron correlations and correlations with motor behavior in extrastriate visual area MT." J Neurosci **33**(50): 19677-19688.
- Leigh, R. J. and D. S. Zee (2006). The neurology of eye movements. Oxford ; New York, Oxford University Press.
- Li, N., K. Daie, K. Svoboda and S. Druckmann (2016). "Robust neuronal dynamics in premotor cortex during motor planning." Nature **532**(7600): 459-464.
- Lisberger, S. G. (2009). "Internal models of eye movement in the floccular complex of the monkey cerebellum." Neuroscience **162**(3): 763-776.
- Lisberger, S. G. (2010). "Visual guidance of smooth-pursuit eye movements: sensation, action, and what happens in between." Neuron **66**(4): 477-491.
- Lisberger, S. G. and A. F. Fuchs (1978). "Role of primate flocculus during rapid behavioral modification of vestibuloocular reflex. II. Mossy fiber firing patterns during horizontal head rotation and eye movement." J Neurophysiol **41**(3): 764-777.
- Lisberger, S. G., E. J. Morris and L. Tychsen (1987). "Visual motion processing and sensory-motor integration for smooth pursuit eye movements." Annu Rev Neurosci **10**: 97-129.

Lisberger, S. G. and T. A. Pavelko (1986). "Vestibular signals carried by pathways subserving plasticity of the vestibulo-ocular reflex in monkeys." J Neurosci **6**(2): 346-354.

Lisberger, S. G. and L. E. Westbrook (1985). "Properties of visual inputs that initiate horizontal smooth pursuit eye movements in monkeys." J Neurosci **5**(6): 1662-1673.

Mauk, M. D., J. F. Medina, W. L. Nores and T. Ohshima (2000). "Cerebellar function: coordination, learning or timing?" Curr Biol **10**(14): R522-525.

May, P. J., R. Hartwich-Young, J. Nelson, D. L. Sparks and J. D. Porter (1990). "Cerebellotectal pathways in the macaque: implications for collicular generation of saccades." Neuroscience **36**(2): 305-324.

Medina, J. F., M. R. Carey and S. G. Lisberger (2005). "The representation of time for motor learning." Neuron **45**(1): 157-167.

Medina, J. F. and S. G. Lisberger (2007). "Variation, signal, and noise in cerebellar sensory-motor processing for smooth-pursuit eye movements." J Neurosci **27**(25): 6832-6842.

Medina, J. F. and S. G. Lisberger (2008). "Links from complex spikes to local plasticity and motor learning in the cerebellum of awake-behaving monkeys." Nat Neurosci **11**(10): 1185-1192.

Medina, J. F. and S. G. Lisberger (2009). "Encoding and decoding of learned smooth-pursuit eye movements in the floccular complex of the monkey cerebellum." J Neurophysiol **102**(4): 2039-2054.

Miles, F. A., J. H. Fuller, D. J. Braitman and B. M. Dow (1980). "Long-term adaptive changes in primate vestibuloocular reflex. III. Electrophysiological observations in flocculus of normal monkeys." J Neurophysiol **43**(5): 1437-1476.

Missal, M. and E. L. Keller (2002). "Common inhibitory mechanism for saccades and smooth-pursuit eye movements." J Neurophysiol **88**(4): 1880-1892.

Noda, H. (1981). "Visual mossy fiber inputs to the flocculus of the monkey." Ann N Y Acad Sci **374**: 465-475.

Noda, H. and T. Fujikado (1987). "Topography of the oculomotor area of the cerebellar vermis in macaques as determined by microstimulation." J Neurophysiol **58**(2): 359-378.

Noda, H., S. Sugita and Y. Ikeda (1990). "Afferent and efferent connections of the oculomotor region of the fastigial nucleus in the macaque monkey." J Comp Neurol **302**(2): 330-348.

O'Leary, J. G. and S. G. Lisberger (2012). "Role of the lateral intraparietal area in modulation of the strength of sensory-motor transmission for visually guided movements." J Neurosci **32**(28): 9745-9754.

Ono, S. and M. J. Mustari (2012). "Role of MSTd extraretinal signals in smooth pursuit adaptation." Cereb Cortex **22**(5): 1139-1147.

Orban de Xivry, J. J. and P. Lefevre (2007). "Saccades and pursuit: two outcomes of a single sensorimotor process." J Physiol **584**(Pt 1): 11-23.

Osborne, L. C., S. S. Hohl, W. Bialek and S. G. Lisberger (2007). "Time course of precision in smooth-pursuit eye movements of monkeys." J Neurosci **27**(11): 2987-2998.

Osborne, L. C., S. G. Lisberger and W. Bialek (2005). "A sensory source for motor variation." Nature **437**(7057): 412-416.

Pitkow, X., S. Liu, D. E. Angelaki, G. C. DeAngelis and A. Pouget (2015). "How Can Single Sensory Neurons Predict Behavior?" Neuron **87**(2): 411-423.

Pouget, A., S. Deneve, J. C. Ducom and P. E. Latham (1999). "Narrow versus wide tuning curves: What's best for a population code?" Neural Comput **11**(1): 85-90.

Ramachandran, R. and S. G. Lisberger (2005). "Normal performance and expression of learning in the vestibulo-ocular reflex (VOR) at high frequencies." J Neurophysiol **93**(4): 2028-2038.

Rambold, H., A. Churchland, Y. Selig, L. Jasmin and S. G. Lisberger (2002). "Partial ablations of the flocculus and ventral paraflocculus in monkeys cause linked deficits in smooth pursuit eye movements and adaptive modification of the VOR." J Neurophysiol **87**(2): 912-924.

Rashbass, C. (1961). "The relationship between saccadic and smooth tracking eye movements." J Physiol **159**: 326-338.

Raymond, J. L., S. G. Lisberger and M. D. Mauk (1996). "The cerebellum: a neuronal learning machine?" Science **272**(5265): 1126-1131.

Robinson, D. A. (1970). "Oculomotor unit behavior in the monkey." J Neurophysiol **33**(3): 393-403.

Robinson, D. A. (1986). Is the oculomotor system a cartoon of motor control? Progress in Brain Research. U. B. B. C. H.-J. Freund and J. Noth, Elsevier. **Volume 64**: 411-417.

Robinson, F. R. and A. F. Fuchs (2001). "The role of the cerebellum in voluntary eye movements." Annu Rev Neurosci **24**: 981-1004.

Robinson, F. R., A. Straube and A. F. Fuchs (1993). "Role of the caudal fastigial nucleus in saccade generation. II. Effects of muscimol inactivation." J Neurophysiol **70**(5): 1741-1758.

Robinson, F. R., A. Straube and A. F. Fuchs (1997). "Participation of caudal fastigial nucleus in smooth pursuit eye movements. II. Effects of muscimol inactivation." J Neurophysiol **78**(2): 848-859.

Roitman, A. V., S. Pasalar, M. T. Johnson and T. J. Ebner (2005). "Position, direction of movement, and speed tuning of cerebellar Purkinje cells during circular manual tracking in monkey." J Neurosci **25**(40): 9244-9257.

Salinas, E. and L. F. Abbott (1994). "Vector reconstruction from firing rates." J Comput Neurosci **1**(1-2): 89-107.

Sato, H. and H. Noda (1992). "Posterior vermal Purkinje cells in macaques responding during saccades, smooth pursuit, chair rotation and/or optokinetic stimulation." Neurosci Res **12**(5): 583-595.

Schoppik, D., K. I. Nagel and S. G. Lisberger (2008). "Cortical mechanisms of smooth eye movements revealed by dynamic covariations of neural and behavioral responses." Neuron **58**(2): 248-260.

Shadmehr, R. and F. A. Mussa-Ivaldi (1994). "Adaptive representation of dynamics during learning of a motor task." J Neurosci **14**(5 Pt 2): 3208-3224.

Shidara, M., K. Kawano, H. Gomi and M. Kawato (1993). "Inverse-dynamics model eye movement control by Purkinje cells in the cerebellum." Nature **365**(6441): 50-52.

Simon, P. L., G. Iain, E. Stefan and T. Peter The oculomotor cerebellum, 'Oxford University Press'.

Soetedjo, R., Y. Kojima and A. F. Fuchs (2008). "Complex spike activity in the oculomotor vermis of the cerebellum: a vectorial error signal for saccade motor learning?" J Neurophysiol **100**(4): 1949-1966.

Sparks, D., W. H. Rohrer and Y. Zhang (2000). "The role of the superior colliculus in saccade initiation: a study of express saccades and the gap effect." Vision Res **40**(20): 2763-2777.

Sparks, D. L. (2002). "The brainstem control of saccadic eye movements." Nat Rev Neurosci **3**(12): 952-964.

Stone, L. S. and S. G. Lisberger (1986). "Detection of tracking errors by visual climbing fiber inputs to monkey cerebellar flocculus during pursuit eye movements." Neurosci Lett **72**(2): 163-168.

Stone, L. S. and S. G. Lisberger (1990). "Visual responses of Purkinje cells in the cerebellar flocculus during smooth-pursuit eye movements in monkeys. II. Complex spikes." J Neurophysiol **63**(5): 1262-1275.

Suzuki, D. A., H. Noda and M. Kase (1981). "Visual and pursuit eye movement-related activity in posterior vermis of monkey cerebellum." J Neurophysiol **46**(5): 1120-1139.

Takagi, M., D. S. Zee and R. J. Tamargo (1998). "Effects of lesions of the oculomotor vermis on eye movements in primate: saccades." J Neurophysiol **80**(4): 1911-1931.

Takagi, M., D. S. Zee and R. J. Tamargo (2000). "Effects of lesions of the oculomotor cerebellar vermis on eye movements in primate: smooth pursuit." J Neurophysiol **83**(4): 2047-2062.

Tanaka, M. and S. G. Lisberger (2002). "Role of arcuate frontal cortex of monkeys in smooth pursuit eye movements. I. Basic response properties to retinal image motion and position." J Neurophysiol **87**(6): 2684-2699.

Tehovnik, E. J., M. A. Sommer, I. H. Chou, W. M. Slocum and P. H. Schiller (2000). "Eye fields in the frontal lobes of primates." Brain Res Brain Res Rev **32**(2-3): 413-448.

Thier, P., P. W. Dicke, R. Haas and S. Barash (2000). "Encoding of movement time by populations of cerebellar Purkinje cells." Nature **405**(6782): 72-76.

Todorov, E. (2002). "Cosine tuning minimizes motor errors." Neural Comput **14**(6): 1233-1260.

Ugolini, G., F. Klam, M. Doldan Dans, D. Dubayle, A. M. Brandi, J. Buttner-Ennever and W. Graf (2006). "Horizontal eye movement networks in primates as revealed by retrograde transneuronal transfer of rabies virus: differences in monosynaptic input to "slow" and "fast" abducens motoneurons." J Comp Neurol **498**(6): 762-785.

Van Essen, D. C., C. H. Anderson and D. J. Felleman (1992). "Information processing in the primate visual system: an integrated systems perspective." Science **255**(5043): 419-423.

Voogd, J., C. K. Schraa-Tam, J. N. van der Geest and C. I. De Zeeuw (2012). "Visuomotor cerebellum in human and nonhuman primates." Cerebellum **11**(2): 392-410.

Westheimer, G. and S. M. Blair (1973). "Oculomotor defects in cerebellectomized monkeys." Invest Ophthalmol **12**(8): 618-621.

Yang, Y. and S. G. Lisberger (2014). "Role of plasticity at different sites across the time course of cerebellar motor learning." J Neurosci **34**(21): 7077-7090.

Zee, D. S., A. Yamazaki, P. H. Butler and G. Gucer (1981). "Effects of ablation of flocculus and paraflocculus of eye movements in primate." J Neurophysiol **46**(4): 878-899.

Zhou, H., Z. Lin, K. Voges, C. Ju, Z. Gao, L. W. Bosman, T. J. Ruigrok, F. E. Hoebeek, C. I. De Zeeuw and M. Schonewille (2014). "Cerebellar modules operate at different frequencies." Elife **3**: e02536.

Biography

I was born in Hinsdale, IL on March 14th, 1988. I attended the University of Illinois at Chicago and graduated in 2010 with a double major in the biological sciences and psychology and a minor in mathematics. Below is a list of my relevant publications.

Conference Publications:

Primary Author:

Raghavan, R.T., Lisberger, S.G. (2015) Differences between Purkinje cell responses in floccular complex and oculomotor vermis during pursuit eye movements. Gordon Research Conference: Cerebellum 2015.

Raghavan, R.T., Prevosto, V., Sommer, M.A. (2014) Lateral cerebellar activity correlated with microsaccades. Society for Neuroscience Abstract 632.18

Raghavan, R.T., Prevosto, V., Darie, R., Sommer, M.A. (2013) Timing activity in the lateral cerebellum. Society for Neuroscience Abstract 647.01

Raghavan, R.T., Lebedev, M.A., O'Doherty, J.E., Nicolelis, M.A.L. (2011) Emergent preparatory neural activity underlying learning in premotor and primary motor cortex. Society for Neuroscience Abstract 279.07

Other Relevant Abstracts:

Prevosto, V. **Raghavan, R.T.**, Sommer, M.A. (2013) Evidence for the involvement of lateral cerebellum in executive control and performance monitoring. Society for Neuroscience Abstract 647.02

Grigsby, E.M., Koval, M.J., Rao, H.M., Mueller, J.K., Prevosto, V., **Raghavan, R.T.**, Deng, Z.-D., Peterchev, A., Egner, T., Platt, M.L., Grill, W.M., Sommer, M.A. (2013) Responses of excitatory and inhibitory neurons to TMS and supposed sham-TMS in alert monkeys. Society for Neuroscience Abstract 784.03

Koval, M.J., Grigsby, E.M., Rao, H.M., Mueller, J.K., Prevosto, V., **Raghavan, R.T.**, Deng, Z.-D., Peterchev, A., Egner, T., Platt, M.L., Grill, W.M., Sommer, M.A. (2013) Transcranial magnetic stimulation has both excitatory and inhibitory effects on the activity of frontal eye field neurons. Society for Neuroscience Abstract 784.09

Grigsby, E.M., Mueller, J.K., Petraglia III, F.W., Prevosto, V., **Raghavan, R.T.**, Kozyrkov, C., Deng, Z.-D., Peterchev, A., Egner, T., Platt, M.L., Grill, W.M., Sommer, M.A. (2012) Neuronal recordings during transcranial magnetic stimulation in the alert primate. Society for Neuroscience Abstract 298.03

Prevosto, V., **Raghavan, R.T.**, Sommer, M.A. (2012) Saccadic response characteristics of lateral cerebellar cortex neurons. Society for Neuroscience Abstract 373.05

Publications:

Raghavan, R.T., Prevosto, V., Darie, R., Sommer, M.A. (2016) Contribution of Cerebellar Loops to Action Timing. *Current Opinion in Behavioral Sciences*